Electronic Properties and Reaction Mechanisms of Polysilanes

(ケイ素骨格高分子の電子物性と反応機構に関する研究)

Shu SEKI

2000 ISIR, Osaka University

Preface

The work of this thesis has been carried out under the guidance of Professor Seiichi Tagawa at the Department of Beam Materials Science, The Institute of Scientific and Industrial Research, Osaka University.

The objective in the present work is to elucidate the nature of Si skeleton in polysilane derivatives and to improve their physical properties by using the radiation chamical processes.

The author would like to dedicate the present paper to my parents and my dearest wife, Sumie.

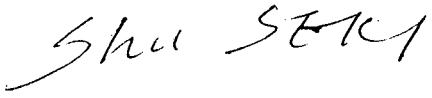

Shu SEKI

The Institute of Scientific and Industrial Research
Osaka University

December, 2000

Contents

Chapter 1 Introduction

1-1 Foreword

Polymers with silicon skeleton, polysilanes were synthesized in the second decade of this century for the first time. However, these 'initial' polysilane materials were poorly investigated at that time, and they attract little scientific interest, because they were insoluble for almost all kinds of organic solvents. On the general account of polymer science and engineering, soluble and high molecular weight polysilane derivatives were necessary in processing, characterization and processing as newly developed polymer materials. Then the first synthesis of variously substituted polysilanes was given great interest and finally came to be staged in many fields, for example, as photoconductors, one-dimensional dimensional semiconductors, resist materials, non-linear optical devices, etc. Many vigorous investigations have been carried out for polysilanes to date, and recently, a variety of the potential properties of polysilanes have been revealed.

1-2 Historical Review

Polysilane derivatives were probably prepared by Kipping[1] for the first time in the early 1920's with the method of coupling reaction of diphenyldichlorosilane, however these 'initial' polysilanes (polydiphenyl-silane) elicited little scientific interest because of its insolubility for any kinds of organic solvents and thermal unstability that meant themal decomposition before melting.[2] After these studies, Burkhard reported the synthesis of simple dialkyl substituted polysilane (polydimethylsilane) by a similar sodium condensation method.[3] But, both these materials were poorly characterized and investigated because of their insolubility and synthetic difficulty that was the need of the high temperature and the high pressure reaction environment with an autoclave system. The next stage studies on polysilane derivatives were broken out in 1970's, 50 years after first synthesis of these polysilanes. Clark reported the synthesis method of polysilane homopolymers without the needs of an autoclave. At around 1975, Yajima et al. reported new utilization of silane polymers in their series of publication and patents in which several kinds of silane polymers were used as precursors of β-silicon carbide.[4] Soon after that, Wesson and Williams described the synthesis of the highly purified poly(dimethyl-silane) which showed slight solubility in some kinds of solvent at high temperature.[5] All of these primary results on polysilanes had been produced by the efforts in the chemists working on alkylated silicon materials, followed by the beginning of studies based on 'multiple' points of view in the field of chemistry and physics.

Diversified studies of polysilanes began about 16 years ago. It was introduced by the success of soluble polysilane polymer and copolymer synthesis. In 1980 Wesson and Williams reported the synthesis of soluble random copolymers containing dimethylsilylene units.[6] Although these materials were more soluble in common organic solvents, they had poor film-forming properties because of their low molecular weight. After that, the same authors reported that a number of soluble block copolymers with sufficient film-forming properties could be prepared by the coupling of various dichlorosilane oligomers. To date, many groups, West, [7] Trujiro, [8] Miller, [9] Zeigler, [10] Matyjaszewski,[11] and so on, have reported various kinds of synthesis routes to obtain soluble polysilanes, and these pioneering studies revealed that the insolubility was not the nature of high molecular weight polysilane materials. Appearance of the soluble polysilane derivatives awakened great interest in the synthesis, characterization, processing and application of polysilanes for newly developed polymer materials. Polysilanes derivatives are polymer materials that means the materials easy to treat, modify and process with the know how of carbon polymers. Contrary, the main chain of polysilanes consists of only silicon atoms, and the electronic structure of the silicon skeleton is drastically different from conventional carbon polymer materials. Actually in a category of studies on polysilanes, these polymers have been regarded as an analogue of silicon based materials such as crystalline silicon, amorphas silicon, etc. The first theoretical aspect of the nature of the silicon skeleton was implied based on the Sadrofy C model.[12] His idea was based on the concepts of Hükel molecular orbitals, supposing non zero resonance integrals between not only sp^3 orbitals of neighboring Si but the orbitals of far Si atoms. Generally, the degree of electron delocalization in the backbone is the function of β_{res}/β_{ovp} : β_{res} means the value of resonance integral between two sp3 orbitals on one silicon atoms, β_{ovp} means that of overap integral. He suggested the value of β_{res}/β_{ovp} in silicon skeleton was higher than the case of carbon backbone polymers. According to the prospects, several semiempilical caluculations and has been carried out on the electronic structures of various substituted polysilanes in the second stage of interest scince 1970's.[13] These studies brought several theoretical anticipation to interesting physical properties of polysilanes, for example, electronic conduction as an analogue of carbon polymers with σ conjugated system (polyacetylene, polytiophene, etc.). Here, the concept of 'σ-conjugated system' was organized for polysilane derivatives though these materials were 'saturated' polymers without σ-orbitals. Nowadays the targets of the investigations have shifted to the nature of silicon skeleton, or physical properties of polysilane as engneering polymer materials, for instance, photo and radiation sensitive material, photoconductor, non-linear optical device, 1-D quantum wires, etc. The studies have become groval and been carried out in various fields.

1-3 Synthesis of Polysilanes

To date, polysilane derivatives are prepared mostly by the Wurtz-type coupling of dichlorodialkylsilane with sodium reflux in organic solvents.[1,2] However, the method has several difficulties such as the poor control of molecular weight and polydispersity. The yields of the polymers are also generally low. Therefore, a lot of groups are working on novel techniques which make it possible to control the configuration of substituents, molecular weight distribution, etc. Here, several conventional and newly developed methods to synthesize polysilanes are introduced.

1. Coupling of dichlorosilane

Maybe Kipping prepared the first substituted polysilane in the 1920s by the condensation of dichlorodiphenylsilane with sodium metal. It is suprising to note that in spite of considerable efforts invested in a search for alternatives, the modified Wurtz coupling of dichlorosilanes remains currently the predominant procedure for the preparation of high molecular weight, linear polysilane derivatives. The reaction is shown in next equation.

For instance, to obtain symmetrically substituted monomers

$$SiCl_4 + 4BrR + 4Mg \rightarrow SiR_4 + 4MgBrCl$$

$$SiR_4 + AlCl_3 + 2CH_3COCl \rightarrow SiR_2Cl_2 + 2CH_3COR \quad (1\text{-}1)$$

For polymerization

$$n\,SiR_2Cl_2 + 2n\,Na \rightarrow (SiR_2)_n + 2n\,NaCl \quad (1\text{-}2)$$

This reaction is usually carried out at elevated temperatures in an solvent using an appropriate alkali metal in dispersion. Potassium metal and sodium-potassium alloys of varying composition have been used extensively for the formation of Si-Si bonds but these reagents often fail to prepare high molecular weight linear polymers and lead to the formation of cyclic oligomers at elevated temperatures, particularly in more polar solvents such as THF. This, coupled with the increased hazards associated with the use and disposal of potassium metal or sodium-potassium alloy, has led to the almost exclusive use of sodium condensation reaction. Recently, however, NaK has been employed at room temperature in conjunction with ultrasonic agitation for the condensation of variety of alkyl-substituted trichlorosilane to form soluble, branched, substituted silane polymers.

Basically, the reaction technique to obtain polysilane derivatives has not revolutionary been changed to date, exceptionlly of unnecessary of autocrave system for high boiling point silicon chrolide monomers. However, the technique has been improved little by little to obtain polymers with adequate properties (molecular weight, substitution pattern and so on) for a variety of investigation. Next ultrasonic activation technique was one of such effective improvement to control molecular weight distribution of polymers and obtain polymers with less defect structures.

Ultrasonic activation

The Wurtz coupling procedure is usually conducted in an inert solvent that boils above the melting point of sodium (97°C). Recent studies using ultrasonic activation to facilitate low-temperature polymerization have provided some interesting results. Matyjaszwski and co-workers have shown that the polymerization of methylphenyl-dichlorosilane yields monomodal high molecular weight polymer when ultrasonic agitation is utilized during and after the monomer addition.[14] At present, this ultrasonic polymerization method is effective only for silane monomers which have the limited kinds of substituents. The low-temperature ultrasonic technique warrants closer investigations for the preparatory and mechanistic purposes. Although the high polymer yields are often comparable to those of the stirred polymerizations at higher temperatures, it may offer some promise as a technique to control the polymer molecular weight distribution.

2. Electrolysis polymerization

All the former methods utilize the coupling reaction of di- or trichlrosilane monomers with high temperature sodium dispersion to obtain polymer materials. It is difficult to control the molecular weight using this reaction, and the polymer yields are considerably low (cost expensive). Therefore the methods are not suitable for mass production. Further, the possibility of the main chain oxidation is still remaining even in the carefully deaerated experimental system. Electrolysis polymerization may solve these problems. Hangge reported that the formation of high polymers by reductive coupling under the Wurtz coupling conditions,[15] suggesting that similar reaction should be possible by using electrochemical reduction at controlled-potential, and actually showed that the silane polymers were obtained in dichlorosilane monomer solution with the electronic fields between magnesium electrodes.[16] Although, the molecular weights of the obtained polymers were relatively low, this method has great potential as polysilane synthesis process, especially as a technique for industrial mass production.

3. Other polymerization procedures

Next two synthesis procedures were recent novel technics to get relatively low molecular weight polymers and origomeric molecules. These reactions seemed to get molecular weight and polymer silicon skeleton structure under good control.

Homogeneous dehydrogenative coupling

This is a method for the preparation of low molecular weight polysilane derivatives from substituted silanes using catalytic quantities of early-transition-metal complexes of titanium and zirconium.[17] The oligomers pre-

pared by this method are atactic, containing 10 to 20 silicon atoms, and are terminated by $SiRH_2$ groups. There are several efforts to generate higher molecular weight polymers using modified catalyst, which suggests the possibility of better stereochemical control in the polymerization. Even with only 10-20 silicon atoms, the current materials may have interesting electronic properties, and the presence of the reactive Si-H function should offer the possibility of introducing novel side chains by subsequent hydrosilylation.

Ring opening polymerization

Several recent reports suggest that certain substituted silane polymers are accessible by ring opening polymerization. The first reported study on the ring opening polymerization was reported by Matyjaszewski et al.[11] They described that the production of a high molecular weight polymer by the ring opening polymerization of octamethoxycyclotetrasilane. These techniques of polymerization have been applied to the synthesis of polysiloxanes, and obtained excellent results.

Other methods to prepare polysilane derivatives have been studied and reported. For example, anionic polymerization of the masked disilenes to obtain high molecular weight polysilanes has been studied by Sakamoto and co-workers.[18] On the other hand, the synthesis results of the cubic octasilicate Si_8R_8: octacilacubanes have been studied by Furukawa,[19] Matsumoto,[20] and Sekiguchi,[21] though these are not the preparation of polymeric materials.

1-4 Thermal Properties of Polysilanes

To date, many kinds of substitute polysilanes can be obtained. The difference in the substitution pattern of polysilanes gives a wide variety of the polymer properties. The products of these substituted polysilanes have glass transition temperature ranging from -76°C to above 120°C. Because of this range of the glass transition temperatures, the polymers themselves range from rubbery elastomers to hard, brittle solids. In general, the incorporation of aryl substituents tends to rise the polymer glass transition temperatures.

Substituted silane high polymers are, in many cases, thermally stable to temperature above 250°C. Some typical thermogravimetric analysis shows almost no weight loss at temperatures below 300°C. This thermal stability is based on the strengths of silicon-silicon bonds(80kcal/mol) and carbon-silicon bonds(90kcal/mol).[22] Although certain aryl substituted polysilanes such as polysilastylene and poly(methylphenylsilane) can apparently be melt cast without decomposition, the sterically hindered bisaryl derivatives undergo irreversible changes around 200°C that are not accompanied by significant weight loss. On the other hand, some symmetrically substituted poly(dialkylsilanes) such as poly(di-n-hexylsilane) thermally decompose with significant weight loss prior to melting.

1-5 Polymer Structure

Nowdays conformational studies of polysilanes show progress in the both theoretical and experimental approach. There are several kinds of theoretical approaches, for example, empirical force field,[23] semiempirical MINDO,[24] CNDO,[25] and ab initio.[26] Computed energy level of the molecular conformation suggests that most stable conformation is all-trans structure (180°twist) of the silicon backbone followed by the gauche structure (60°twist) at near the energy level. Further, computed barriers to internal rotation are also very low. Therefore, several factors, such as temperature, may cause the transition from one state to other. However, these theoretical calculations are limited only for the simple model structures, especially ab initio calculation is impossible for almost all actual polymers except for all hydrogen terminated polysilane. Thus, the conformations of the practically important, tractable polysilanes, which have long alkyl or aryl substituents on silicon, have not been reliably predicted by theory, although some trends are now apparent. Long substituents may cause side chain-side chain interactions, and the silicon backbone has only low torsional barriers. Thus, molecular conformation can be changed easily by substituents, and then, the conformations other than the usual all trans and all gauche will be important in these structures, for example, 7/3 helix structure.

For analysis of polymer microstructure of polysilanes, a number of ^{29}Si NMR studies using INEPT pulse sequences on soluble polysilane derivatives in solution have been reported.[27] According to these studies, broad and structured silicon resonances are observed for unsymmetrically alkyl- substituted homopolymers prepared by Wurtz coupling. It is characteristic of a random, atactic, distribution of stereocenters. However, the patterns of the resonances are apparently different for some polymers with aromatic substituents attached to the backbone, such as poly(methylpenylsilane). In the case of these polysilanes, the peak intensities within the silicon multiplets suggest a nonrandom collection of stereocenters in the polymers.

Infrared spectra for a wide variety of substituted polysilanes have been also measured, and many papers describe infrared spectra data.[28] Rabolt reported that according to IR and Raman spectroscopy data, both the side and main chains disordered at elevated temperatures in the case of poly(di-n-alkylsilane), and these polymers presented a disordering phase transition point at 40-50°C.[29]

Fluorescence and fluorescence excitation spectra give a lot of information of the backbone conformation and the electronic structure of grand state as well as UV absorption spectra.[30] Itoh determined the dependence of the relative fluorescence quantum yield of poly(dialkylsilane) on temperature, and suggested that

the energy transfer was occurring intramolecularly from helical to rodlike conformational segments.[31] Namely, the energy transfer yield and rate increase with decreasing temperature especially at the transition temperature, where the rodlike segment content increases sharply.

1-6 Electronic Structure

Unique electronic structure may be the most important reason why polysilane derivatives attract attention as engineering materials. Recently, polysilane's electronic structure has been investigated by the analogy of other silicon backbone materials. Here, such newly developed approaches will be introduced.

Polysilanes belongs to one category of silicon backbone materials which include silane origomers, silicon clusters and amorphous and crystalline silicones. However, these materials have been investigated independently in two different fields. Mostly, crystalline and amorphous silicones are studied in the field of solid-state physics, whereas polysilanes and related molecules are studied in the field of organosilicon chemistry. Application fields of these two categories of silicon backbone materials are also completely different until recently. For example hydrogeneted amorphous silicon and crystalline silicone are well known as typical two materials of the most useful semiconductors for electronic and optical devices, whereas polysilanes have been investigated for application as a precursor of SiC ceramics, UV photoresist, etc. However, polysilanes and related materials have not been effectively applied for electronic materials bringing out their potential of unique electronic structure.

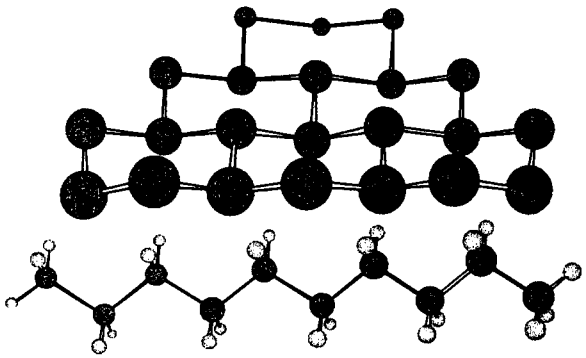

Figure 1-1. Schematic view of an unit plane in crystalline silicon and a silicon skeleton in perhydrogenated polysilane.

In 1983, Wolford et al. discovered a new type of hydrogenated amorphous silicon, called polysilane alloy, which include a large number of silicon hydride polymers.[32] Their structures were studied by Matsumoto et al., and it was clarified that polysilane alloys are materials with intermediate properties between the amorphous silicon and organosilane polymers.[33] Maybe this was the first time when polysilanes encountered to the field of solid state physics, and they were recognized potential electronic materials. To date, the polysilane derivatives have been treated as an one-dimentional analogue of the silicon catenated materials which are the most practical semiconducting materials.[34]

The crystalline Si lattice structure is the same as that of diamond. The bonding between Si atoms is by σ bonds, with s electrons delocalized over whole lattice. A unit plane of this silicon crystal lattice is illustrated in the figure 1-1. A unit plane consists of unit chains, and the chains are formed by bonding unit dimmers along (110) or (101) crystal axis. Sub lattices cut from the crystalline silicon lattice can be described by using this unit structure. As shown in fig. 1-1, a polysilane has a skeleton which is cut from silicon crystal unit lattice, and a network polymer has just a structure of unit plane. This dimensional consideration suggests that the electronic structure of any silicon backbone materials can be treated by same procedure of calculation.

Band gap energies of zero, one, two and three dimensional material were estimated by Takeda et al. as an analogy of silicon crystal.[35] Disilane which is a typical zero dimensional material has the energy of 6.5 eV, although it is not suitable to call 'band gap energy', and polysilane (one dimension), network polysilane or polysilane alloy (two dimensional) and crystalline silicon (three dimensional) have the band gap energies of 4eV, 2.5eV and 1.1eV, respectively.

The electronic structure of silicon based polymers are determined basically from the backbone dimension as discussed before. However, in addition, two important factors must be considered in determining accurate and detailed structures. One is side chain effects and the other is backbone conformation effects. The band gap energy (Eg) is the difference between the edges of the conduction band and valence band. The effective mass of electrons and holes are estimated by parabolic approximation; a large curvature corresponds to a small effective mass and a small curvature corresponds to a large mass. With this band concept, light absorption and luminescence are interpreted as follows. Namely, light is absorbed by the transition from valence band to conduction band. Therefore, the broadening of the absorption spectrum originates basically from one dimensionality of the joint density of states, which is described by $1/(E-Eg)^{1/2}$. Excited electrons and holes relax to the bottom of the band and then recombine radiatively. Thus, the photoluminescence spectra are very sharpened. The energy difference between two peaks is called the Stokes shift. Polysilane's band structures are calculated by a semiempirical LCAO method.[35] The ab initio method seems not to be able to exactly estimate absolute energy level of the excited states, that is the conduction band. According to the data calculated by Mintmire [36] and Matsumoto,[26] hydrogenated polysilane's band edge states with different parities exist at G point (k=0), which shows that the polysilane is a direct semiconductor, and further the band gap energy is 4.5eV. Both valence and conduction band edge states are composed mainly of skeleton Si atomic orbitals. The valence band edge is the σ bonding state of the skeleton

Si $3p_x$ orbitals, and the conduction band edge is the σ^* antibonding state of the skeleton Si 3s atomic orbital.

The same groups reported also substitution effects on polysilane band structure. The substitution effects of alkyl side chains have two characteristics : the unchanged state of the direct-type band structure and the systematic change in the band gap value and the position of the pseudo π band, which are related to the electron donating property of alkyl side chains. The summary of their calculation data is that the band gap tends to be compressed when larger alkyl groups are substituted, but that the amount of reduction is not significant because of weak electronic contribution from the side chains. On the other hand, substitution of aryl side chains results in a different band structure. Effects of directly attached phenyl groups on polysilane band structure were also investigated theoretically by Matsumoto[37] and experimentally by Diaz,[38] Loubriel[39] and so on. Theoretical calculation data suggests the existence of the states localized at phenyl side chains and the σ–π interaction between delocalized skeleton σ band and localized π states. Poly(methylphenylsilane) ; PMPS has 3.9 eV band gap energy caluculated and the caluculation study predicts next substitution effects.

Skeleton-sidechain interaction due to π-like coupling results in σ–π band mixing between the skeleton Si $3p_x$ and side chain phenyl p HOMO states. The symmetric π HOMO can mix with the delocalized σ valence band, resulting in the formation of two delocalized σ band. The asymmetry of the other π HOMO states cancels this σ–π mixing effect, and the obtained states remains strongly localized in the individual phenyl groups. On the other hand, σ^*-π^* band mixing does not take place because of the orbital symmetry. π^* states are localized at phenyl substituents and thus are not dispersed.

This substitution effects of aryl (phenyl) groups were confirmed by experimental approaches. Diaz measured the oxidation potentials of a variety of alkyl-substituted and aryl-substituted polysilanes. In spite of oxidation potential between 1.4 V and 1.6 V for dialkylpolysilane, the direct bonding of an atyl substituents to the backbone as in PMPS reduces the oxidation potential by 0.4 V to 1.0 V in accordance with the predicted strong destabilization of silicon backbone HOMO through interaction with a substituent π orbital. The destabilization of the HOMO is also consistent with the red shifts of UV absorption bands observed for phenyl substituted polysilane derivatives. Further, Loubriel have studied the photoelectron spectra of a number of polysilanes, and concluded that while alkyl substituents cause little perturbation of the backbone silicon orbitals, significant orbital interactions result from the appendant aryl substituents such as phenyl or naphthyl to backbone.

1-7 Radiations and Polysilanes

Polysilanes and their photolysis have attracted great interest because of their potential use as resist materials in the field of microlithography. Actually, Trefonas et al.,[40] Zeigler et al.,[41] Hofer et al.[42] and Miller et al.[43] reported that molecular weight reduction and photovolatilization was caused by UV light exposures for a variety of polysilanes. Based on the applicational view, silicon containing polymers and their reactions induced by several kinds of radiations have been widely investigated to date, for instance, electron beam induced reactions which have played a significant role in two layer resist processes,[44] that for ion beams which have been recieving renews interest as a candidate for the manufacture of semiconductors in the future,[45] and the reactions upoun irradiation to γ-rays to elucidate the basic mechanisms of polysilanes for radiation sources.[46]

Radiation induced reactions have been revealed to be the useful tools not only for the resist systems but for the investigation of electronic structures of polysilanes, especially of their σ-conjugated system. They can promote the ionic species of polysilanes very effectively. Ionic species of Si based molecules have been firstly studied for cyclic and linear polysilanes.[47] Cyclic origosilanes form radical anions by reduction with alkali metal, and also form radical cations by oxidation with $AlCl_3$. The ionic species have an unpaired electron delocalized over the silicon skeleton. This implied that the excess electrons could be mobile along Si conjugated chains. However the way of the investigation had unfortunately been very limited, and there had been no way for the chaged polymer molecules in the chemical processes. Only the few studies had been reported until the period when the radiation chamical processes had given the breakthrough to the investigation, although the their energy states should be important not only for the nature of σ-conjugated system but for their physical properties because the radical ions precisely simulated the polysilane molecules which was just conducting the charge carriers on their skeleton. Charged molecules of polysilanes were produced by a pulse radiolysis technique, and displayed a transient absorption band at near UV region with very high extinction coefficients.[48] The transient spectra suggest that an excess electron or a hole is delocalized over a Si segment in linear polysilanes. This indicates that the conjugated molecular orbital is responsible for the absorption spectra of the ionic species, and the similar experiments have been extensively carried out for σ-conjugated molecules including origosilanes and origogermanes.[49] Charged radicals of network polysilanes and polygermanes were also investigated by the technique.[50] The spectroscopy suggested the localized states of excess electrons on the network Si and Ge skeletons. These experimental results predicts that the degree of excess electron delocalization, hence, the mobility of charge carriers will be very sensitive to the backbone structures in the polysilane derivatives.

Almost all the studies on the charged σ-conjugated molecules have been carried out to date by using pulse radiolysis technique as discussed above. Especially, the technique has been only the way for the spectroscopic study on charged radicals of polymeric materials, and becoming the standard technique in the field.

1-8 Summary

Polysilane derivatives contain only silicon atoms catenated together to form a linear backbone. Silicon, among elements, is almost unique in its ability to homocatenate and form stable long linear chains in a manner similar to carbon, which forms an almost limitless variety of carbon backbone polymers. Stable silicon backbone polymers have been prepared that contain up to a few tens thousands monomer units in a single chain. Recently, a number of soluble high molecular weight polygermane derivatives have also been reported.

It has been recognized that the properties of silicon catenation differed significantly from carbon catenation. This was manifested most dramatically by their curious electronic spectra, which suggested significant interaction and electronic delocalization within the σ-bonded skeleton. Theoretical and experimental approaches have revealed the nature of the 'σ-conjugation system', and now, a completely different concept which is quoted from the field of solid state physics is applied for the analysis of the several unique properties of polysilanes.

Chapter 1 Reference

[1] Kipping, F. S. J. Chem. Soc. 1921, 119, 830.
[2] Kipping, F. S. J. Chem. Soc. 1924, 125, 2291.
[3] Burkhard, C. J. Am. Chem. Soc. 1949, 71, 963.
[4] Yajima, S.; Hyashi, J.; Omori, M. J. Am. Ceram. Soc. 1976, 59, 324.
[5] Wesson, J. P.; Williams, T. C. J. Polym. Sci., Polym. Chem. Ed. 1979, 17, 2833
[6] Wesson, J. P.; Williams, T. C. J. Polym. Sci., Polym. Chem. Ed. 1980, 18, 959.
[7] for his review, West, R. In Chemistry of Organic Silicon Compounds; Patai, S., Rapport, Z., Eds.; Wiley: New York, 1989, pp 1207.
[8] Trujillo, R. E. J. Organomet. Chem. 1980, 198, C27.
[9] for their review, Miller, R. D.; Hofer, D.; McKean, D. R.; Willson, C. G.; West, R.; Trefonas, P. T. In materials for microlithography; ACS Synposium Series 266; Thompson, L. F., Willson, C. G., Frechet, J. M. J., Eds.; American Chemical Society: Washington, DC, 1984; Chapter 14.
[10] for their review, Zeigler, J. M,; Schilling, F. C.; Bovey, F. A.; Lovinger, A. J. In Silicon Based Polymer Science; Advances in Chemistry Series 224; Zeigler, J. M., Fearon, F. W., Eds.; American Chemical Society: Washington, DC, 1990; Chapter 28.
[11] Matyjaszewski, K.; Chen, Y. L.; Kim, H. K. In Inorganic, and Organometallic Polymers; ACS Symposium Series 360; Zeldin, M., Wynne, K. J., Allcock, H. R., Eds.; American Chemical Society: Washington, DC, 1988; Chapter 6.
[12] for example, Pitt, C. G. In Homoatomic Rings, Chains, and Macromolecules of Main Group Elements; Edited by Rheingold, A. L.; Elsevier: Amsterdam. 1977.
[13] Su, W. P.; Schrieffer, J. R.; Heeger, A. J. *Phys. Rev. Lett.* 1979, **58**, 937.: Rice, M. J. *Phys. Lett.* 1979, **A71**, 152.
[14] Kim. H. K.; Matyjaszewski, K. J. Am. Chem. Soc. 1988, 110, 3321.
[15] Hengge, E.; Firgo, H. J. Organomet. Chem. 1981, 212, 155.
[16] Hengge, E.; Litsher, G. Angew. Chem., Int. Ed. Engl. 1976, 15, 370.
[17] Aitken, C. T.; Harrod, J. F.; Samuel, E. J. Am. Chem. Soc. 1986, 108, 4059.
[18] Sakamoto, K.; Obsts, K.; Hirata, H.; Nakajima, M.; Sakurai, H. J. Am. Chem. Soc. 1989, 111, 7641.
[19] Furukawa, K.; Fujino, M.; Matsumoto, N Appl. Phys. Lett. 60, 1992, 2744.
[20] Matsumoto, H. et al. J. Chem. Soc. Chem. Commun. 1988, 1083.
[21] Sekiguchi, A. et al. J. Am. Chem. Soc. 114, 1992, 6291.
[22] Walsh, R. Acc. Chem. res. 1981, 14, 246.
[23] Damewod, J. R.; West, R. Macromolecules 1985,18, 159.: Welsh, W. J.; DeBolt, L.; Mark, J. E. Macromolecules 1986, 19, 2978.
[24] Verwoerd, W. S. J. Comput. Chem. 1982, 3, 445.
[25] Takeda, K.; Matsumoto, N.; Fukuchi, M. Phys. Rev. B 1984, 30, 5871.
[26] Matsumoto, N.; Teramae, H. J. Am. Chem. Soc. 1991, 113, 4481.
[27] Maxka, J.; Mitter, F. K.; Powell, D. R.; West, R. Organomet. 1991, 10, 660.
[28] Todesco, R. V.; Basheer, R. J. Polym. Sci., Polym. Chem. Ed. 1986, 24, 1943.: Zhang, X. H.; West, R. J. Polym. Sci., Polym. Chem. Ed. 1984, 22, 159.: Fujino, M.; Matsumoto, N.; Ban, H.; Sukegawa, K. J. J. Polym. Sci., Polym. Lett. Ed. 1988, 26, 109.: Cui, C. X.; Kertesz, M. Macromolecules 1992, 25, 1103.
[29] Rabolt, J. F.; Hofer, D.; Miller, R. D.; Fickes, G. N. Macromolecules 1986, 19, 611.
[30] for example, Klinggensmith, K. A.; Downing, J. W.; Miller, R. D.; Michl, J. J. Am. Chem. Soc. 1986, 108, 7438.
[31] Ito, O.; Terazima, M.; Azumi, T. J. Am. Chem. Soc. 1990, 112, 444.: Ito, O.; Terazima, M.; Azumi,; Matsumoto, N.; Takeda, K.; Fujino, M. Macromolecules 1989, 22, 1718.
[32] Wolford, D. J.; Reimer, J. A.; Scott, B. A. Appl. Phys. Lett. 1983, 42, 369.
[33] Matsumoto, N.; Furukawa, S.; Takeda, K. Solid State Commun. 1985, 55, 881.
[34] Brus, L. J. Phys. Chem. 98, 1994, 3575.
[35] Takeda, K.; Teramae, H.; Matsumoto, N. J. Am. Chem. Soc. 1986, 108, 8186.
[36] Mintmire, J. W.; Oritz, J. V. Macromolecules 1088, 21, 1189.
[37] for a review, Matsumoto, N.; Takeda, K.; Teramae, H.; Fujino, M. In Silicon Based Polymer Science;

Advances in Chemistry Series 224; Zeigler, J. M., Fearon, F. W., Eds.; American Chemical Society: Washington, DC, 1990; Chapter 28.

[38] Diaz, A. F.; Miller, R. D. J. Electrochem. Soc. 1985, 132, 834.

[39] Loubriel, D.; Zeigler, J. M. Phys. Rev. B 1986, 33, 4203.

[40] Trefonas, P.; West, R.; Miller, R.D.; Hofer, D. J. Polym. Sci., Polym. Lett. Ed. 1983, 21, 823.

[41] Zeigler, J.M.; Harrah, L.A.; Johnson, A.W. Proc. SPIE 1985, 539, 166.

[42] Hofer, D. C.; Miller, R. D.; Willson, C. G. Proc. SPIE 1984, 469, 16.

[43] for a review, Miller, R. D.; Michl, J. Chem. Rev. 1989, 89, 1359

[44] Bowden, M. J. ACS Symposium Series 266; American Chemical Society; Washington DC; 1984; p.39.

[45] Taylor, G.N.; Wolf, W.W.; Moran, J.M. J. Vac. Sci. Technol. 1981, 19, 872.

[46] Miller, R.D. Advanced in Chemistry Series 224; American Chemical Society; Washington DC; 1990; p.413.

[47] West, R.; Carberry, E. *Science* 1975, **189**, 179.; Carberry, E.; West, R.; Glass, G. E. *J. Am. Chem. Soc.* 1969, **91**, 5446.; Kira, M.; Bock, H.; Hengge, R. *J. Organomet. Chem.* 1979, **164**, 277.

[48] Ban, H.; Sukegawa, K.; Tagawa, S. *Macromolecules* 1987, **20**, 1775; Ban, H.; Sukegawa, K.; Tagawa, S. *Macromolecules* 1988, **21**, 45; Ban, H.; Tanaka, A.; Hayashi, N.; Tagawa, S.; Tabata, Y. *Radiat. Phys. Chem.* 1989, **34**, 587.

[49] Mochida, K.; Kuwano, N.; Nagao, H.; Seki, S.; Yoshida, Y.; S. Tagawa *Inorg. Chem. Commun.* 1999, **2**, 238.; Mochida, K.; Kuwano, N.; Nagao, H.; Seki, S.; Yoshida, Y.; S. Tagawa *Chem. Lett.* 1999, 3.; Mochida, K.; Hata, R.; Chiba, H.; Seki, S.; Yoshida, Y.; S. Tagawa *Chem. Lett.* 1998, 263.

[50] Watanabe, A.; Matsuda, M.; Yoshida, Y.; Tagawa, S. ACS Symposium Series 579; American Chemical Society; Washington DC; 1994; p.408.

Chapter 2 Synthesis of Polysilane Derivatives

Recently, several synthesis routes have been developed because of applicational needs in various fields, as described in the introduction. Nowdays the trend of polysilane synthesis studies may be roughly divided into two categories. One category intends to control molecular weights, distribution, mainchain configuration, defects structure, etc, i. e. to control directly its structure of the polymer backbone. The other approach is trying to connect various kind of side chain groups to polymer backbone, and change polymer properties indirectly utilizing the corelation between substituents and main chain. Here, the synthesis studies of polysilanes have been related to the first category. In the present chapter, general procedures and tips of the polymer synthesis are introduced with several experimental results in this study.

2-1 Introduction

As already mentioned, there are two currents of the polysilane syntesis studies. The first approach, which aims to change the main chain structure of the polymers, may be concluded to be the effort of the dimention control. Since the early stage of the polysilane studies, silane monomer, origomer and polymers have been treated as analogical materials of silicon crystal and amorphas semiconductor. Therefore, the electronic structure of the polysilanes has been analized by a model of electronic band structure, which is a concept of solid state physics. Matsumoto et. al. reported the reduced band gap energy with systematically dimention controlled polysilanes[1], that is, monosilane and disilane being treated as zero dimentional materials, polysilane as one, network structure polysilane (this polymer has many blanching and crosslinking structure) as two and amorphas and crystal silicons as three dimentional material. These polysilanes and network polysilanes are synthesized by similar route, [2] Wurtz coupling, with different monomers. Whereas Wurtz coupling reaction is most widely applied for polysilane synthesis in these days, it can poorly control the polymer molecular weight and distribution. Further, from the view point of engineering application, the electronic structure in solid state is very important. However, previous studies in solid state polysilane, especially polymer film, were not so many, because the polymers synthesized in conventional conditions lacked film-forming properties which is closely related to polymer molecular weights. Generally, high molecular weight polymer material shows good film-forming properties. Therefore, the auhtor's synthesis intended to get mainly high molecular weight of the polymer. As a result, the author succeeded to obtain better film forming high polymers by means of the modified Wurtz coupling. In this chapter, such methods and results of modified Wurtz coupling reaction will be described.

2-2 General Procedures

At first, the synthsis process of the conventional Wurtz coupling must be mentioned. Figure 2-1 shows schematic procedure of the polymarization. In many cases, sodium metal is used for desalting regant. Because the surface of sodium metal is inactive at room temperature, it is needed to maintain system temperature above the melting point of sodium (92°C) during reaction proceeding. Since the temperature of this reflux system is settled by boiling point of the reflux solvent, available solvents are limited (inert for sodium and polymers, boiling point higher than sodium, etc). Considering these limmitations, toluene was used for the reflux solvent. On the other hand, the 'early' polysilanes had poor solubility, which is described in the former chapter, and generally polysilanes and origosilanes do not show good solubility especially in non polar solvent such as alkanes. For that reason, an idea of utilization of alkanes as reflux solvent has not come out. However, there are alkanes having various boiling points and viscosities with different molecular weights, and they are very easy for treatment at high temperature. These characteristics of alkanes are suitable for the delicate reaction control, though it is possible that polymers precipitate with proceeding polymerization reaction, and as a consequence is termination of polymerization reaction.

Table 2-1. Synthesis results of PMPS by Wurtz coupling in a variety of solvents

Solvent	T_r [a] (°C)	t_r [b](min)	c[c]	Mw[d]	yield (%)
Toluene	110	60	5g / 100 ml	9000	32
Toluene	110	240	5g / 100 ml	13000	45
Octane	140	180	5g / 100 ml	19000	25
Decane	155	180	5g / 100 ml	24000	21
Undecane	185	180	5g / 100 ml	40000	55
Dodecane	195	180	5g / 100 ml	56000	34

[a] T_r, reaction temperature; [b] t_r, reaction time; [c] c, concentration of monomers; [d] Mw, weight average molecular weight.

Poly(methylphenylsilane) has phenyl substituents, that is intermolecule π-conjugation system. It was already pointed out by Takeda et al. with semiempilical calculation method (CNDO) that π*-orbitals in the phenyl substituent can corelate to sigma-conjugation system of polymer main chain. This colelation is very interesting as a material for electronics. Therefore, this experiment attempted to obtain poly(methylphenylsilane) ; PMPS with better film forming properties.

It has already been known that PMPS shows the thermal degradation phenomena at the temperature above 250°C even in a deaerated atmosphere. Based on this data of PMPS, several kinds of solvents which have their boiling point between 92°C and 250°C were choozen here, toluene (b. p. = 110°C), xylene (145°C), octane (126°C), undecane (180°C) and dodecane (210°C). The starting monomer was dichloromethylphenylsilane for all kind of the solvents, and this monomer was made by Shinetsu Chemical Corperation. Alkanes could not compeletely dissolve synthesized polymers after reaction being finished. Then there are two routes to obtain solid polysilane. One is to precipitate the polymers with adding methyl- or ethylalchols followed by filteration and washing by water (separating sodium chrolide), and the other is to completely disolve the polymers by additing tetrahydrofran (THF), and precipetate them after filteration. The latter method was used here because it has less possibility of remaining sodium chloride than the former. Argon gas flowing the whole system contain oxigen less than 0.1 ppm, and all kinds of the solvents were purified by two times distillization. Therefore the reaction system contamination by the gas and the solvent can be neglected.

Polymer molecular weights were measured by gel permation chromatography (GPC) system that is a product of Shimadzu Corporation. The values of Mw, Mn and the molecular weight distribution were calibrated by polystylene standards.

2-3 Synthesis Results

Table 2-1 summerizes weight average molecular weights (Mw) of the syntesized PMPS together with the reaction condition for each solvent. At first, it is clear that the Mw values of the obtained polymers become larger with increasing reaction temperature. The surface of the dispersed (melted) sodium metal must be highly activated at high temperature, and then, the dechlorination reaction of one silicon segment seems to be hardly terminated by making dungling bonds. There are two possibilities of the termination process of the reaction, that are hydrogenated chain ends and chlorinated chain ends. In these considerable dungling bonds, paticuraly reaction efficiency of chloride chain end can increase with raising temperature. Further, in the highly heated system, movement of each molecule is predicted to become larger in solution. Naturally, mobile molecular segments are more likely to encounter each other at higher temperature, and as a result, the reaction between segments seems to contribute to produce large molecules.

A similar model of the polymerization can be considered from the results of molecular weight distribution changes that are shown in Figure 2-2. Generally, most polysilane synthesis yield materials with polymodal (bimodal in the case of PMPS) molecular weight distribution. For example, in the polymerization of PMPS using toluene, the majour product of the polymer ranges at Mw = 3000 - 10000 (polystylene caliblation standard) with its percentage of 90-95, and the rest polymer is distributed around Mw = 300000 - 1000000. In spite of this fact, all polymers obtained using alkanes have different molecular weight distribution in comparison with the case of toluene. The yields of higher molecular weight compornent increase in the heated system, though the peak itself seems to be reduced to lower molecular weight.

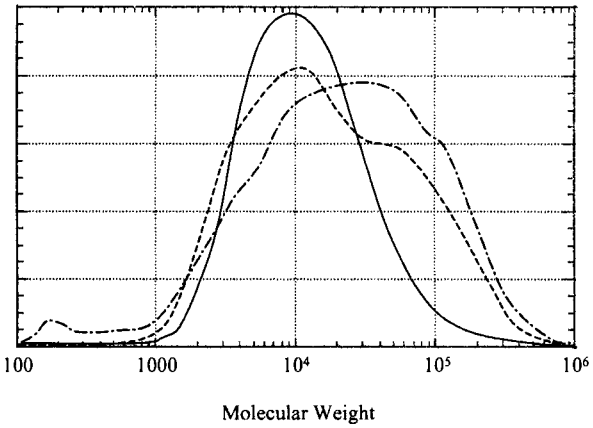

Figure 2-1. Molecular weight distribution of PMPS obtained in a variety of reaction conditions. A solid line denotes the distribution of PMPS obtained in toluene, dashed: in undecane, dot-dashed: in dodecane.

For these phenomena of PMPS polymerization, Zeigler[3] and Miller[4] proposed a next model. Their model rationalizes the obserbed effects in terms of the effective monomer concentration at the sodium interface. This in turn is ditermined by the rate of diffusion of monomer to the sodium surface, which depends in part on whether the surface is predomonantely open and readily accessible or is covered with growing polymers. After a finate initiation period, dispersed particles of sodium are undoubtedly covered with growing polymers. In a good solvent, the chains are predominantely extended permitting relatively unimpeded access of the monomer to sodium surface, and then, a large number of comparatively low molwcular weight polymers can be produced. In a poor solvent, the attached polymer chains tend to collapse to the surface forcing monomer to diffuse through the growing chain to reach the surface of sodium, therefore most of the diffused and reached monomers may contribute to further growing of polymer chain. However, if the solvent is too poor, the polymer collapses upon itself and precipitates, thus limiting the molecular weight in this fashon. These groups also investigated the effects of additives on polymerization yields.[5] They reported that addition of diglyme or polyether improve polymer yields for the polymerization of

PMPS, poly(di-n-hexylsilane);PDHS and poly(n-dodecylsilane). This effect indicaes that polymerization reaction of these polysilanes is mainly promoted by silyl anions because such regants act on silyl cations with sequestering effects. This model of the polymerization mechanism also makes good explanation for the result of high polymer generation at higer monomer concentration as shown in table 2-1. In the case of polymerization promoted only by radical anion, it is natural that high monomer concentration induces the yield of high mlecular weight polymers.

2-4 Summary

All kinds of alkanes (Octane, Undecane and Dodecane) showed good nature as reflux solvent for the polymerization of dichloromethylphenylsilane monomer with Wurtz coupling method. Further, high molecular weight polymers could be obtained by the alkanes, and their weight average molecular weights became larger with increase of boiling point of the alkanes, that is, reaction temperature. With the conventional Wurtz coupling method (toluene reflux solvent), it was possible to produce polysilane high polymers at higher monomer concentration.It should be noted that all polysilanes obtained by these modified Wurtz coupling methods have good film forming properties for any processes which are spin coating, solvent cast, bar coating, etc.

Chapter 2 Reference

[1] Matsumoto, N.; Takeda, K.; Teramae, H.; Fujino, M. In Silicon Based Polymer Science; ACS Symposium Series 224; Zeigler, J. M., Fearon, F. W., Eds.; American Chemical Society: Wachington, DC, 1990; Chapter 28.

[2] Furukawa, K.; Fujino, M.; Matsumoto, N. Macromolecules 1990, 23, 3423.: Bianconi, P. A.; Weidman, T. D. J. Am. Chem. Soc. 1988, 110, 2342.: Watanabe, A. Macromolecules 1993, 26, 2111.

[3] Zeigler, J. M.; Polym. Prepr. 1986, 27, 109.: Zeigler, J. M.; Harah, L. A.; Johnson, A. W. Polym. Prepr. 1987, 28, 424.

[4] Miller, R. D.; Michl, J. Chem. Rev. 1989, 89, 1359.

[5] for a summary, Miller, R. D.; Hofer, D.; McKean, D. R.; Willson, C. G.; West, R.; Trefonas, P. T. In materials for microlithography; ACS Synposium Series 266; Thompson, L. F., Willson, C. G., Frechet, J. M. J., Eds.; American Chemical Society: Washington, DC, 1984; Chapter 14.

Chapter 3 Polysilanes with Structural Defects

To date, experimental results and theoretical calculations on polysilanes and related materials suggested that their conjugated σ bondings in silicon skeleton, called σ conjugated system strongly contributed the physical properties of these materials such as photoconductivity, nonlinear optical properties, low dimensional semiconduction phenomenon and so on. The theoretical background of the concept of σ-conjugated system is introduced in this section.

3-1 Basis of σ-conjugated Systems

Since last decade, several kinds of electronic conductive organic materials have been discovered, and especially conductive polymers have been vigorously investigated because of easy synthesis and processing of polymer materials. Most of typical electronic conductive polymers, for example polyacetylene were unsaturated carbon backbone polymers which have a σ conjugated system along polymer backbone until recently, and the electron and hole transport mechanism of such σ conjugated materials is now becoming clear with efforts of theoretical and experimental approaches. One electron theory model that stress electron-lattice coupling have been successful in interpreting the observed solid state properties of polyacetylene. The model suggests that charge carriers; holes and electrons on polyacetylene main chain crook lattice structure around themselves and stabilized in the potential bottom followed by increase of their effective mass, which is so-called polaron state.

It is already known that polysilanes also have similar electronic structure and properties as the unsaturated carbon-backbone polymers whereas polysilanes' main chain is completely saturated. From the view point of carbon conjugated polymer analogues, the one electron theory model; polaron model were extended and applied for silicon conjugated polymers by Rice at 1987 for the first time.[1] Their model predicted the presence of charge-neutral polaron and bipolaron states on polysilanes with localized intragap levels and infrared vibrational characteristics which are similar to those found in carbon conjugated polymers with non-degenerate (structural) ground states (by Brazovski). Further they estimated that the width of the neutral polaron is only a few bond length, thus providing a specific mechanism for energy localization. Next, theoretical prospects of the polaron model of a polysilane will be discussed.

Polaron states on polysilanes

The microscopic model is defined by the Hamiltonian as follows.

$$\hat{H} = 2\Delta_0 N + \sum_j \left(Br_j^{-1} + \frac{1}{2} M R_j^2 \right) - \Delta \sum_{j,\sigma} \left(a_{j,\sigma}^* b_{j-1,\sigma}^* + H.c. \right) - \sum_{j,\sigma} V_{j,j-1} \left(a_{j,\sigma}^* b_{j-1,\sigma}^* + H.c. \right) \quad (3\text{-}1\text{-}1)$$

It describes N (number of atoms) A atoms of mass M whose instantaneous position and velocities in a trans chain backbone (along x axis) are denoted by R_j and dR_j/dt, respectively (j=1,2,-,N). A denotes a Si atom, and the formula of the monomer unit of the polymer is taken to be SIR_2. It is assumed that the electronic states of the backbone are derived from interaction of atom Si sp3 like orbitals, a orbital; $\Psi_a(x\text{-}R_j)$ and b orbital; $\Psi_b(x\text{-}R_j\text{-}1)$, which point along the same Si-Si bond. The other atomic hybrid orbitals, pointing along Si-R bonds, are assumed to be effectively decoupled from the a and b orbitals on account of strong bonding with the side chain groups R. The matrix element describing the interaction of the a and b orbitals is denoted by $V_{j,j-1}$ and taken to have the specific form $V_{j,j-1}=D_{rj}^{-2}$, where D is a constant and $r_j=|R_j-R_{j-1}|$. At the same time, a repulsive interaction $U_j=Br_j^{-1}$ is assumed to exist between the same pair of atoms, j and j-1, where B and l are constants. Together, $V_{j,j-1}$ and U_j microscopically define the electron lattice interaction. $a_{j,\sigma}$ and $b_{j,\sigma}$ are fermion operators which create an electron with spin s in the a and b orbitals respectively of the atom j. Δ denotes the matrix element between a and b orbitals on the same atomic site and $4\Delta_0$ denotes the atomic sp^3 promotion energy. The energies in an equation using Hamiltonian (3-1-1) are measured relative to the atomic energies and there is one electron per orbital. Apart from the crucial detail that the matrix element $V_{j,j-1}$ couples the electrons to the instaneous positions of the Si atoms, the electronic part of the Hamiltonian is essentially a Sandorfy C model suggested by Pitt at 1977.[2]

The ground state of the equation based on Hamiltonian (3-1-1) is that of a covalent semiconductor with the bonds of equal length r and an electron energy spectrum e_k given by next equation,

$$\varepsilon_k - \Delta_0 = \pm\left[V^2(r) + \Delta^2 + 2V(r)\Delta\cos(ka)\right]^{1/2} \equiv \pm E_k \quad (3\text{-}1\text{-}2)$$

Here, $V(r) = +D/r^2$, $2a=2r\sin\theta$ is the period of the trans chain, 2θ is the tetrahedral bond angle, and the allowed wave vector k are defined in the extended zone $-\pi \le ka < \pi$. The covalent energy gap, Eg, is just equal to $2[V(r) - \Delta]=2a$. If $\Delta \neq 0$, the bonds become coupled and the charge delocalizes from them toward the aromatic sites. Δ is a parameter which specifies the degree of delocalization of a pair of electrons in a local band. Minimizing the total

energy E(r) per bond with respect to r, the equilibrium bond length r_0 is able to be fixed as next equation,

$$\frac{B}{r_0^l} = \frac{4V}{l(N-l)} \sum_k \frac{W_k}{E_k} \tag{3-1-3}$$

and it reads to the result of

$$E_b = 2\Delta_0 - \frac{2}{l(N-l)} \sum_k E_k \left(1 - \frac{2VW_k}{lE_k^2} \right) \tag{3-1-4}$$

for the binding energy $E_b=E(r_0)$ per bond, where $W_k=V+\Delta\cos(ka)$ when $V=V(r_0)$. Similarly, $K(r)=\partial^2 E/\partial r^2$ may be evaluated to give

$$K = \frac{2(l-2)\beta}{3(N-l)} \sum_k W_k E_k^{-1} - \frac{2\gamma^2}{N-l} \sum_k \Delta_k^2 E_k^3 . \tag{3-1-5}$$

This is the bond stretch constant $K=K(r_0)$, where $\Delta_k=\Delta\sin(ka)$, and $-\gamma$ and β are respectively the first and second derivatives of V(r) evaluated at $r=r_0$. The frequency of the transverse optical (TO) phonon of the polymer is $\omega_{TO}=(4K/M)^{1/2}\cos\theta$. The sums in eqations (3-1-3), (3-1-4), and (3-1-5) are easily evaluated in terms of elliptic functions. Together with the formula for Eg they may be used in principle, to determine the four microscopic parameters B, *l*, D and Δ, from the experimentally observed values of r_0, E_b, K and Eg. A set of parameters that have been obtained in this way is $V=D/r_0^2=3.4$eV, D=1.3eV, l=6.2eV and $B/r_0^l=2$eV reported by Rice in 1987.[3] As already mentioned in the chapter 1, ground state band structure that are much more realistic than the band structure described by this simplified model have been calculated by Takeda, and it should be mentioned in comparison that their data also show a correlation between the value of the bandgap energy and the nature of the pendant group and assess the extent to which the backbone states mix with those of the side chains. However, it should be appreciated that these more realistic band states are no less unstable towards polaron formation than the simpler band states considered here.

Here, theoretical basics of polysilane band structure are discussed above. Next, the author will consider the states available in the polymer for the addition or excitation of electrons or holes. In such case, calculational treatment, for example calculated ground state band structures mentioned above, is limited and very difficult for complex systems such as substituted polysilanes. However the simplified model can be applied for polaron and bipolaron model of polysilane's silicon skeleton caused by electron phonon coupling. A polaron and bipolaron model solution has been already obtained by Abkowitz,[4] and the procedure will be discussed.

Because of the nature of the ground state it is supposed that polysilane molecules are relaxed by polaron formation that involves bond length relaxation. If the author requires the latter to leave the length of the polymer unchanged, the author is led to consider a static displacement pattern of the form of a TO phonon, that is $y_j=(-1)^j(u_j/2\cos\theta)$, where y_j denotes the displacement in the y direction of the j th atom from its ground state equilibrium position R_j^0. If the bond relaxation amplitude u_j is sufficiently small and only slowly varying over interatomic distances, it is possible to expand Hamiltonian (3-1-1) about $\{R_j^0\}$ and express the orbital amplitudes for electronic states with levels e_n close to the gap edges as $a_{j,n}=(-1)^j A_n(x)$ and $b_{n,j}=-(-1)^j B_n(x)$, where x denotes an arbitrary point along the polymer axis in continuum description $ja\rightarrow x$. The electronic states and $u_j=u(x)$ are then found to be determined by the simultaneous solution of

$$e_n A_n(x) = Q_-(x) B_n(x)$$
$$e_n B_n(x) = Q_-(x) A_n(x)$$
$$w(x) = -\frac{2\gamma^2}{K_0} \sum_n \left[p_n(x) - p_n(\infty) \right] \tag{3-1-6a,b,c}$$

where $Q_\pm(x)$ are the operator given by next formula

$$Q_\pm(x) = -a - (a^2/2)V\nabla_x^2 + v(x) \pm V_a \nabla_x \tag{3-1-7}$$

and $p_n(x)$ are the local bond orders given by

$$p_n(x) = -\frac{\left[A_n^*(x) B_n(x) + c.c. \right]}{2} \tag{3-1-8}$$

Equation (6c) is the potential $w(x) = \gamma u(x)$ felt by the electrons as a result of u(x), Vn is the occupation of the n th level, and K_0 is the unscreened force constant given by the first term of eqn. (3-1-5). A_n and B_n are normalized according to

$$\int (dx/a) \left[|A_n(x)|^2 + |B_n(x)|^2 \right] = 1 \tag{3-1-9}$$

and the total energy of the polymer E is expressed by

$$E = \sum_n v_n \varepsilon_n + \frac{K_0}{2} \int \frac{dx}{a} u(x)^2 \tag{3-1-10}$$

where in eqations (3-1-9) and (3-1-10) the integral extends over $x = N/a \rightarrow$ infinity, and the levels en are measured relative to Δ_0. Equation (3-1-8) and the requirement of eqn. (3-1-9) completely specify the coupled electron lattice system in the continuum limit.

The polaron solution of eqn. (3-1-8) has already obtained by Rice. A form of the solution is expressed as $u(x)=(\varepsilon^2/\alpha\gamma)\mathrm{sech}^2(x/\xi_p)$, where $\varepsilon=(V\Delta)^{1/2}(a/\xi_p)$. The characteristic length ξ_p denotes the half width of the polaron. Considering this solution of the eqn. (3-1-8), next views of the electronic states of polysilanes are speculated.

(a) A pair of localized intragap states with energies of

$$E_{\pm} = \pm\left(\alpha^2 - \varepsilon^2\right)^{1/2} \equiv \pm\varepsilon_p$$

(3-1-11)

and with wavefunctions $A_{\pm}(x)=F_0(x+x_0)$ and $B_{\pm}(x)=F_0(x-x_0)$, where $F_0(x)=(a/4\xi_p)^{1/2}\mathrm{sech}(x/\xi_p)$ and $x_0=(V/2\alpha)a$. The polaron half width ξp is next,

$$\xi_p = \xi_p(v) = \left(2K_0\Delta V/\alpha\gamma^2\right)(a/v)$$

(3-1-12)

Here, if v is equal to $v_+ + 2 - v_-$, two parameters of v+ and v- present the electronic occupations of the upper and lower intragap levels respectively.

(b) Conduction band(+) and valence band(-) states with energies

$$\varepsilon_{\pm}(k) = \pm\left[\alpha^2 + \Delta V(ka)^2\right]^{1/2} \quad (k \neq 0)$$

(3-1-13)

and wavefunctions as

$$A_{\pm,k}(x) = f_k(x + x_0)$$

$$f_k(x) = \sqrt{\frac{a}{2L_k}}\exp(-ikx)\left[k\xi_p + i\tanh(x/\xi_p)\right]$$

(3-1-14,15)

and $L_k=L[1+(k\xi_p)^2]+2\xi_p$. The wave vector k are obtained from $kL=2\pi t+\theta_k$, where $t=0, \pm1, \pm2,....$, and $\theta_k=2\tan^{-1}(1/k\xi_p)$ is the phase shift experienced by the band states in their transmission through the region of the polaron.

Thus, theoretically expected spectrum of polysilanes is revealed. By the way, The presence of the polaron removes one electron from the valence band leading to valence band charge deficit. Thus, the total charge Q of the polaron is found to be $Q=e(v^+ + v_- - 2)$, where e denotes the unit charge of a electron. Since the intragap level may accommodate zero, one or two electrons, next type of polaron is considered, that is a paramagnetic polaron (v=1) with charge $\pm 1e$ or a spinless bipolaron (v=2) with charge of $\pm 2e$, and or a charge neutral polaron (v=3,4) states. These considerations suggest the presence of intragap state of excited polysilane main chain formed by polaron or bipolaron state, namely possibility for the presence of stable polaron state with excited electron and holes, and further suggest bipolaron states are likely to be formed by th interaction between polarons. On the other hand, a spectrum of excited (electron or hole doped) polysilane is predicted to have UV band with red shift and IR band according to subband gap transition, in other words, vibrational absorption.

Section 3-1 Reference

[1] Rice, M. J. Phys. Lett. A, 1979, 71, 152.

[2] Pitt, C. G. In Homoatomic Rings, Chains, and Macromolecules of Main Group Elements; Edited by Rheingold, A. L.; Elsevier: Amsterdam. 1977.

[3] Rice, M. J.; Phillpot, S. R. *Phys. Rev. Lett.* 1987, **58**, 937.

[4] for a review, Abkowitz, M. A.; Rice, M. J.; Stolka, M. Phil. Mag. B 1990, 61, 25.

3-2 Reaction Mechanisms of Polysilanes with Structural Defects

This section discusses the stability of radicals produced under γ-irradiation for phenyl substituted polysilanes with different backbone structure. Poly(methylphenylsilane) and structural defect-containing phenyl substituted polysilanes were irradiated by ^{60}Co γ-rays in the solid state. Temperature dependence of the EPR signal intensity from the radicals induced by radiolysis was measured. The radicals appeared to be more stable as the induced defect density in the backbone structure was increased, indicating that the structure defects on the polymer backbone may play a role in stabilizing silyl radicals. The migration of unpaired electrons was also observed from chain ends to chain center leading to stable radical species. The estimated-branched structures were less than 3.5 % in the linear polysilane obtained by conventional Wurtz coupling condensation.

3-2-1 Introduction

Wurtz coupling reaction of dichlorosilane is often the choice method for synthesizing polysilane derivatives. However, when this method is used it is impossible to avoid the creation of structural defects, such as branching, oxidized sites, etc., in the silicon skeleton. While the occurrence of structural defects may be widespread, the relationship between the defect structure and various physical properties of polysilanes has not been elucidated. Fujiki reported the synthesis of structural defect-containing poly(methylphenylsilane), as well as the relationship between the fraction of the induced defects and the intensity of broad emission band observed around 2.9 eV[1]. Fujiki reported that the branching structure in the silicon skeleton could be influenced by changing the $SiRCl_3/SiRR'Cl_2$ monomer ratio in the coupling reaction, and observed broad emission bands in addition to 3.4-3.6 eV emission band of the linear polysilane. The intensity of the new emission band increased with the structural defect density in the silicon skeleton and this band was ascribed to the photoluminescence from the defect structure. It was suggested that the defect density in linear polysilane was < 1%, considering the relative emission intensities.

There is another point of view that considers the polysilane derivatives as silicon materials of low dimensionality. Matsumoto et al., considered the polysilanes as one dimensional silicon materials, amorphous and crystalline silicon as the three dimensional silicon materials, and polysilanes with network silicon skeleton were considered to be two dimensional silicon materials[2]. Their modeling calculations showed the band gap energy of 1D-Si, 2D-Si to be 3.4 eV and 2.5 eV, respectively. For the 3D-Si it was 1.7 eV for amorphous silicon and 1.1 eV for crystalline silicon. The reduction of the band gap energies was ascribed to the extension of the σ-conjugated system in the silicon skeleton. Their experimental results on photoluminescence of these silicon materials supported these calculations. They also suggested that the increasing defect (branching) structure density in silicon skeleton could develop into a silicon network, i.e., conversion from 1D-Si to 2D-Si with an extended σ-conjugated system. Brus also discussed silicon optical and electronic properties as a function of dimensionality.[3] Brus focused on the luminescence spectra of these silicon materials, and suggested a model of structural change from direct to indirect gap materials with increasing dimensionality of the silicon skeleton.

Many polysilanes have a strong UV absorption band which originates from the σ to σ* transition. Photochemistry of polysilanes has been considered to involve chain scission on exposure to UV light, and several groups[4] have reported the potential use of polysilanes as UV photoresist material. There are reports on the characteristics of the UV light induced reactive intermediates of polysilanes using EPR spectroscopy. McKinly et al., observed radicals of di-n-pentyl and methylpentyl substituted polysilanes in n-octane and n-pentane solution at 200 K - 350 K induced by 248-330 nm light.[5] Their data showed EPR spectra consisting of a doublet of doublets, which were assigned to two unpaired electrons on silicon atoms in the low temperature region, giving rise to a triplet state at higher temperature. Thus a silicon centered radical pair was formed as a result of UV light exposure. They proposed three primary reaction routes: silylene extraction, homolytic cleavage and alkyl side chain elimination followed by polymer skeleton scission. Todesco, et al., also reported UV light induced radical formation in poly[dimethylsilane-co-methyl(1-napthylsilane)] in methyltetrahydrofuran[6]; however, their EPR spectrum turned out to be that of solvent radicals. As the above-mentioned studies illustrate, the reactive intermediates and the stability of these polymer materials in photo- and radiation- induced reactions have not been adequately elucidated. In contrast, many investigations have been reported for small silane and oligosilane molecules. Silyl radical formation in alkyl substituted silicon centered molecules were observed by many groups in the 1970's. Benett, et al.,[7] and Krusic, et al.,[8] reported trimethylsilyl radical formation on exposure for UV light. Benett, et al.,[9] and Cooper, et al.,[10] also presented the EPR spectra of dimethyl(trimethylsilyl)silyl radicals generated by UV light exposure. The observed coupling constant of β-hydrogen in this radical was considerably larger than that of Me_3Si and was ascribed to the conjugative interaction of the neighboring silicon atom.

The present section describes the observation of silyl radicals in solid state poly(methylphenylsilane) (PMPS), PMPS containing structural defects, and poly(phenyl-silane) (PPS) with silicon skeleton network. PMPS is one of the most popular polysilanes because of its stability in the solid state, ease of handling and good film forming properties. Furthermore, PMPS has σ-conjugated substituents, and the phenyl group itself is bulky in comparison to alkyl side chains, so that PMPS has a more rigid silicon skeleton than the other al-

kyl-substituted polysilanes. PMPS is one of the most suitable polysilanes as an optical and photoconductive material. This section discusses the stability of reactive intermediates in these polymers and the effect of defect structures in the main chains.

3-2-2 Experimental

Linear PMPS was synthesized by the conventional sodium condensation (Wurtz Coupling) method from methylphenyldichlorosilane monomer. Defect-containing PMPS was synthesized by the same procedure with the monomer mixture of methylphenyl-dichlorosilane and p-tolytrichlorosilane.

The ratio of the mixture was changed from 0.27 wt % to 20 wt %. For poly(phenylsilane) (PPS) with network silicon skeleton, phenyltrichlorosilane was taken as monomer. All chlorosilanes were doubly distilled products from Shinetsu Chemical Co. Ltd. Polymerization reactions were carried out in Ar atmosphere, in 100 ml of toluene with 20 ml diethylene-glycoledimethylether as reflux solvent, except for the polymerization of PPS. PPS was prepared using decane as a reflux solvent in order to obtain relatively high molecular weight polymer. The monomer was added into the reaction vessel and mixed with molten sodium metal over a four-hour period. PMPS and defects-containing PMPS solutions were precipitated using isopropyl alcohol after filtration to remove NaCl, and the precipitates were dried under vacuum. To eliminate the remaining NaCl, toluene solutions of these polymers were transferred into separatory funnels, washed with water, and precipitated twice with toluene-isopropyl alcohol and tetrahydrofuran(THF)-methanol mixture. PPS was first precipitated by direct addition of isopropyl alcohol into the reaction vessel, and washed with water after filtration. The purification was carried out using the same procedure as for PMPS. PMPS and defects-containing PMPS showed good solubility in toluene, THF, methyl THF (MTHF), chloroform and in dichloromethane. PPS was partially soluble in toluene, and the insoluble component was removed by filtration. The amount of residual Cl atoms were confirmed to be less than 0.1 % in solid PPS by elemental analysis. For defect-containing polysilanes, the ratio of branching structure for each polymer was confirmed by NMR using JEOL EX-270 1H NMR spectrometer in the Institute of Scientific and Industrial Research, Osaka on Shimadzu C-R3A gel permeation chromatography (GPC) system. Phase transition temperatures were measured on the Perkin-Elmer DSC-7 system.

Electron spin resonance measurements were carried out using a Varian X-band EPR spectrometer. The microwave power used was typically 0.2 mW that was increased to 5 mW for measurements above 250 K. Polymer samples in suprasil quartz cells were evacuated to 10^{-4} Pa, and irradiated by ^{60}Co γ-ray source in the Chemistry Division at Argonne National Laboratory to the dose of 1.9 - 3.8 kGy. After the irradiation at 77 K, samples were transferred to a liquid helium cryostat, and EPR measurements were carried out at temperatures from 4 K to 270 K.

For optical measurements, samples in 1 cm quartz cells were dissolved in MTHF and evacuated. Frozen solutions were irradiated with ^{60}Co γ-rays at 77 K with a dose of 1.9 kGy, and the absorption spectra were measured by a Varian Cary UV-Vis-NIR spectrometer after bleaching the solvated electron absorption band in MTHF.

Table 3-2-1. Polymerization results and characteristics of polysilane samples.

Entry	*D*	*Mw*	T_g(K)
1	0.0	3.2×10^4	379 K
2	0.045	1.6×10^4	385 K
3	0.090	1.2×10^4	392 K
4	0.18	1.1×10^4	399 K
5	1.0	2.4×10^4	---

a D, Si based defect density per total Si units; *Mw*, weight average molecular weight; *Tg*, glass transition temperature.

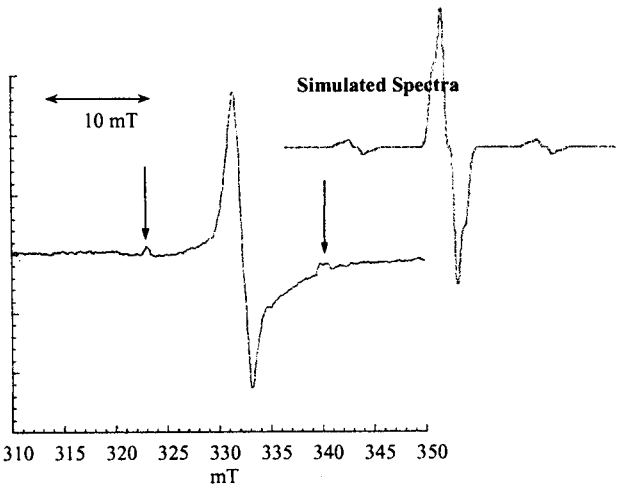

Figure 3-2-1. EPR spectrum of defect-containing γ -irradiated PMPS at 6 K with simulated spectrum of -MePhSi-MePhSi· using coupling constants in refs. 13 and 15.

3-2-3 Results and Discussion

Table 3-2-1 shows the polymerization results for PMPS, defect containing PMPS and PPS. The ratio of tolyl and methyl protons measured by ^{1}H NMR spectra establish that the concentration of defect structures was proportional to the ratio of trichlorosilane / dichlorosilane monomers. The changes in phase transition temperatures as shown in table 3-2-1 support the presence of the defect structures in the silicon skeleton. The molecular weights of these polymers decrease slightly with increase in defect densities.

In The authors' previous work the authors described the γ-radiolysis induced silyl radicals in poly(dimethylsilane).[11] The silyl radicals were quite stable and were probably created via the main chain scission of the silicon skeleton. Several other studies

suggested the creation of silyl radicals induced by photolysis and by other types of ionizing radiation.[4,5] There has been little discussion on the relative stability of radical species in polysilanes. Figure 3-2-1 shows the EPR spectrum of γ-irradiated defect containing PMPS at 6 K. The spectrum exhibits weak hyperfine satellites owing to the presence of ^{29}Si (relative abundance 4.7%; spin = 1/2). A simulated EPR spectrum, calculated using values of coupling constants previously observed in γ-irradiated poly(dimethylsilane)[11] and diphenyl-silyl radicals[12] is also shown in the fig. 3-2-1.

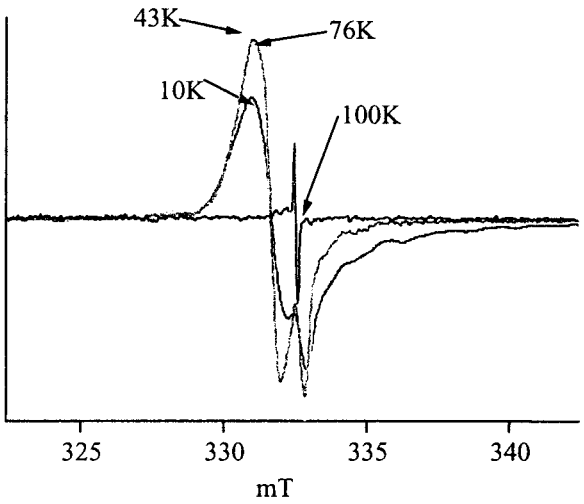

Figure 3-2-2. Temperature dependence on EPR signals of linear PMPS.

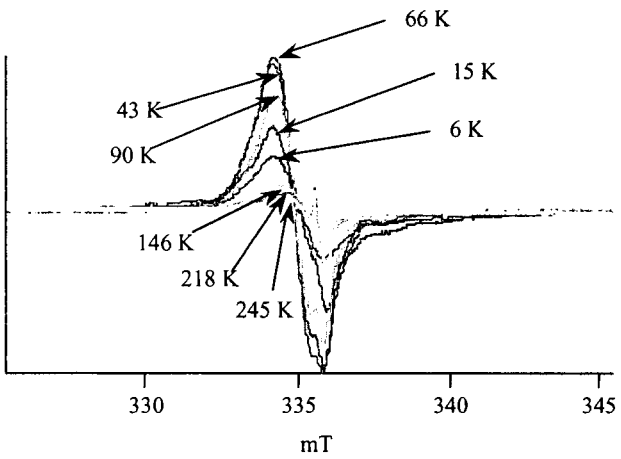

Figure 3-2-3 Temperature dependence on EPR signals of defect-containing PMPS with the defect density at 0.090.

The spectrum was simulated using a Gaussian approximation lineshape with 0.28 mT linear, typical for EPR spectra in amorphous polymer solids. The observed spectrum exhibits the same features as the simulated spectrum of silyl radicals with small differences in the peak width; i.e. 1.41 mT for observed spectrum and 1.38 mT for the simulated spectrum respectively. The coupling constant of ^{29}Si is 18.2 mT in good agreement with previously reported values for coupling constants in silyl radicals.[12] Thus the EPR spectrum is assigned to the silicon centered neutral radical. Because of the asymmetry of the amorphous polymer, the spectrum was broadened due to small coupling constants of hydrogen atoms of phenyl groups (reported as 0.097, 0.092, and 0.045 mT for p-, o-, and m-hydrogen, respectively).[13]

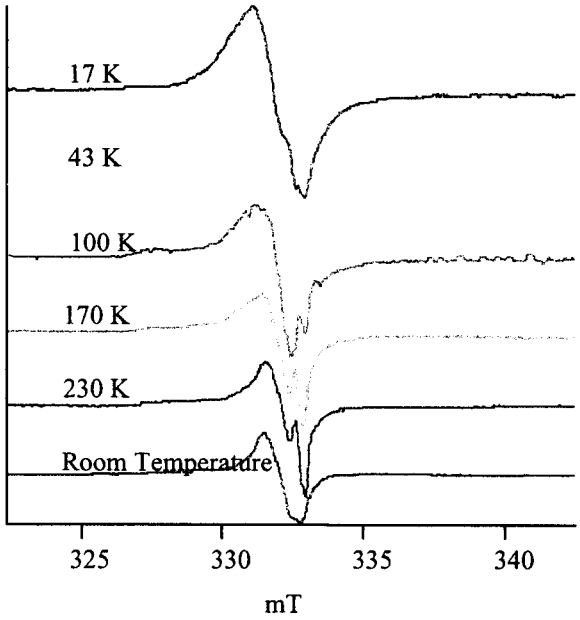

Figure 3-2-4. Temperature dependence of EPR signal of the polysilane with network-like silicon skeleton.

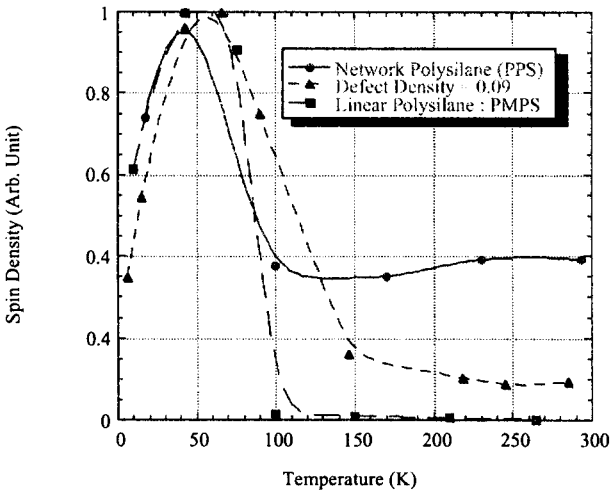

Figure 3-2-5. Temperature dependence of EPR signal intensity of PMPS, defect-containing PMPS (defect density of 0.090) and PPS.

In figure 3-2-2 the author illustrates the temperature dependence of the EPR signal intensity of γ-irradiated linear PMPS. The EPR signals could not be resolved because the coupling constants of phenyl protons of silicon centered radicals are small. In the aryl substituted linear PMPS, a broad signal was observed below 90 K. The signal was ascribed to silicon centered neutral silyl radicals as described before. The g-factor of the radical is estimated to be 2.0066 at all temperatures. The signal intensity decreased rapidly at higher temperature, and the signal completely disappeared at 100 K suggesting re-

combination of silyl radicals with increasing temperature. Figures 3-2-3 and 3-2-4 show similar temperature dependence for defect-containing PMPS and PPS with network silicon skeleton, respectively. The defect density of the PMPS, which represents the ratio of the branched Si units to the total Si units, is 0.09. It is evident that the EPR peak intensity decreases with an increasing number of branched Si structures on the silicon skeleton. The shapes of these EPR signals are nearly the same for PPS and the g-factor is 2.0036. Therefore it appears that once silicon centered neutral silyl radicals are formed in these polysilanes, they are trapped and stabilized at branching sites of the silicon skeleton. However, the spectra are shifted to higher magnetic field in γ-irradiated defect containing PMPS. The g-factors of the observed radicals are also changed from 2.0064 at 15 K to 2.0038 at 245 K. This indicates the overlap of two radical species that are assigned to –MePhSi˙ radicals produced by main chain scission, and to –PhSi˙ radicals by side chain scission reactions.

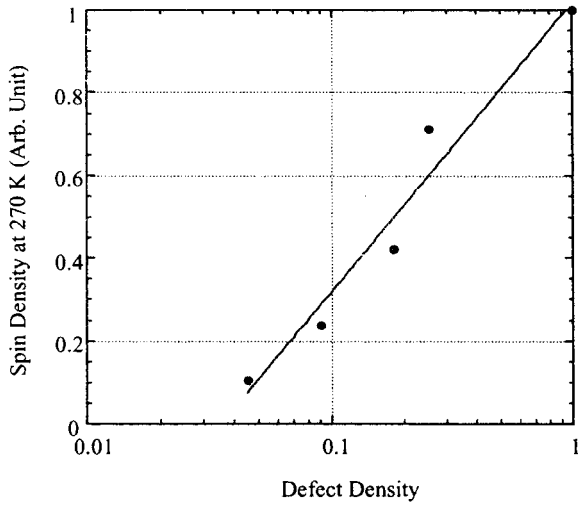

Figure 3-2-6. Dependence of spin density on defect density as calculated from EPR spectra observed at 270 K.

Figure 3-2-5 shows the temperature dependence of the EPR signal intensity for γ-irradiated polysilanes. The signal intensity does not change above 200 K for PPS and defects-containing PMPS. This allows one to estimate total spin density of –PhSi˙ type radicals, as a function of defect density, as shown in figure 3-2-6. The spin density is not proportional to the defect density but appears to be approximately proportional to logarithm of defect density. This may be due to migration of unpaired electrons from chain end to the branched sites with rising temperature. The radical at the branched site shows greater stability compared to the chain end radicals. Therefore the presence of branched structures enhances the chain scission reaction. One can use this to estimate the defect density in linear polysilanes and to compare it with the NMR-based estimates mentioned in the experimental section. No EPR signal is observed for γ-irradiated linear PMPS at 270 K suggesting that the amount of branched sites is less than 3.5 % in the polymer.

Figure 3-2-7 shows the results of optical spectroscopy of these polysilanes after γ-radiolysis in the MTHF matrix at 77 K. Electrons created by the ionizing radiation in the MTHF matrix are transferred to the solute polysilane molecules producing radical anions of the polysilane.

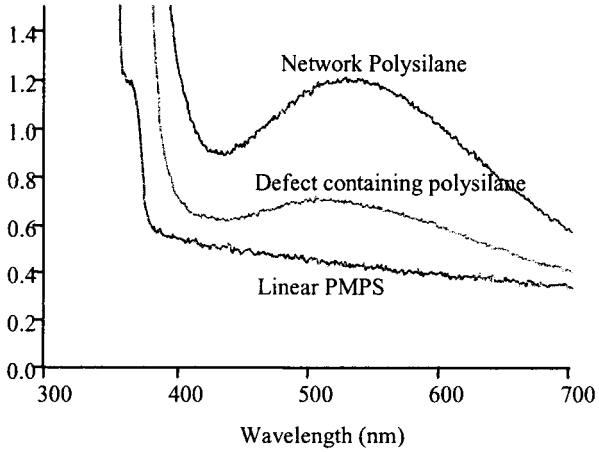

Figure 3-2-7. UV-VIS absorption spectra of polysilane MTHF solutions (77K) irradiated by γ-rays to a dose of 1.9kGy. Solute concentration was 30 mmol/l in all solutions used.

The authors have reported electron beam pulse radiolysis studies, where anion and cation radicals on linear and branched polysilane molecules were found to exhibit simultaneously a sharp UV absorption band around 370 nm and a broad IR band.[14] Extinction coefficients of the radical anions decrease with the increase in defect density, while the absorption maxima occurred in the same wavelength range. In the case of linear PMPS, a weak absorption band was observed at 375 nm that can be ascribed to the anion radicals of PMPS. However, the anionic species were not observed in defect-containing PMPS and PPS. Figure 3-2-6 also illustrates a new, broad absorption band observed at 520 nm and 540 nm for defect-containing PMPS and network PPS, respectively. The intensity of this band was seen to increase and shift to longer wavelength upon increasing the density of defect structures in the silicon skeleton. This absorption was also observed in the presence of 50 mM CCl_4, a typical scavenger of anionic species, indicating that absorption was due to neutral species. This new absorption band must be due to the neutral silyl radicals generated as a result of direct or indirect excitation of the solute polysilane molecules. This implies that relatively stable silyl radical species occur at the branching site of highly branched PMPS and PPS at 77 K, while the silyl radicals in the predominantly linear PMPS are less stable and recombine more readily.

3-2-4 Summary

Neutral silyl radicals in solid aryl substituted polysilanes were less stable than radicals derived from dimethyl substituted polysilanes. The defect (branch) structure in the silicon skeleton appears to be able to stabilize silyl radicals, and highly branched silyl radicals

exhibited remarkable stability, even close to room temperature.

Conjugation effects of the silicon skeleton on these radical species may be small, and the unpaired electrons were concentrated on the highly branched silicon atoms. These branched silyl radicals exhibited optical absorption around 540 nm in MTHF matrix at 77 K. The unpaired electrons migrated from the chain ends to the chain center leading to stable radical species. Therefore EPR spectroscopy can be used to assess the presence of branched structure in the silicon skeleton. The estimated-branched structures were less than 3.5 % in the linear polysilane obtained by conventional Wurtz coupling condensation.

Section 3-2 Reference

[1] Fujiki, M. Chem. Phys. Lett. 1992, 198, 177.

[2] Matsumoto, N.; Takada, K.; Teramae, H.; Fujino, M. Advances in Chemistry Series 224; American Chemical Society; Washington DC; 1990; p.515.

[3] Brus, L. J. Phys. Chem. 1994, 98, 3575.

[4] Miller, R. D.; Michl, J. Chem. Rev. 1989, 89, 1359; Taylor, G.N.; Wolf, W.W.; Moran, J.M. J. Vac. Sci. Technol. 1981, 19, 872.; Trefonas, P.; West, R.; Miller, R. D.; Hofer, D. J. Poly. Sci., Poly. Lett. Ed. 1983, 21, 823.; Zeigler, J.M.; Harrah, L.A.; Johnson, A.W. Proc. SPIE 1985, 539, 166.; Hofer, D. C.; Miller, R. D.; Willson, C. G. Proc. SPIE 1984, 469, 16.

[5] McKinly A. J.; Karatsu, T.; Wallraff, G. M.; Miller, R. D.; Sooriyakumaran, R.; Michl, J. Organ. 1988, 7, 2567.

[6] Todesco, R. V.; Kamat, P. V. Macromolecules 1986, 19, 196.

[7] Benett, S. W.; Eaborn, C.; Hudson, A.; Hussain, H. A.; Jackson, R. A. J. Organ. Chem. 1969, 16, 36.

[8] Krusic, P. J.; Kochi, J. K. J. Am. Chem. Soc. 1969, 91, 3938.

[9] Benett, S. W.; Eaborn, C.; Hudson, A.; Jackson, R. A.; Root, K. D. J. J. Chem. Soc, A 1970, 348

[10] Cooper, J.; Hudson, A.; Jackson, R. A. Mol. Phys. 1972, 23, 209.

[11] Seki, S.; Tagawa, S.; Ishigure, K.; Cromack, K. R.; Trifunac, A. D. J. Rad. Phys. Chem. Radiat. Phys. Chem. 1996, 47, 217.

[12] Wick, A. K. Helv. Chim. Acta 1970, 53, 819.

[13] Geoffroy, M.; Lucken, E. A. C. Helv. Chim. Acta 1970, 53, 813.

[14] Ban, H.; Sukegawa, K.; Tagawa, S. Macromolecules 1987, 20, 1775.; Ban, H.; Sukegawa, K.; Tagawa, S. Macromolecules 1988, 21, 45.

3-3 Energy Relaxation in Polysilanes with Structural Defect

The electronic structure of a charged polysilane molecule is studied in the present section. The transient absorption spectroscopy was carried out for radical cations and anions of aryl-substituted polysilane molecules with Si based defects by means of nanosecond pulse radiolysis technique. Radical cations and anions of polysilanes displayed near UV and IR absorption maxima at ca. 3.2~3.4 eV and 0.5~1 eV, respectively. They are ascribed to interband and subband transition of polaron states and/or charge resonance states (CR) between σ-conjugated segments. The transition energy of the bands were strongly affected by the defects showing remarkable blue shift in IR absorption. The energy of IR absorption band was interpreted as the degree of electron-phonon coupling. The energy rapidly increased from ca. 0.5 eV with an increase in the defect density, and saturated at ca. 0.85 eV for radical cations and 0.95 eV for radical anions. It indicated that excess electrons and holes relatively localized at the defect structures, while as the charges were delocalized in a conjugated segment in linear polysilanes.

3-3-1 Introduction

Ionic species of Si based molecules have been studied for cyclic and linear polysilanes.[1] Cyclic origosilanes form radical anions by reduction with alkali metal, and also form radical cations by oxidation with $AlCl_3$. The ionic species have an unpaired electron delocalized over the silicon skeleton. Charged molecules of polysilanes were produced by a pulse radiolysis technique, and displayed chromophores at near UV and IR region with very high extinction coefficients.[2] The transient spectra suggest that an excess electron or a hole is delocalized over a conjugated segment in a molecule. This indicates that the conjugated molecular orbital (σ-conjugation) is responsible for the absorption spectra of the ionic species.

Organopolysilane solid films show high electric resistance but became p-type semiconductor in the presence of strong electron acceptors.[3] This suggests that the polymer essentially have semiconducting path for the carriers along a main chain. Thus an ionized molecule simulates one conducting holes or electrons on the silicon chain. Several studies have reported on the energy states of excess electrons on π conjugated polymers such as polyacetylene.[4] They suggested that the polaronic interaction occurs between the electrons and backbone phonons. Recently, the one-electron-theory model has been extended to tetrahedrally bonded polymers as polysilanes, and predicted small electron-lattice interaction.[5] The polaron model gives better interpretation to hole transport in polysilanes, however the direct observation of the state have not carried out yet. Thus the transient spectroscopy by the pulse radiolysis technique is useful to elucidate the polaron states on σ conjugated system.

A Wurtz coupling reaction of dichlorosilane with alkali metal is often the choice for the polymerization of polysilane derivatives. However when the polymers are obtained by the method, they contain small amount of structural defects, such as branching points and oxidated sites. Fujiki reported empirical linear relationship between the defect density and the relative intensity of broad photoluminescence at visible region in poly(methylphenylsilane) (PMPS).[6] Hole transport in polysilanes with structural defects was also investigated by microwave absorption and DC time-of-flight techniques.[7] The values of charge carrier mobility apparently depended on the density of Si based defects. This indicates that physical properties of linear polysilanes are dominated by the presence of the structural defects that disturb the σ-conjugated system along a silicon skeleton.

The present section describes the transient absorption spectra of radical cations and anions of PMPS, PMPS with Si-based structural defects, and poly(phenylsilane) (PPS). The spectra were obtained by nano-second pulse radiolysis technique with a wide wavelength range from 300 nm to 1600 nm. Their optical properties were quantitatively discussed in relation with the amount of Si-based structural defects. The binding energy of excess electrons and holes is estimated on the basis of the polaron model, leading to elucidate the effects of structural defects on the σ-conjugated system in polysilanes.

Table 3-3-1. Characteristics of polysilane derivatives

Entry	Feed Ratio	D[a]	*Mw*[b]	*Mw/Mn*[c]	T_g[d](K)
PMPS	0	0	3.2×10^4	2.3	379
PSi(D = 0.0083)	0.01	0.0083	3.5×10^4	2.6	383
PSi(D = 0.065)	0.07	0.065	2.8×10^4	2.7	385
PSi(D = 0.11)	0.1	0.11	2.6×10^4	3.1	389
PSi(D = 0.23)	0.25	0.23	2.7×10^4	2.9	390
PPS	1	1	4.5×10^4	1.8	-

[a] D, Si based defect density per total Si units; [b,c] *Mw and Mn*, weight and number average molecular weight; [d] T_g, glass transition temperature.

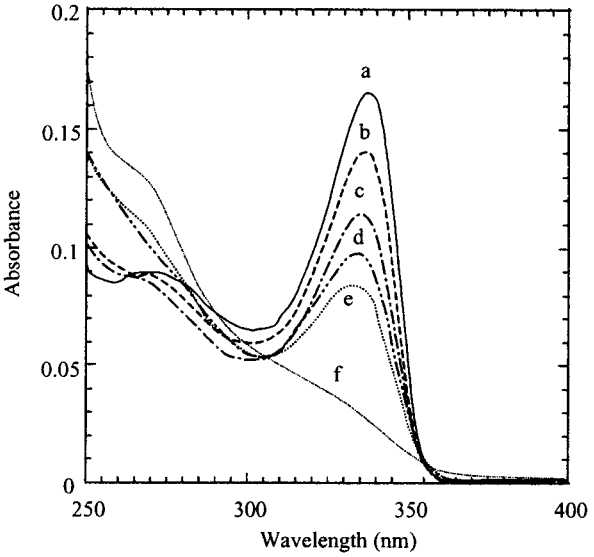

Figure 3-3-1. Absorption spectra of polysilanes in a THF solution at 2.0 x 10^{-5} mol/dm^3 conc. (base mol unit). a : PMPS, b : PSi (D = 0.0083), c : PSi (D = 0.065), d : PSi (D = 0.11), and e : PSi (D = 0.23).

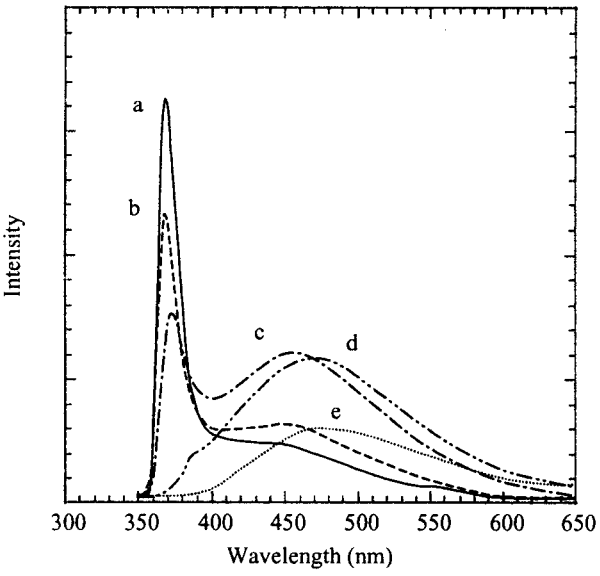

Figure 3-3-2. Fluorescence spectra of polysilanes in a THF solution. a : PSi (D = 0.0083), b : PSi (D = 0.065), c : PSi (D = 0.11), d : PSi (D = 0.23), and e : PPS

3-3-2 Experimental

General. PMPS was synthesized by the conventional sodium condensation (Wultz Coupling) method from the methylphenyldichlorosilane monomer. Defect-containing PMPS was synthesized by same procedure with a monomer mixture of methylphenyldichlorosilane and p-toryltrichlorosilane. The ratio of the mixture was changed from 0.15 wt % to 25 wt %. Phenyltrichlorosilane was used as a monomer for the synthesis of PPS with network silicon skeleton. All chlorosilanes were doubly distilled products from Shin-Etsu Chemical Co. Ltd. Polymerization reactions were carried out in an Ar atmosphere, in 100ml of dry toluene which was refluxed with sodium during 10 h and distilled before use. The monomer was added into the reaction vessel and mixed with sodium dispersion during 12 hours. The sodium micro-dispersion in toluene was purchased from Acros Co. LTD. PMPS and defect-containing PMPS solutions were precipitated in iso-propylalchol (IPA) after filtration passing through a 0.45 μm PTFE filter to roughly eliminate NaCl, and precipitates were dried under vacuum. The toluene solutions of these polymers were transferred into separatory funnel, washed with water to eliminate the remaining NaCl, and precipitated twice with toluene-isopropylalchol and tetrahydrofran(THF)-methanol. PPS was first precipitated by direct addition of IPA into the reaction vessel, and then washed with water after filtration. PMPS and defect-containing PMPS showed good solubility for toluene, THF, 2-methyltetrahydrofran (MTHF), chloroform and dichloromethane. Because of the less solubility of PPS, the soluble fraction was collected against THF and dichlorometane. The amounts of residual Cl atoms were confirmed to be less than 0.1 % in all polysilanes by elemental analysis. The Si based defect density (D) was confirmed from the ratio of the ^1H contents in p-tolyl and methyl groups determined by a JEOL EX-270 NMR spectrometer at 270 MHz. A ^{29}Si NMR spectra were also recorded using a JEOL EX-600 NMR spectrometer at 120 MHz. The molecular weight distributions in all the polymers were measured with a Shimadzu C-R3A gel permeation chromatography (GPC) system with polystylene calibration standards. Glass transition temperatures were measured with a Perkin-Elmer DSC-7 system. The UV-visible absorption spectra were recorded by a Shimadzu UV-3100 PC system. The photoluminescence spectra were measured with a Perkin-Elmer LS-50B.

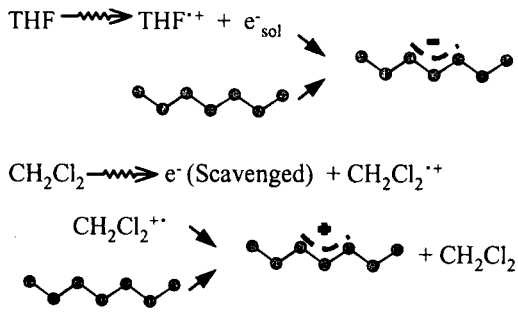

Figure 3-3-3. Scheme of the reaction and the resulting polymer radical anions and cations. Polymer molecule is simply represented by the skeleton of catenating Si atoms.

Pulse Radiolysis. .The pulse radiolysis measurements were performed with L-band electron linear accelerator at the Radiation Laboratory of the Institute of Scientific and Industrial Research, Osaka University. All the polysilanes were dissolved into THF and CH_2Cl_2 at 0.05 mol/dm^3 conc. (base mol unit). The THF solutions were evacuated, and the CH_2Cl_2 solutions were bubbled by Ar gas during 5 min. before irradiation. The samples were irradiated with a 2 nsec single electron pulse at room temperature. A Xe flash lamp was used as a source of analyzing light with continuous sepctrum from 300

nm to 1600 nm. The analyzing light was monitored with Ritsu MC-10N monochromator, and detected by PIN Si (Hamamatsu S1722) or InGaAs (Hamamatsu G3476) photodiodes. The signals were corrected by a Sony/Tektronics SCD1000 transient digitizer. The typical instrument function was ca. 8 nsec.

Low Temperature Matrix Spectroscopy. The low temperature matrix experiment was carried out using a ^{60}Co γ-ray source at the ISIR Osaka University. PMPS, PSi (D = 0.0083), and PSi (D = 0.065) were dissolved into MTHF or 2-buthylchrolide which were purchased from Dojin Chemical Co. LTD at 10 mM conc. (base mol unit). The author could not perform the experiment for polysilanes with more defects because of the less solubility at 77 K against the solvents. The solutions were evacuated and sealed into quartz cells. The irradiation was performed at 77 K, 3.7 kGy/h during 6 hours. The samples were exposed to 527 nm laser light after the irradiation to breach the chromophores of trapped solvated electrons in MTHF, or radical cations of BuCl. The radical anions and cations of the polysilanes were formed in MTHF and BuCl, respectively after the breaching.

NMR Spectroscopy. PMPS. ^{1}H-NMR(270.05 MHz, $CDCl_3$) δ 0.2(br), 7.1(br); ^{29}Si-NMR(119.19MHz, $CDCl_3$) δ -39.2, -39.8, -41.2. PSi(D=0.0083). ^{1}H-NMR(270.05 MHz, $CDCl_3$) δ 0.2(br), 2.3(br), 7.2(br); ^{29}Si-NMR(119.19MHz, $CDCl_3$) δ -39.2, -39.8, 41.2. PSi(D=0.065). ^{1}H-NMR(270.05 MHz, $CDCl_3$) δ 0.2(br), 2.3(br), 7.1(br); ^{29}Si-NMR(119.19MHz, $CDCl_3$) δ –35, -39.2, -39.8, 41.2, -46. PSi(D=0.11). ^{1}H-NMR(270.05 MHz, $CDCl_3$) δ 0.2(br), 2.3(br), 7.2(br); ^{29}Si-NMR(119.19MHz, $CDCl_3$) δ –35, -39.2, -39.8, 41.2, -46. PSi(D=0.23). ^{1}H-NMR(270.05 MHz, $CDCl_3$) δ 0.2(br), 2.3(br), 7.2(br); ^{29}Si-NMR(119.19MHz, $CDCl_3$) δ –35, -39.2, -39.8, 41.2, -46. PPS. ^{1}H-NMR(270.05 MHz, $CDCl_3$) δ 7.2(br); ^{29}Si-NMR(119.19MHz, $CDCl_3$) δ –60.

3-3-3 Results and Discussion

Table 3-3-1 shows the polymerization results for PMPS, defect-containing PMPS and PPS. The obtained values of D are proportional to the monomer feed ratio of trichlorosilane and dichlorosilane. A ^{29}Si NMR study on the structural defect-containing polysilanes reported additional broad signals that were ascribed to the Si-Si bond elongation at branching points, suggesting that branching points were actually induced in the polymer

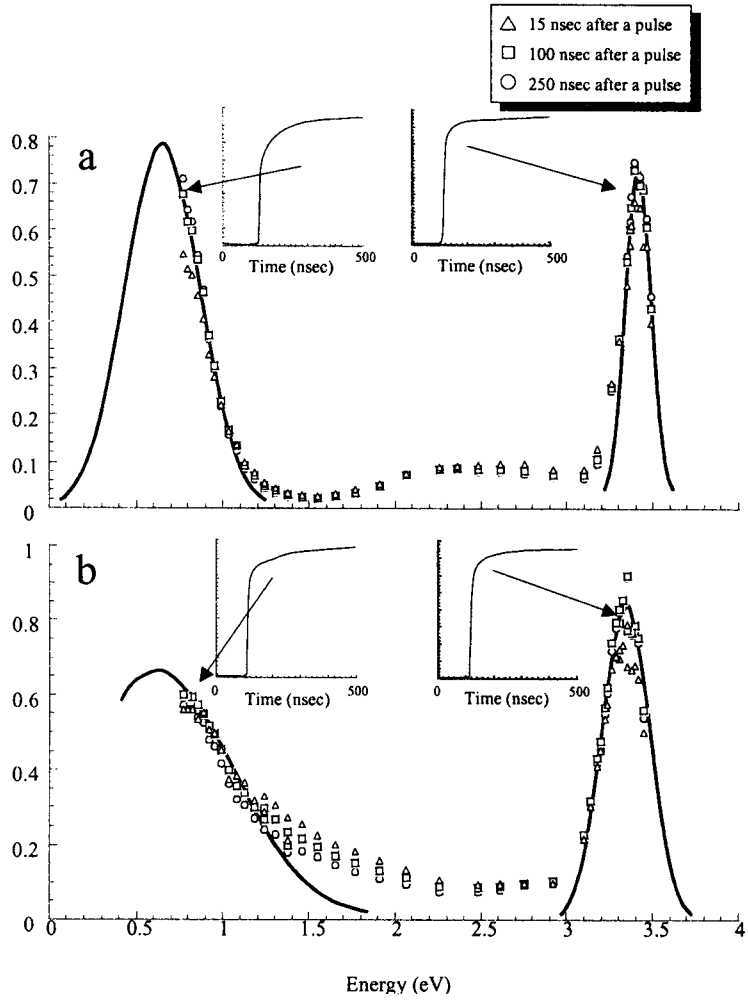

Figure 3-3-4. Transient absorption spectra of radical anions : a and radical cations : b of PMPS at the 15, 100, and 250 nsec after a pulse. Superimposed figures indicate the kinetic traces of transient absorption.

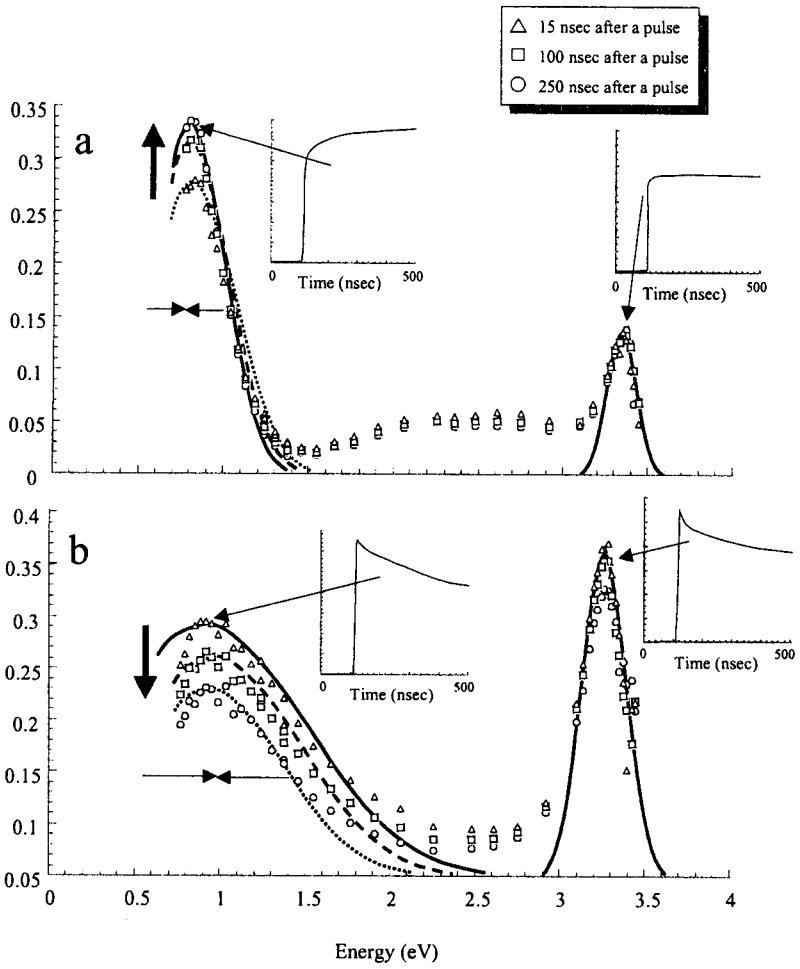

Figure 3-3-5. Transient absorption spectra of radical anions : a and radical cations : b of PSi (D = 0.23) at the 15, 100, and 250 nsec after a pulse. Superimposed figures indicate the kinetic traces of transient absorption.

main chain.[6] The presence of defects in a main chain is also supported by the changes in glass transition temperatures that increase gradually with increasing D as shown in table 3-3-1.

The molecular weights of these polymers used in the present study are also summarized in table 3-3-1. These polysilanes initially show bimodal molecular weight distribution. Because the number of defects is predicted to depend on the molecular weight of PMPS,[6] the high molecular weight fraction was eliminated. This gives the

Table 3-3-2. Transient absorption band of polysilane derivatives

D	Anion IR λ_{max} ($X10^3$ nm)	λ_{max} Energy (eV)	Cation IR λ_{max} ($X10^3$ nm)	λ_{max} Energy (eV)
0	2.10[a]	0.59	2.25[a]	0.55
0.0083	1.90[a]	0.65	2.05[a]	0.60
0.065	1.47	0.84	1.55	0.80
0.11	1.40	0.89	1.50	0.82
0.23	1.30	0.95	1.45	0.86

D	Anion UV λ_{max} (nm)	λ_{max} Energy (eV)	Cation UV λ_{max} (nm)	λ_{max} Energy (eV)
0	369	3.36	364	3.41
0.0083	370	3.35	364	3.41
0.065	369	3.36	366	3.39
0.11	373	3.31	368	3.37
0.23	379	3.25	372	3.33

[a] The values of λ_{max} were determined by the low temperature matrix experiment

small dispersion and the similar value of their molecular weights.

Figure 3-3-1 shows the absorption spectra of the polysilanes in THF. The absorption maxima shift from 337 nm to 332 nm with increasing D. PPS has no peak at the region with a tail observed over 400 nm. An extinction coefficient at the absorption maximum was decreased from 9.2 x 10^3 to 4.8 x 10^3 with the increase in D from 0 to 0.23. A full width of half maximum (fwhm) of the band also changes from 0.22 eV for PMPS to 0.31 eV for PSi (D = 0.23), respectively. The UV absorption of PMPS was already ascribed to the transition exciton states in a Si conjugated segment. The present results indicate that defect structure increase the energetic dispersion of the exciton state.

Photoluminescence spectra of the polysilanes are illustrated in figure 3-3-2. Defect containing polysilanes show two emission bands: S emission observed at around 370 nm with fwhm of ca. 0.1 eV, and B emission at visible region with large fwhm of ca. 0.7 ~ 1 eV. The B emission shows remarkable red shift and becomes broader with the increase in D. The S emission was ascribed to a relaxation process of exciton states. As reported previously, the excitation spectrum of B emission is not identical to the absorption spectrum of the polymer, but exhibits broad band around 4 eV with a tail ranging to ca. 3 eV. This indicates that a different energy state on Si main chain is responsible to the B emission, such as the localized exciton states at defect structures. It is also supported by the presence of tail structures in absorption spectra of defect containing polysilanes.

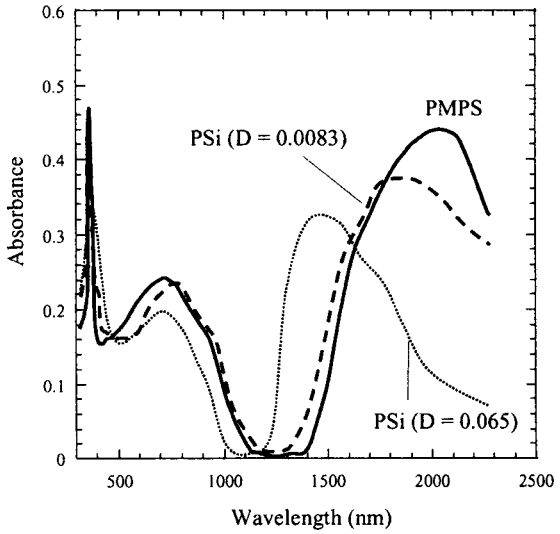

Figure 3-3-6. Absorption spectra of polysilanes in MTHF solutions at 77 K. The solutions were irradiated by ^{60}Co γ-rays at 15.7 kGy, and solvated electrons were breached by the exposure to a 527 nm laser light during 1 min. Solid, dashed, and dotted lines indicate the spectra of PMPS, PSi (D = 0.0083), and PSi(D = 0.065), respectively.

The transient spectroscopy of radical anions and cations of the polysilanes was performed by means of the electron beam pulse radiolysis. In each THF or dichloromethane solution, incident electrons cause the reactions as illustrated in the figure 3-3-3. The anionic or cationic species of polysilanes are then formed within an electron pulse width (fwhm = 8 nsec).

The observed transient spectra in THF and CH_2Cl_2 are shown in the figures 3-3-4 and 3-3-5, for PMPS and PSi (D = 0.025), respectively. Two absorption bands are observed at near UV (UV band) and IR (IR band) regions for both radical anions and cations of the polymers. Both UV and IR bands indicate the similar time dependence for all cases as shown in the superimposed figures. The maximum of IR band was confirmed by the low temperature matrix experiment as displayed in figure 3-3-6 for radical anions of PMPS and PSi (D = 0.0083). The transition energies of UV band (E_{UV}) and IR band (E_{IR}) were 3.36 and 0.59 eV, respectively for PMPS radical anions. The sum of the two absorption energies becomes ca. 3.95 eV showing good agreement with calculated band gap energy (Eg) in PMPS. For cations of PMPS, E_{UV} and E_{IR} were estimated to be 3.41 and 0.55 eV, also indicating the same total transition energy as Eg. This suggests the presence of an interband level occupied by an excess electron or a hole. The width of UV and IR bands decreased with the observation time in figs. 3-3-4 and 3-3-5. The shrinking suggests the decrease in the energetic dispersion of interband levels.

Table 3-3-3. Relative extinction coefficients of the UV band

D	Relative ε at λ_{max} of Radical Anions	Relative ε at λ_{max} of Radical Cations
0	1.0	1.0
0.0083	0.80	0.76
0.065	0.58	0.42
0.11	0.54	0.26
0.23	0.39	0.16

A polysilane molecule already revealed to have a backbone consisting of conjugated helical segments joined to each other by a disordered part. An excess electron or a hole on a polymer migrates into the most stable conjugated segment within the observation time range, thus the intersegment charge transfer may be responsible to the decrease in the dispersion. Figure 3-3-7 shows a series of transient absorption spectra observed for radical anions of the polymers. The spectra of radical cations are also shown in figure 3-3-8. The UV band slightly shifts to longer wavelength region with increasing D over 0.065. In contrast, the IR band presents remarkable blue shift with the increase in D. The absorption energies of UV and IR bands are summarized in table 3-3-2. The value of E_{IR} estimated for PSi (D = 0.065) by the matrix experiment corresponds to that observed by the pulse radiolysis as shown in figs. 3-3-6 and 3-3-7. The sum of E_{UV} and E_{IR} is almost same for both cations and anions of a polymer. The total transition energy presents Eg that increases from 3.9 to 4.2 eV with increasing D from 0.0 to 0.23. The IR band reflects the sub-band transition between valence band and interband levels in the radical anions, and also reflects the transition between interband

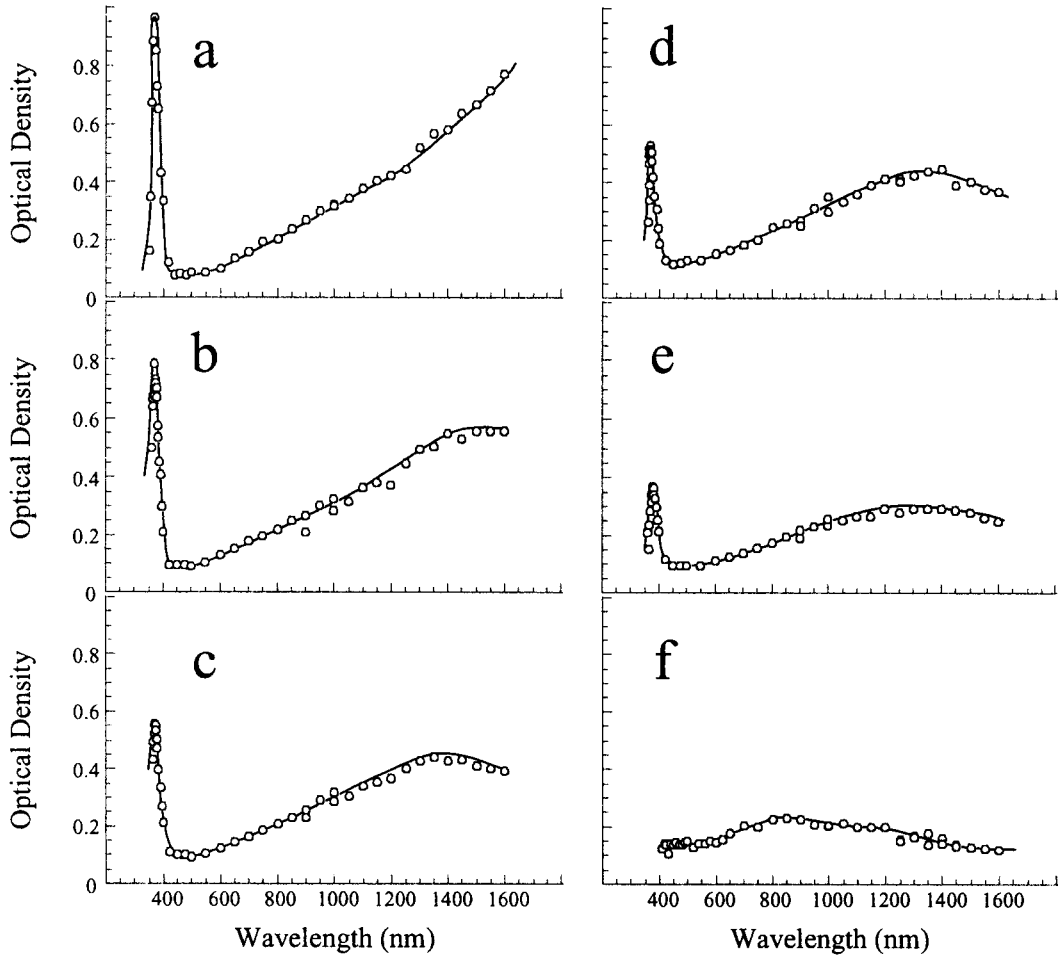

Figure 3-3-7. Transient absorption spectra of radical anions of the polymers at 15 nsec after a pulse. a : PMPS, b : PSi (D = 0.0083), c : PSi (D = 0.065), d : PSi (D = 0.11), e : PSi (D = 0.23), and f : PPS.

levels and conduction band in the radical cations. The present pulse radiolysis technique predominately produces singly charged molecules, thus the interband level may be promoted by polaron interaction between a charge and phonons in a silicon skeleton, and/or charge resonance (CR) interaction between two adjoining σ-conjugated segments. Because of the same total transition energy as Eg in PMPS, and little difference in the total energy of radical cations and anions, the polaron interaction is responsible to the formation of the interband levels. Thus E_{IR} denotes the binding energy (δε) of a polaron state on a Si segment. The value of δε gradually increases with increasing D, and saturates at 0.95 eV and 0.86 eV for the anions and the cations as shown in figure 3-3-9. The kinetic traces of the IR band are summarized in figure 3-3-10 and 3-3-11 for radical cations and anions, respectively. The IR band attributed to the radical anions decays faster when the polymer contains the large number of defects, while showing the same kinetic traces for radical cations. The molecular weight of the polymers was monitored before and after the irradiation to the THF solutions. The G-values (number of reactions per absorbed 100 eV) of main chain scission is estimated at 0.087 and 0.23 for PMPS and PSi (D = 0.23), respectively. This indicates that the radical anion may be a precursor of a chain scission reaction, and an excess electron is localized at the defect on a silicon skeleton leading to side and/or main chain dissociation reactions.

Several groups have been studied the electronic states of conjugated polymer chains with unpaired electrons, suggesting polaron, bipolaron, and charge neutral polaron states.[4,5] It was predicted that the lattice relaxation played a crucial role in determining the state of an electron or a hole on a conjugated polymer chain, such as polyacetylenes.[4,5] Based on the Sandrofy C model,[8] the following formula is obtained as the relation between the polaron width and the binding energy,

$$\delta\varepsilon \approx \left(\frac{\Delta V}{2\alpha}\right)\left(\frac{a}{\zeta_p}\right)^2 \qquad (3\text{-}3\text{-}1)$$

where δε denotes the binding energy of a polaron, a denotes a lattice unit of a trans-chain segment, and ξ_p is the polaron width. V is the matrix element describing the interaction between two atomic orbitals consisting a covalent bond, and Δ also denotes the matrix element between two atomic orbitals of a Si atom. α is represented by,

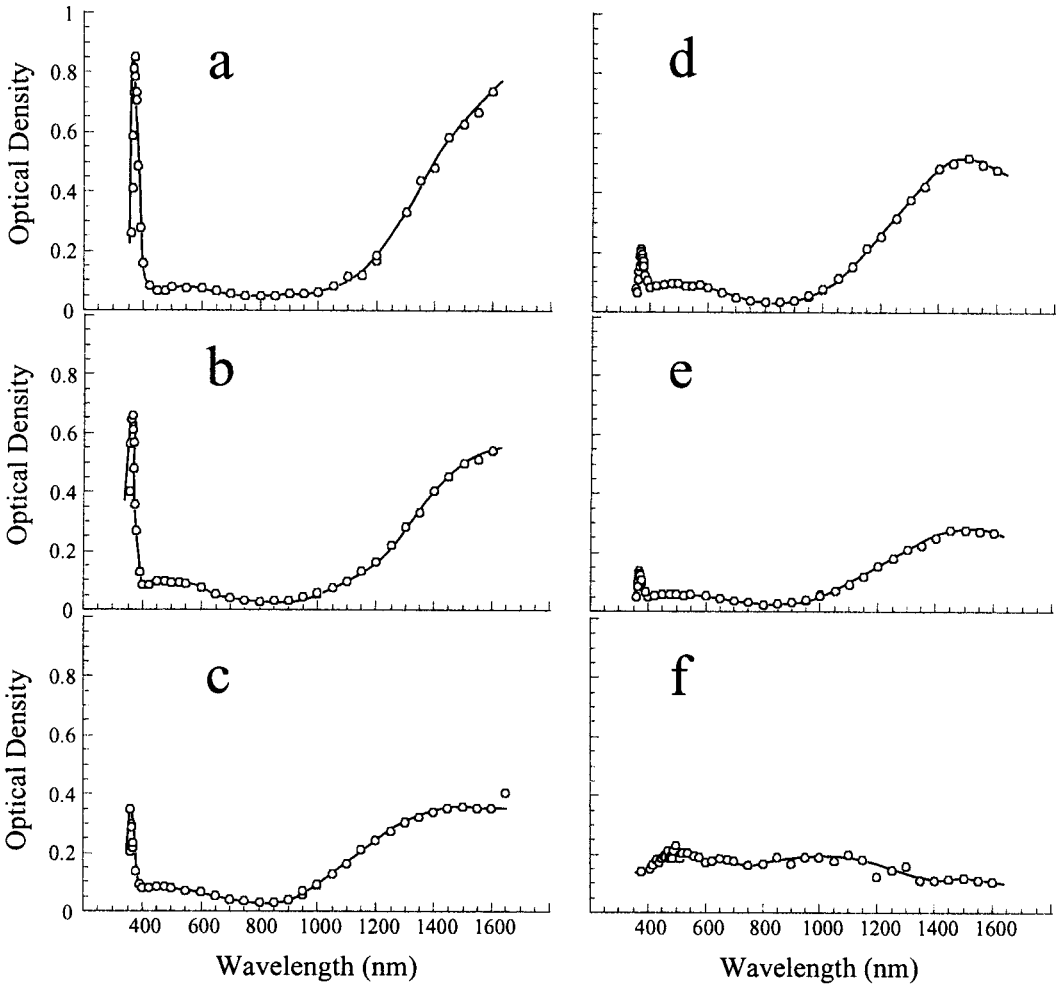

Figure 3-3-8. Transient absorption spectra of radical cations of the polymers at 15 nsec after a pulse. a : PMPS, b : PSi (D = 0.0083), c : PSi (D = 0.065), d : PSi (D = 0.11), e : PSi (D = 0.23), and f : PPS.

$$\alpha \equiv [V(r) - \Delta] \tag{3-3-2}$$

$$r = \frac{a}{\sin\theta} \tag{3-3-3}$$

where 2θ is the tetrahedral bond angle. Thus, Δ is a parameter which specifies the degree of delocalization of σ electrons on a σ-conjugated segment while V described the localization of a pair electrons in a local bond.

The relative polaron width on the polymers can be estimated based on the equation (3-3-1). With the previously reported values of Δ and V in poly(dimethylsilane), the value of $(\Delta V/2\alpha)$ can be estimated as ca. 1 eV.[9] The observed binding energy of positive and negative polarons is also ca. 1 eV in the polymer containing high defect density such as PSi (D = 0.23), giving $\xi_p/a \sim 1$. It suggests the highly polarized polaron state localized on a single Si unit. The polaron relatively delocalizes on a Si conjugated segment in the polysilanes with fewer defects because of the smaller values of $\delta\varepsilon$.

The aryl-substituted polysilanes with Si-based defect structures were already reported to show a broad emission band around 2.9 eV.[6] The intensity of the new emission band had good empirical relation to the amount of silicon branching in the backbone.

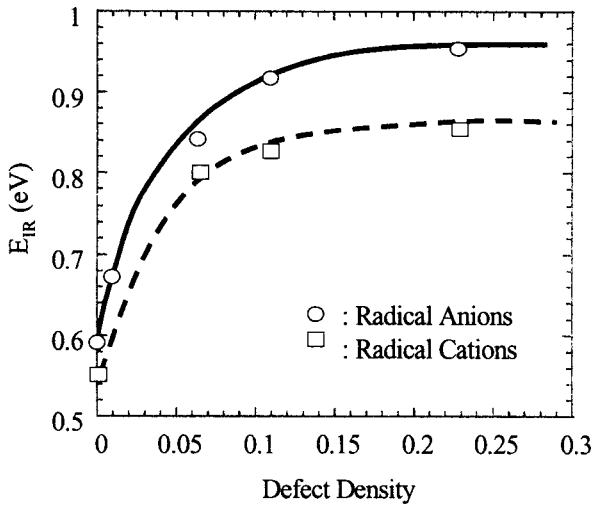

Figure 3-3-9. Dependence of E_{IR} on D. Circles indicate E_{IR} of radical anions, and squares indicate E_{IR} of radical cations

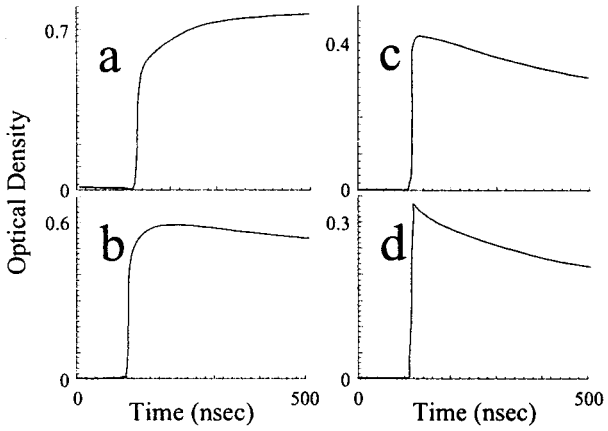

Figure 3-3-10. Kinetic traces of transient absorption of the radical anions in the IR region. a : PMPS monitored at 1600 nm, b : PSi (D = 0.065) monitored at 1450 nm, c : PSi (D = 0.11) monitored at 1350 nm, and d : PSi (D = 0.23) monitored at 1250 nm.

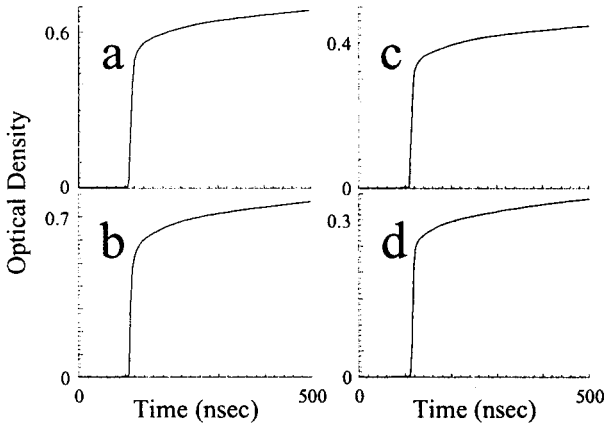

Figure 3-3-11. Kinetic traces of transient absorption of the radical cations in the IR region. a : PMPS monitored at 1600 nm, b : PSi (D = 0.065) monitored at 1550 nm, c : PSi (D = 0.11) monitored at 1500 nm, and d : PSi (D = 0.23) monitored at 1400 nm.

The density of silicon branching in a PMPS was estimated at < 1% considering the relative emission intensity. The authors also reported the number of silicon branching in a PMPS obtained by Wurtz coupling reaction. It was less than 3.5 % which was determined by EPR spectroscopy for silyl radicals migrated into branching points.[10] The potential density of defects in a PMPS was also estimated by the empirical relationship between the hole drift mobility and the defect density, leading to be the value of 0.14 %. In the present study, the relative extinction coefficient of the UV band : ε_{rel} is remarkably affected by the presence of structural defects as shown in figs. 3-3-7 and 8, and as summarized in table 3-3-3. Figure 3-3-12 displays a semi-logarithmic plotting of E_{IR} and ε_{rel} vs D. By the fitting of the plotting, following empirical formula were obtained,

$$\varepsilon_{rel} = 0.25 - 0.27 \cdot \log D \qquad (3\text{-}3\text{-}4)$$

$$\varepsilon_{rel} = -0.11 - 0.42 \cdot \log D \qquad (3\text{-}3\text{-}5)$$

where equation (3-3-4) is obtained as the relation in radical anions, and equation (3-3-5) also represents the relation in radical cations. ε_{rel} = 1 gives the potential density of defects in the PMPS used in the present study, giving D = 1.7 x 10^{-3} from eqn. (3-3-4) and 2.2 x 10^{-3} from eqn. (3-3-5), respectively. The plotting of E_{IR} vs D also gives the following formula,

$$E_{IR} = 1.1 + 0.21 \cdot \log D \qquad (3\text{-}3\text{-}6)$$

$$E_{IR} = 1.0 + 0.19 \cdot \log D \qquad (3\text{-}3\text{-}7)$$

they are respectively obtained as the relation of radical anions and cations. The values of D in the PMPS are evaluated by E_{IR} = 0.59 in equation (3-3-6) and E_{IR} = 0.55 in equation (3-3-7), suggesting D = 4.1 x 10^{-3} and D = 4.2 x 10^{-3}. Thus when the Wurtz coupling reaction is used to synthesize the polysilanes, it is still difficult to prevent the polymer from induced defect structure. However, the molecular weight of the polymer (Mw = 3.2 x 10^4, Mn = 1.8 x 10^4) suggests the degree of polymerization to be a few hundreds. Therefore a few defect structures is maximally present in a PMPS molecule.

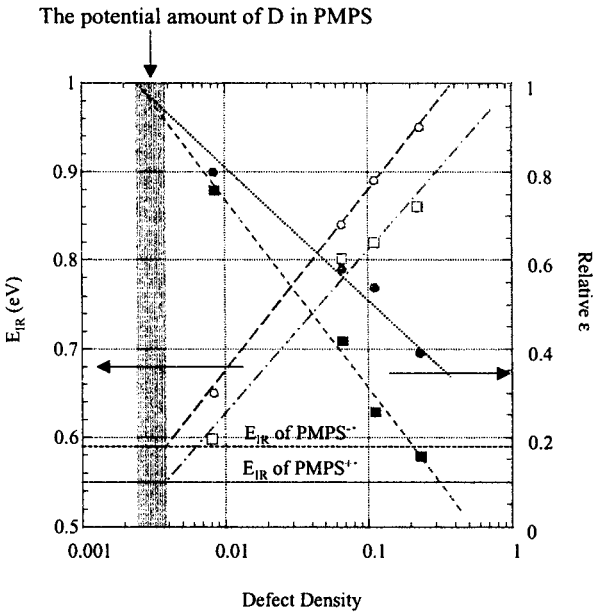

Figure 3-3-12. Semi-logarithmic plotting of E_{IR} and ε_{rel} vs D. The thresholds denote the measured E_{IR} of radical anions and cations of PMPS, which was obtained the conventional Wurtz coupling reactions without using trichlorosilanes.

3-3-4 Summary

The electronic states of excess electrons or holes were investigated by nano-second pulse radiolysis technique. Transient absorption spectroscopy was carried out for radical cations and anions of polysilanes with Si based defect structures. The radical cations and anions of polysilanes displayed near UV and IR absorption maximums at ca. 3.2~3.4 eV and 0.5~1 eV, respectively. They are ascribed to the interband and the subband transition of polaron states. The values of E_{UV} and E_{IR} were

strongly affected by the defect density showing remarkable blue shift in IR absorption. The E_{IR} was interpreted as the degree of electron phonon coupling which rapidly increased with the increasing defect density and saturated at ca. 0.85 eV for radical cations and 0.95 eV for radical anions. This indicates that excess electrons and holes are localized at the defect structures in specimens with more defects, while the charge was relatively delocalized in a conjugated segment in the polysilanes with fewer defects. The author obtains the empilical relation between E_{IR} and D, also between ε_{rel} and D, giving the potential density of Si based defect structures in PMPS as $1\sim5 \times 10^{-3}$.

Section 3-3 Reference

[1] West, R.; Carberry, E. *Science* 1975, **189**, 179.; Carberry, E.; West, R.; Glass, G. E. *J. Am. Chem. Soc.* 1969, **91**, 5446.; Kira, M.; Bock, H.; Hengge, R. *J. Organomet. Chem.* 1979, **164**, 277.

[2] Ban, H.; Sukegawa, K.; Tagawa, S. *Macromolecules* 1987, **20**, 1775; Ban, H.; Sukegawa, K.; Tagawa, S. *Macromolecules* 1988, **21**, 45

[3] West, R.; David, L. D.; Djurovich, P. I.; Stearly, K. L.; Srinivasan, K. S. V.; Yu, H. *J. Am. Chem. Soc.* 1981, **102**, 7352.

[4] Su, W. P.; Schrieffer, J. R.; Heeger, A. J. *Phys. Rev. Lett.* 1979, **58**, 937.; Rice, M. J. *Phys. Lett.* 1979, **A71**, 152.

[5] Rice, M. J.; Phillpot, S. R. *Phys. Rev. Lett.* 1987, **58**, 937.

[6] Fujiki, M. *Chem. Phys. Lett.* 1992, **198**, 177.

[7] van Walree, C. A.; Cleiji, T. J.; Jenneskens, L. W.; Vlietstra, E. J.; van der Laan, G. P.; de Haas, M. P.; Lutz, E. G. *Macromolecules* 1996, **29**, 7362; Seki, S.; Yoshida, Y.; Tagawa, S.; Asai, K.; Ishigure, K.; Furukawa, K.; Fujiki, M.; Matsumoto, N. *Phil. Mag. B* submitted for publication.

[8] for a review, Pitt, C. G. In *Homoatomic Rings, Chains, and Macromolecules of Main Group Elements*; Rheingold, A. L. Ed.; Elsevier: Amsterdam, 1977.

[9] Kumada, M.; Tamao, K. *Adv. Organomet. Chem.* 1968, **6**, 80.; Pollard, W. B.; Lucovsky, G. *Phys. Rev* 1982, **B26**, 3172.

[10] Seki, S.; Cromack, K. R.; Trifunac, A. D.; Yoshida, Y.; Tagawa, S.; Asai, K.; Ishigure, K. *J. Phys. Chem.* 1998, **B102**, 8367.; Seki, S.; Cromack, K. R.; Trifunac, A. D.; Tagawa, S.; Ishigure, K.; Yoshida, Y. *Radiat. Phys. Chem.* 1993, **47**, 217

3-4 The Effects of Structural Defects on Hole Drift Mobility

The effects of a silicon-based structural defect on the hole transport properties of poly(methylphenylsilane) were studied by the DC time-of-flight technique. The defect was chemically introduced as a silicon branching of the silicon backbone by copolymerizing methylphenyldichrolosilane and *p*-tolyltrichlorosilane with sodium. The author obtained a good empirical relation between the hole drift mobility at a zero electric field limit ($\mu_{E=0}$) and the defect density. The value of $\mu_{E=0}$ decreased exponentially from 4 x 10^{-4} to 5 x 10^{-6} ($cm^2/V\cdot sec$) with an exponential increase in defect density from 0.0024 to 0.18. On the basis of Bässler's disorder formalism, hole transport in the polymers was quantitatively analyzed revealing the different contributions of diagonal and off-diagonal disorder with defect density. The degree of fluctuation in the density of state mainly determined the hole drift mobility in specimens with fewer defects, while intersite hopping distance controlled the mobility in the polymers with more defects.

3-4-1 Introduction

Polysilanes containing only silicon in the backbone have attracted considerable attention[1] because of their interesting optoelectric properties such as photovolatilization,[2] nonlinear optical effects,[3] and photoconductivity.[4] These properties originate from the delocalization of Si-Si σ-electrons along main chains called σ-conjugated systems.[5] Although solid state polysilanes have a high electric resistance as insulators, they become p-type semiconductors in the presence of strong electron acceptors.[6] This suggests that the silicon skeleton of polysilane derivatives can intrinsically provide a semiconducting path for holes. Photoconductivity is one of the most practical features of polysilane derivatives. Several detailed studies have been carried out on hole transport phenomena in polysilanes,[4,7] and they showed that polysilanes have the highest hole drift mobility values as amorphous polymer materials without any dopants despite the fact that the polymers consisted of saturated silicon chains. The values in polysilanes are lower than those in amorphous and crystalline silicon which are 3 dimensional analogs of polysilane derivatives. A polysilane molecule has already been revealed to have a backbone consisting of conjugated helical segments joined to each other by a disordered Si conformation. The Poole-Frenkel hopping model provides a better interpretation of the hole transport in 1 dimensional polysilanes,[7,8] indicating the presence of a localized state in a conjugated segment isolated by a disordered and/or metastable conformation of silicon catenation.

Recent studies on charge carrier transport have developed theoretical and experimental treatments of drift mobility in disordered molecular solids.[8,9] Charge transport phenomena in a solid system are considered to be dominated by disorder which can be separated into diagonal and off-diagonal disorder.[8] Generally in the polymer systems, lack of long range order, hence local disorder, cause a transport band to split into multiple hopping sites. This is called diagonal disorder. Further fluctuation in the intersite distance also affects the carrier transport in the medium, and this is described as off-diagonal disorder. Hole transport in polysilane derivatives has often been analyzed using the term of disorder, and it has already been revealed to typically obey the disorder formalism.[8,10] It is also suggested that the several localized states of carriers present in a silicon chain, and the hole transport is controlled by hopping between σ-conjugated segments.

The localized state may be ascribed to a conjugated helical segment, and hoppoing probability between the localized states must depend on the conjugation length and the intersegment distance in silicon skeletons. It is predicted that branching points in the Si catenation change the local molecular structure of polysilane derivatives, and control the length of each conjugated segment and the intersegment distance. Local deformations in the molecular structure are also expected to act as trapping sites for holes conducted along a silicon chain. Van Walree et al. used the microwave conductivity technique to observe charge migration in alkyl substituted polysilanes containing silicon branches, and reported a large decrease in the degree of charge migration caused by the silicon branching.[11] The branching points were concluded to act as scattering points for charge carriers, thus hole mobility value is expected to decrease in polysilanes with silicon branching.

Hole transport was also observed in polysilanes with a variety of molecular weights.[12] The observed drift mobility values increased with increasing molecular weight, indicating changes in the backbone structure with increasing molecular weight. This also suggests that the intermolecular hopping process plays a significant role in the hole transport in polysilanes. The contribution of intermolecular hopping may be clarified by observing the hole transport in polysilanes with structural defects which have controlled σ-conjugated segments in their skeletons.

Table 3-4-1. Characteristics of polysilane derivatives[a]

Entry	D	M_w	T_g(K)
PMPS	0	3.2 x 10^4	379
PSi (D = 0.0024)	0.0024	2.9 x 10^4	381
PSi (D = 0.0060)	0.0060	2.4 x 10^4	379
PSi (D = 0.018)	0.018	2.2 x 10^4	383
PSi (D = 0.045)	0.045	2.3 x 10^4	386
PSi (D = 0.090)	0.090	1.9 x 10^4	395
PSi (D = 0.18)	0.18	2.8 x 10^4	401

[a] D, Si based defect density per total Si units; *Mw*, weight average molecular weight; *Tg*, glass transition temperature.

This section reports the direct observation of hole transport in aryl-substituted polysilanes with structural defects by using the time-of-flight (TOF) technique. The author discusses the TOF signals and hole drift mobility in the polysilanes by a quantitative treatment of each disorder factor. The hole mobility values are discussed as a function of the silicon branching density. The hole mobility dependence on defect density allows the author to estimate the mobility value in polysilanes with no branching structure. The potential amount of silicon branching is also determined in a linear polysilane obtained by a conventional Wurtz coupling reaction.

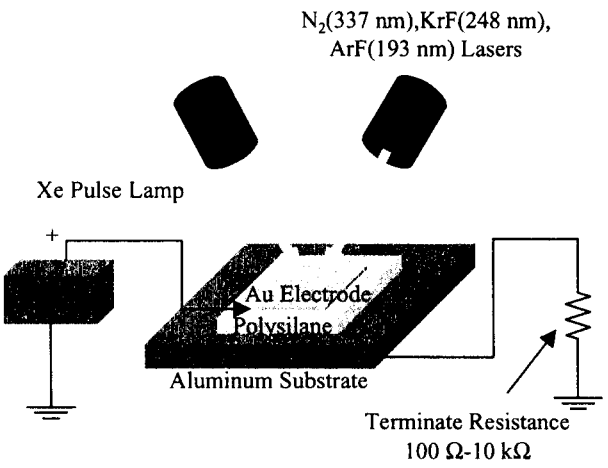

Figure 3-4-1. Schematic diagram of the measurement system of TOF.

3-4-2 Experimental

Linear poly(methylphenylsilane) (PMPS) was synthesized by the conventional sodium condensation method from methylphenyldichlorosilane monomer. Defect-containing PMPS was synthesized by the same procedure with a mixture of methylphenyldichlorosilane and *p*-tolytrichlorosilane monomers. The ratio of the mixture ranged from 0.3 wt % to 20 wt %. All the chlorosilanes the author used were doubly distilled products from Shin-Etsu Chemical Co. Ltd. The polymerization reactions were carried out in an Ar atmosphere, in 100 ml toluene with 20 ml diethyleneglycoledimethylether as the solvent. The monomer was put into the reaction vessel and mixed with sodium dispersion for 15 hours at 75°C. Sodium dispersion in toluene was purchased from Acros Co. LTD. Solutions of PMPS and defect-containing PMPS were precipitated using isopropyl alcohol after filtration to remove NaCl, and the precipitates were dried in a vacuum. Toluene solutions of the polymers were transferred into separatory funnels, washed with water, and precipitated twice with toluene-isopropyl alcohol and a tetrahydrofuran (THF)-methanol mixture to eliminate residual NaCl. PMPS and PMPS containing defects showed good solubility in toluene, THF, 2-methyltetrahydrofuran (MTHF), chloroform and dichloromethane. The amount of residual Cl atoms was confirmed to be less than 0.1 % in all the polysilane derivatives by elemental analysis. For polysilanes containing defects, the ratio of branching structure for each polymer was confirmed from the H contents of p-tolyl and methyl substituents determined by a JEOL EX-270 ^{1}H NMR spectrometer in the Institute of Scientific and Industrial Research, Osaka University. The molecular weight distributions in all the polymers were measured with a Shimadzu C-R3A gel permeation chromatography (GPC) system. Glass transition temperatures were measured with a Perkin-Elmer DSC-7 system.

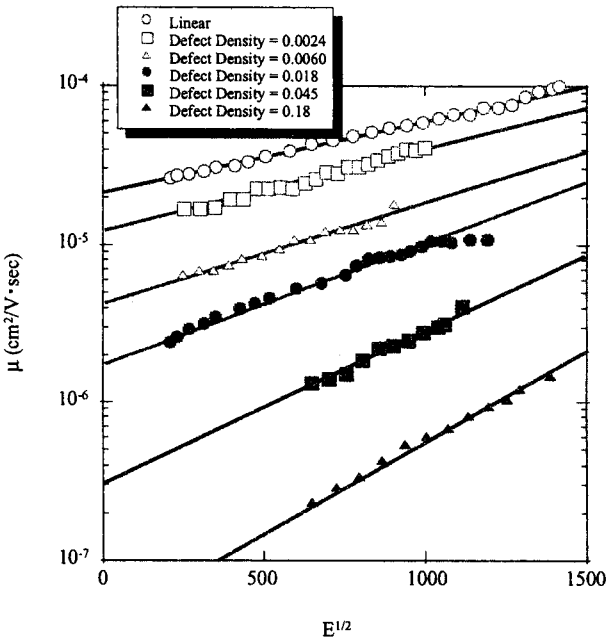

Figure 3-4-2. Semilogarithmic plot of hole drift mobility μ against $E^{1/2}$ in all defect-containing polysilanes at 295 K.

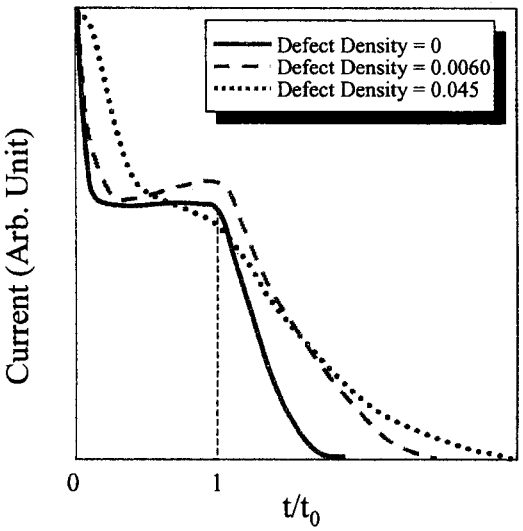

Figure 3-4-3. TOF signals measured in PMPS (solid), PSi (D = 0.0060) (dashed), and PSi (D = 0.045) (doted) at 295 K, E=6.5x10^5 V/cm. All curves are normalized at their average flight time.

Photo-generated carrier drift mobility was measured by the current-mode TOF technique. Polymer films were coated on an Al substrate at 10 ~ 20 μm thick. They

were in turn coated with a semitransparent Au top electrode as illustrated in figure 3-4-1. The schematic diagram of Time-of-Flight carrier mobility measurement system was also shown in fig. 3-4-1. Current transient could be photoexcited at the upper surface of the film using attenuated 337 nm and 248 nm pulses from N_2 and Lambda Physik Compex102 KrF excimer lasers. The pulse energy was generally attenuated down to a 100 $\mu J/cm^2$ · pulse, with a pulse width of 4 ~ 10 nsec. The experiment was carried out in an environmental chamber in which the temperature could be varied from 180 K to 380 K, and stabilized to better than 1 K. The signal voltage was developed across a sensing resistor (300 ~ 30kΩ) in a circuit whose overall time constant was kept below the transient time, and acquired by a Tektronics TDS420A digitizing oscilloscope. TOF observation was carried out in a 243 K to 313 K temperature range except for the highly defect induced polysilanes (defect density over 0.045) which crack when cooled below 270 K.

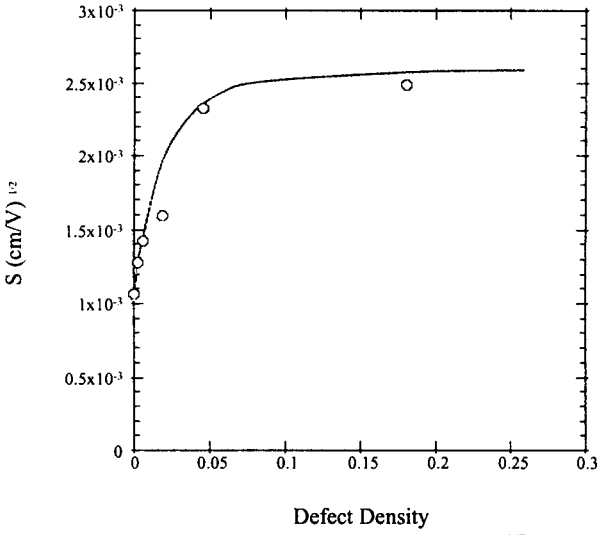

Figure 3-4-4. Changes in the slope of log $\mu(E^{1/2})$ line plotted to defect density in the polymers. The slope fitted the data obtained at 295 K.

3-4-3 Results and Discussion

The obtained polymers and their characteristics are summarized in table 3-4-1. The glass transition temperature of the polymers increases gradually with defect density in the polymers. This indicates that the backbone structure is affected by the numbers of branching points. A ^{29}Si NMR study on polysilanes containing structural defects reported additional broad signals that were ascribed to Si-Si bond elongation at branching points.[13] It suggested that branching points were actually induced in the polymer main chain. TOF measurements of hole drift mobility were carried out at 295 K for the polymers. The mobility values: μ were calculated from the mean arrival time of the carriers, which was inferred from the time at which the tangents to the plateau and tail intersected in the TOF signals. However the plateau region was almost indistinguishable in the signal observed with PSi (Defect Density : D = 0.18). Figure 3-4-2 plots log μ of linear and defect-containing polysilanes against $E^{1/2}$. The μ value in polysilanes is reported to increase with E in a Poole-Frenkel fashion in spite of showing saturation in a low field.[8-10] The obtained log μ(E) is also proportional to $E^{1/2}$ for all defect-containing polysilanes. However, μ(E) saturated in a higher field region for defect-containing polysilanes than for PMPS. The hole drift mobility value drops two orders of magnitude in PSi (D = 0.18) in comparison with that in PMPS. This generally indicates that silicon branching acts as a hole trapping site, and both intra- and inter-molecular hopping probability decreases in polysilanes containing defects.

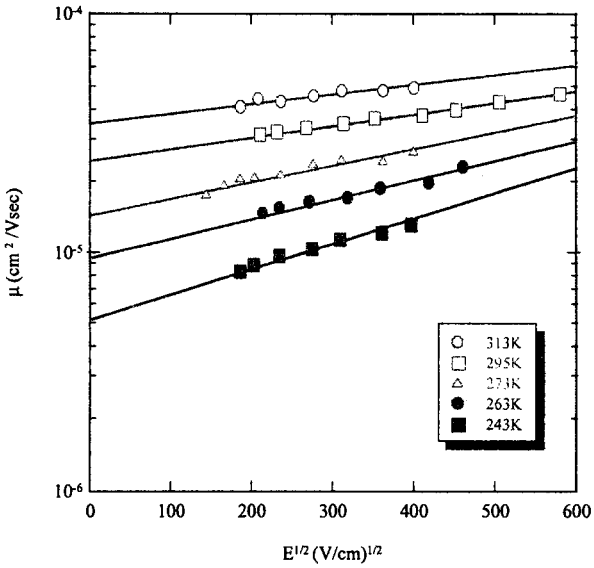

Figure 3-4-5. Semilogarithmic plot of hole drift mobility μ against $E^{1/2}$ in PMPS at a variety of temperature.

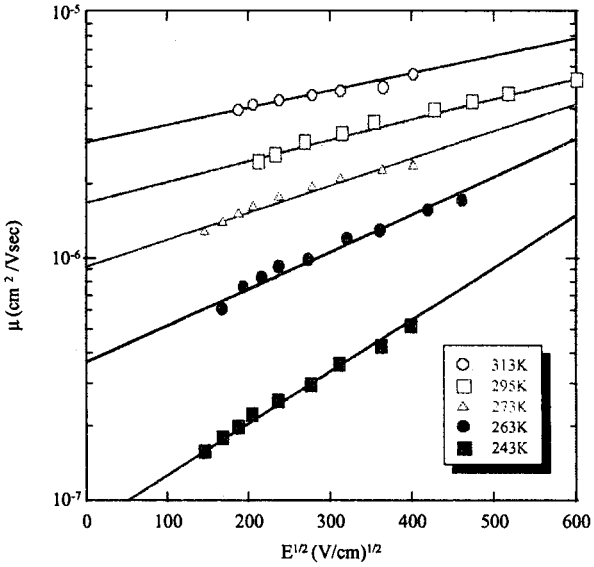

Figure 3-4-6. Semilogarithmic plot of hole drift mobility μ against $E^{1/2}$ in PSi (D = 0.018) at a variety of temperature.

Figure 3-4-3 shows a series of normalized TOF signals for PMPS, PSi (D = 0.0060), and PSi (D = 0.045) at 295K, E = 6.5 x 10^5 V/cm. The anomalous broadening of

the TOF signals is due to the non-thermal field-assisted spreading of the drifting hole plane. There is a large deformation in the signals for the polymers containing a large number of defect structures. A signal obtained in PSi (D = 0.0060) shows a slight transient increase in the current at plateau region. The author obtained symmetrical signals upon exposure to light pulses with energy in the 1 mJ/cm^2 · pulse to 30 $\mu J/cm^2$ · pulse range. This suggests that delayed geminate pair dissociation is responsible for the increase in plateaus rather than the space-charge effects caused by high density excitation. The deformation of signals in PSi (D = 0.045) is due to not only delayed geminate pair dissociation but competition between several different hole transport routes leading to the sudden trapping of charge carriers in a low field. The yield of photo-generated holes can also be estimated by integration of transient current. The yields relative to PMPS are 0.48 and 0.099 for PSi (D = 0.0060) and PSi (D = 0.045), respectively. The large decrease with increases in defect density suggests that defects strongly affect the mechanism which releases holes from the excited state upon exposure to UV light, and decrease the efficiency of geminate pair dissociation.

The authors' previous study reported that the optical properties of the polymer changed with defect density.[14] The intense UV absorption, which had been ascribed to the transition to exciton states, shows a gradual blue shift and broadening with increasing defects. This suggests that the density of states (DOS) must be changed in the polymeric system. The deformation of TOF signals should be predominately ascribed to disorder transition with increasing defects. Bässler suggested a disorder formalism in which carrier transport phenomena are quantitatively analyzed using the Monte-Carlo technique. Charge carrier mobility in a disordered molecular solid should obey the following expression of the form,[8,15]

$$\mu(T,E) = \mu_0 \exp\left[-\left(\frac{2\sigma}{3kT}\right)^2\right] \times \exp\left[C\left\{\left(\frac{\sigma}{kT}\right)^2 - \Sigma^2\right\}\sqrt{E}\right] \quad (3\text{-}4\text{-}1)$$

where σ is the width of DOS reflecting the diagonal disorder parameter , Σ is the intersite distance reflecting the off-diagonal parameter, and C is an empirical constant.

The experimental results on field dependence of μ are analyzed with the equation to gain an insight into the effect of disorder parameters. Figure 3-4-4 plots the slope of μ in fig. 3-4-2 versus the defect density in the polymers. S is represented by,

$$S = C\left\{\left(\frac{\sigma}{kT}\right)^2 - \Sigma^2\right\} \quad (3\text{-}4\text{-}2)$$

S rapidly increases with defect density, and saturates at about 2.5 x 10^{-3} $(cm/V)^{1/2}$ for defect densities over 0.1. This suggests that there is a rapid increase in σ with increasing defect density, and that the contribution of σ to hole mobility is larger than that of Σ in defect-containing polysilanes. Defect structures in the silicon skeleton disturb its σ-conjugation, and shorten the conjugation length leading to an increase in energetic disorder. The anomalous broadening of the TOF signals shown in fig. 3-4-3 also supports the notion of an increase in σ. The author discusses the temperature dependence of μ for the polymers to distinguish the contributions from the two parameters.

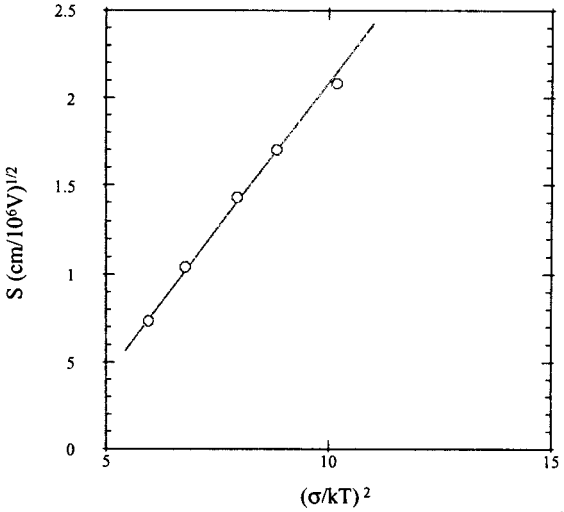

Figure 3-4-7. The slope parameter : S of log μ vs. $E^{1/2}$ plots to diagonal disorder : (σ/kT) in PMPS.

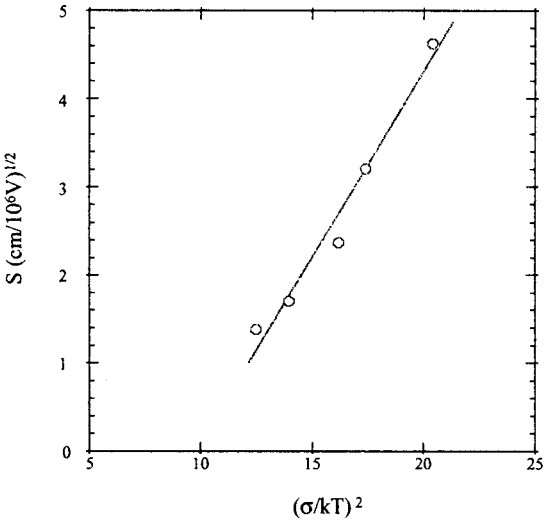

Figure 3-4-8. The slope parameter : S of log μ vs. $E^{1/2}$ plots to diagonal disorder : (σ/kT) in PSi (D = 0.018).

Figures 3-4-5 and 3-4-6 plot the field dependence of μ at various temperatures for PMPS and PSi (D = 0.018) which is chosen as a typical defect-containing polysilane. The hole mobility in this temperature and electric field range seems to obey the Poole-Frenkel law,

$$\ln \mu \propto SE^{1/2} \quad (3\text{-}4\text{-}3)$$

with good agreement for both polymers. The slope S of the field dependence in PSi (D = 0.018) is clearly larger at any temperature than the corresponding S value in PMPS. This suggests a large σ contribution to hole

transport in defect-containing polysilanes. Σ is determined by the non-Arrhenium type plotting of zero field limit mobility which is obtained by extrapolating figs. 3-4-5 and 3-4-6. The S values are plotted against a temperature dependent diagonal disorder parameter $(\sigma/kT)^2$ in figs. 3-4-7 and 3-4-8 for PMPS and PSi (D=0.018), respectively. The slope in the figures gives parameter C in equation (3-4-1) as 3.1×10^{-4} and 3.9×10^{-4} $(cm/V)^{1/2}$ for PMPS and PSi (D = 0.018), respectively. C shows good agreement with previously reported values of experimental and Monte-Calro simulation results in PMPS. However in PSi (D = 0.018), the obtained C is very large compared with other polymers. This is due to the thermally induced contribution of off-diagonal disorder in the temperature range. The Σ values are also obtained from the intersection of the S(σ/kT) line with S = 0 yielding Σ = 1.8 for PMPS and Σ = 3.2 for PSi (D = 0.018). The obtained values of Σ are summarized in table 3-4-2. The Σ values are almost constant around 1.8 followed by rapid increase in Σ with increasing defect density over 0.018, which suggests that the intermolecular hopping probability is reduced when there is a certain number of defects in the skeleton.

Figures 3-4-9 and 3-4-10 plot zero field limit mobility $\mu_{E=0}$ in various defect-containing polysilanes versus 1/T and $1/T^2$, respectively. The non–Arrhenius type plotting (fig. 3-4-10) provides a better fit for the obtained results. Arrhenius plotting gives the carrier activation energy by the following formula,[15,16]

$$\mu(E,T) = \mu_0 \exp\left[-\frac{\varepsilon_0 - \beta E^{1/2}}{kT_{eff}}\right] \quad (3\text{-}4\text{-}4)$$

where $1/T_{eff} = 1/T - 1/T_0$, ε_0 denotes zero field activation energy, which was proposed by Gill for hole transport in poly(vinylcarbazole).[16] T_0 can be calculated by the Arrhenius plotting of μ parametric in applied voltage. In the present case, T_0=398 K and 402 K are obtained for PMPS and PSi (D = 0.018), respectively.

The obtained activation energy is summarized in table 3-4-2 for the polysilanes. The values of σ in eqn. (3-4-1) can be calculated from the $(1/T)^2$ dependence in fig. 3-4-10. The obtained values are also summarized in table 3-4-2. Prefactor mobility μ_0 is also estimated by extrapolation of the non-Arrhenius type plotting. The zero field activation energy suddenly increases when defect structures are introduced with a density of more than about 0.003. The author predicts that a small number of defect structures will not affect the conjugation length in the silicon skeleton, and that the holes will delocalize to the same degree in the polysilane with a small number of defects (e.g. defect density = 0.0024) as in PMPS. However, the absolute value of hole drift mobility in PSi (D = 0.0024) is half that in PMPS, indicating a reduction in intermolecular hopping probability caused by the defect points. The author also suggests that off-diagonal disorder, that is the intersite hopping distance, controls the hole transport in the polysilanes containing a large number of defects, in contrast to the dominant effect of diagonal disorder on hole transport in polysilanes with a small number of defects. The DOS width exhibits the same tendency as the activation energy. There is little difference in the DOS width in PMPS and PSi (D = 0.0024), which is supported by optical measurements indicating little difference in the extinction coefficient and FWHM of the UV absorption band in the polymers.[13]

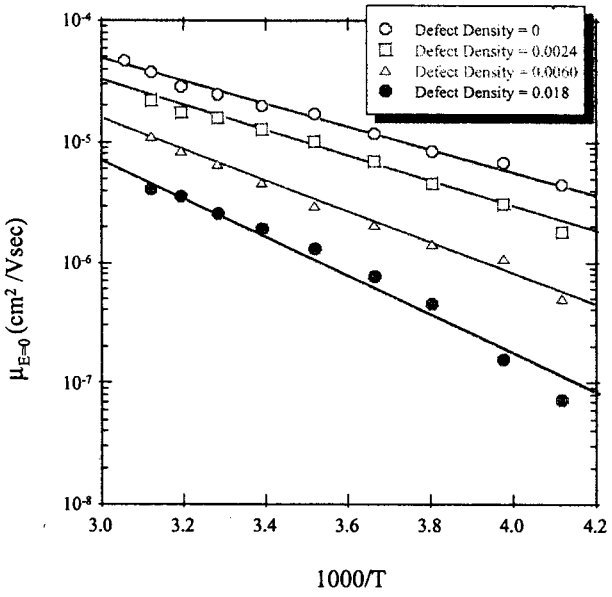

Figure 3-4-9. Arrhenius plots of hole drift mobility in PMPS, PSi (D = 0.0024), PSi (D = 0.006), and PSi (D = 0.018). Lines indicate least-squares fit to each data set leading to activation energy.

Table 3-4-2. Activation energy and density of states in defect induced polysilanes

D	μ_0 (cm^2/V·sec)	ε_0/k (K)	ε_0 (eV)	$(2\sigma/3k)^2$ (K^2)	σ (eV)	Σ
0	4.3×10^{-4}	1.9×10^{3}	0.16	2.69×10^{5}	0.066	1.8
0.0024	2.7×10^{-4}	2.0×10^{3}	0.17	2.74×10^{5}	0.068	1.8
0.0060	2.2×10^{-4}	2.5×10^{3}	0.22	3.45×10^{5}	0.076	1.9
0.018	1.1×10^{-4}	3.9×10^{3}	0.34	5.34×10^{5}	0.094	3.2
0.045	2.3×10^{-5}	5.6×10^{3}	0.49	8.38×10^{6}	0.11	3.6

Table 3-4-3. Polaron formation energy and energetic disorder of DOS in polysilanes calculated by Bässler and Borsenberger's equation[a]

Defect Density	E_p (eV)	σ (eV)
0	0.28	0.059
0.0024	0.33	0.066
0.0060	0.46	0.075
0.018	0.56	0.095

[a] Ep, polaron formation energy; σ, diagonal disorder parameter.

The increasing values of σ also suggest the presence of a backbone-derived localized state attributed to a local deformation of the chain structure. The holes in the skeleton possibly interact with backbone phonons giving polaron states. The formation energy of the positive polarons increases with increasing D. This leads to a decrease in the probability of intersite hopping, and also to a decrease in drift mobility. This prospect is experimentally supported by the nonlinearity of the plots of both log μ vs T^{-1} and T^{-2} (figs. 3-4-9 and 3-4-10), indicating that neither form (3-4-1) nor (3-4-4) can satisfactorily explain the present results. Bässler and Borsenberger suggested models for the treatment of μ which take the contribution of polaron formation energy into account.[17] The following equation gives the temperature dependence in the rate of hopping υ_{ij} between sites i and j which have potentials of ε_i and ε_j, respectively,

$$\upsilon_{ij} = \upsilon_0 \exp\left(-2\gamma a \frac{\Delta R_{ij}}{a}\right) \times \exp\left(-\frac{E_p}{2kT}\right) \exp\left[-\left(\frac{\varepsilon_j - \varepsilon_i}{kT}\right)\right] \quad ;\varepsilon_j > \varepsilon_i$$

$$\upsilon_{ij} = \upsilon_0 \exp\left(-2\gamma a \frac{\Delta R_{ij}}{a}\right) \exp\left(-\frac{E_p}{2kT}\right) \quad ;\varepsilon_j < \varepsilon_i \qquad (3\text{-}4\text{-}5)$$

where υ_0 is the prefactor hopping rate, γ an inverse wavefunction decay constant, ΔR_{ij} the intersite distance between site i and j. E_p denotes the polaron formation energy, thus $E_p/2$ reflects the excess activation energy ascribed to the deviation of the Arrhenius type plotting from linearity as shown in fig. 3-4-9 Equation (3-4-5) leads to the following temperature dependence of the zero-field mobility,

$$\mu(T, E=0) \propto \exp\left[-\left(\frac{2\sigma}{3kT}\right)^2 - \frac{E_p}{2kT}\right] \qquad (3\text{-}4\text{-}6)$$

and the differential of equation (3-4-6) yields the effective Arrhenius activation energy Δ^{eff} as

$$\Delta^{eff} = -k\frac{\partial}{\partial(1/T)}\ln\mu(E=0) = \frac{8\sigma^2}{9kT} - \frac{E_p}{2} \qquad (3\text{-}4\text{-}7)$$

The value of log $\mu_{E=0}$ in fig. 3-4-9 is fitted at each limited section by a quadratic function by the least squares method, and the obtained slope at each temperature is plotted versus 1/T in figure 3-4-11. Based on equation (3-4-7), the slope provides the values of σ, and E_p is estimated as Δ^{eff} at T= ∞. The obtained values of σ and E_p are summarized in table 3-4-3. The σ values show good agreement with that obtained by analysis with the disorder-controlled transport theory in table 3-4-2. However, E_p gradually increases with increasing D. Local deformation in the molecular structure at branching points may be responsible for the increasing E_p, and μ is also interpreted as being controlled by polaron formation in the polysilanes with a small number of defects.

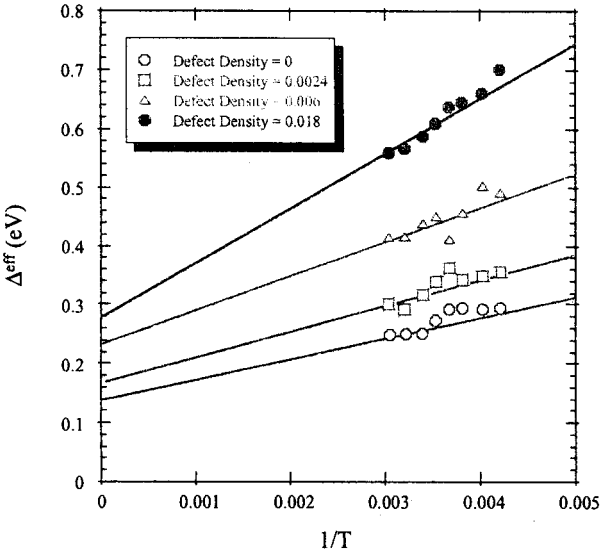

Figure 3-4-11. Effective activation energy: Δ^{eff} vs. T^{-1}.

The S value is interpreted as representing the overall effects of diagonal and off-diagonal disorder, and is sensitive to the presence of structural defects in the backbone. This indicates that the zero field limit mobility rapidly decreases with increasing defect density. $\mu_{E=0}$ is considered to be an approximate reflection of the degree of delocalization of a hole in a segment at a given temperature, and clearly depends on the defect density in polysilanes as shown in fig. 3-4-3. Figure 3-4-12 plots $\mu_{E=0}$ vs defect density with a threshold which denotes the $\mu_{E=0}$ obtained in the PMPS used in the present study. The following relationship is obtained empirically,

$$\mu(E=0) = 6.2\times10^{-8}\times D^{-1.3} \qquad (3\text{-}4\text{-}8)$$

where D denotes the Si based defect density per total Si units. Aryl-substituted polysilanes with Si-based de-

fect structures have already been reported to show a broad emission band around 2.9 eV.[12] The intensity of the new emission band related well to the amount of silicon branching in the backbone. This suggests that the density of silicon branching in linear polysilane was < 1% considering the relative emission intensity. The authors' previous study also suggested that the residual amount of silicon branching in polysilane obtained by the Wurtz coupling reaction was less than 3.5 %. This was determined by EPR spectroscopy for silyl radicals which had migrated into branching points.[13] In the present study, the potential number of defect structures can be evaluated from the intersection of the extrapolated $\mu(E = 0, D)$ line with the threshold. The calculated defect density is 1.4×10^{-3} for PMPS *obtained in this study without using trichlorosilane.* Thus when the Wurtz coupling reaction is employed to synthesize the polysilanes, it is still difficult to prevent the polymer from induced defect structure. However, the molecular weight of the polymer (Mw = 3.2×10^4, Mn = 1.8×10^4) suggests the degree of polymerization to be a few hundreds. Therefore, a maximum of one or two defect structures are present in a polysilane molecule. It has been considered that hole mobility in linear polysilane molecules is determined by intramolecular hopping between σ-conjugated segments in the silicon skeleton. The present results suggest that intermolecular hopping processes can compete with intramolecular hopping processes. This view is also substantiated by the relatively large effects of off-diagonal disorder on hole mobility in slightly defect induced polysilanes.

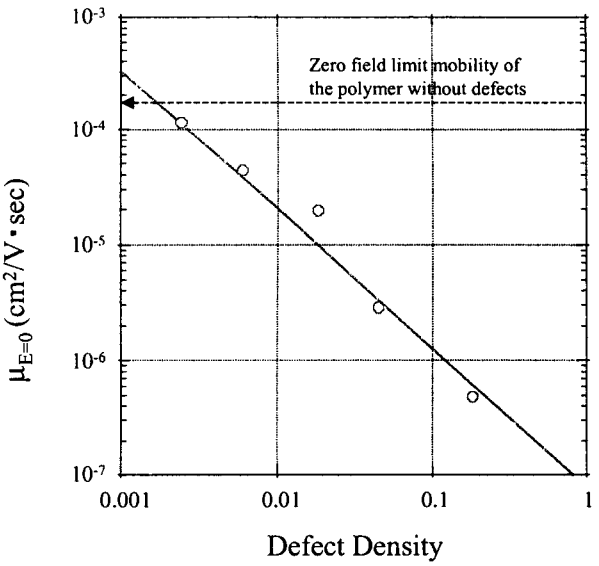

Figure 3-4-12. Dependence of zero field limit mobility $\mu_{E=0}$ on defect density in the polymers. Dashed line denotes the value of hole drift mobility in PMPS obtained by Wurtz condensation in the present study.

3-4-4 Summary

The author studied the hole transport properties in PMPS with controlled defect densities by the DC TOF technique. The hole drift mobility value strongly depends on the defect density, and is two orders of magnitude lower in PSi (D = 0.18) than in PMPS. The author analyzed the observed TOF signal and hole drift mobility in the polymers on the basis of Bässler's disorder formalism. Hole transport in polymers with a lower defect density was dominated by the degree of fluctuation in the density of states, though the mobility was controlled by the intersite hopping distance in specimens with higher defect densities. The value of $\mu_{E=0}$ was sensitive to the presence of structural defects in the backbone, and decreased exponentially from 4×10^{-4} to 5×10^{-6} ($cm^2/V \cdot sec$) as the defect density increased exponentially from 0.0024 to 0.18. The empirical relation was clearly obtained between defect density and $\mu_{E=0}$ in the present section. It is also suggested that a few defect structures should be introduced in a silicon skeleton by using the Wurtz coupling reaction.

Section 3-4 Reference

[1] for a review, Miller, R. D.; Michl, J. *Chem Rev.* 1989, **89**, 1359.

[2] Zeigler, J. M.; Harrah, L. A.; Johnson, A. W. *Proc. SPIE* 1985, **536**, 166.; Hofer, D. C.; Miller, R. D.; Wilson, C. G. *Proc. SPIE* 1984, **246**, 16.

[3] Kajar, F.; Messier, J.; Rosilo, C. *J. Appl. Phys.* 1986, **60**, 3040.

[4] Kepler, R. G.; Zeigler, J. M.; Harrah, L. A.; Kurtz, S. R. *Phys. Rev.* 1987, **B35**, 2818.; Fujino, M. *Chem. Phys. Lett.* 1987, **136**, 451.; Stolka, M.; Yuh, H. J.; McGrane, K.; Pai, D. M. *J. Polym. Sci., Polym. Chem. Ed.* 1987, **25**, 823.

[5] Su, W. P.; Schrieffer, J. R.; Heeger, A. J. *Phys. Rev. Lett.* 1979, **58**, 937.;Rice, M. J.; Phillpot, S. R. *Phys. Rev. Lett.* 1987, **58**, 937.; Rice, M. J. *Phys. Lett.* 1979, **A71**, 152.; Phillpot, S. R. *Phys. Lett.* 1987, **31**, 43.; Takeda, K.; Fujino, M.; Seki, K.; Inokuchi, H. *Phys. Rev.* 1987, **B36**, 8129.

[6] West, R.; David, L. D.; Djurovich, P. I.; Stearly, K. L.; Srinivasan, K. S. V.; Yu, H. *J. Am. Chem. Soc.* 1981, **102**, 7352.

[7] Kepler, R. G.; Zeigler, J. M.; Harrah, L. A.; Kurtz, S. R. *Bull. Am. Phys. Soc.* 1984, **29**, 509.; Kepler, R. G.; Zeigler, J. M.; Harrah, L. A.; Kurtz, S. R. *Bull. Am. Phys. Soc.* 1984, **28**, 362.; Abkowitz, M. A.; Knier, F. E.; Yuh, H. J.; Weagley, R. J.; Stolka, M. *Solid State Commun.* 1987, **62**, 547.; Abkowitz, M. A.; Rice, M. J.; Stolka, M. *Phil. Mag.* 1990, **B61**, 25.

[8] Bässler, H. *Phys. Stat. Sol.* 1993, **B175**, 15

[9] Dieckmann, A.; Bässler, H.; Borsenberger, P. M. *J. Chem. Phys.* 1993, **99**, 8136.; Borsenberger, P. M.; Pautmeier, L. T.; Bässler, H. *Phys. Rev.* 1992, **46**, 12145.; Schönherr, G.; Bässler, H.; Silver, M. *Phil. Mag.* 1981, **B44**, 47.; Pautmeier, L.; Richert, R.; Bässler, H. *Phil. Mag. Lett.* 1989, **59**, 325.; Yuh, H. J.; Stolka, M. *Phil. Mag.* 1988, **B58**, 539.

[10] Yokoyama, K.; Yokoyama, M. *Phil. Mag.* 1990, **61**, 59.; Yokoyama, K.; Yokoyama, M. *Solid St. Commun.* 1989, **70**, 241.; Dohmaru, T.; Oka, K.; Yajima, T.; Miyamoto, M.; Nakayama, Y.; Kawamura, T.;

West, R. *Phil. Mag.* 1995, **B71**, 1069.
[11] van Walree, C. A.; Cleiji, T. J.; Jenneskens, L. W.; Vlietstra, E. J.; van der Laan, G. P.; de Haas, M. P.; Lutz, E. G. *Macromolecules* 1996, **29**, 7362.
[12] Fujiki, M. *Chem. Phys. Lett.* **1992**, 198, 177.
[13] Seki, S.; Cromack, K. R.; Trifunac, A. D.; Yoshida, Y.; Tagawa, S.; Asai, K.; Ishigure, K. *J. Phys. Chem.* 1998, **B102**, 8367.
[14] Seki, S.; Cromack, K. R.; Trifunac, A. D.; Tagawa, S.; Ishigure, K.; Yoshida, Y. (1995) *Radiat. Phys. Chem.* , **47**, 217
[15] Abkowitz, M. A.; Bässler, H.; Stolka, M. *Phil. Mag.* **1991**, B63, 201.; Pai, D. M. *J. Chem. Phys.* 1970, **52**, 2285.
[16] Gill, W. D. *J. Appl. Phys.* 1972, **43**, 5033.
[17] Bässler, H.; Bosenberger, P. M.; Perry, R. J. *J. Polym. Sci. Polym. Phys.* 1994, **B32**, 1677.

Chapter 4 Polysilanes as Radiation Sensitive Materials

4-1 Reactive Intermediates

The present section reports the observation of silyl radicals induced by γ-ray irradiation of solid polysilane. In spite of extensive studies of the photo and radiation chemistry on oligosilane molecules, there have been few studies on high molecular weight polysilane. Several previous studies of photolysis of polysilanes have suggested that the predominant intermediates should be silyl radicals generated by homolysis of the silicon skeleton of polysilanes. However the direct observation of silyl radical formation has not been reported until recently. Irradiation of solid poly(dimethylsilane) with γ-rays induced EPR signals that are explained by silyl radical formation as a result of main chain scission in polysilane.

4-1-1 Introduction

Polysilanes have been presumed to undergo main chain scission upon exposure for UV light, and potential uses of polysilanes as UV photoresist materials has already been reported by several groups. However, the reactive intermediates of photo- and radiation induced reactions has not been delineated in these polymer materials. Only a few investigatiors have reported on the natures of UV light-induced reactive intermediates of polysilanes by means of EPR spectroscopy. McKinly et al. reported that 248-330 nm light induced radical species in alkyl substituted polysilanes (di-n-pentyl and methylpenthyl substituted polysilanes) in n-octane and n-pentane solution at 200 K – 350 K.[1] The structure of the initial persistent radicals observed was -SiR_2-Si· R-SiR_2- indicating alkyl side chain scission rather than main chain silicon-silicon bond scission. This implied that the silicon-centered biradical formation occurred as a result of UV light exposure, and they proposed the following three primary reaction routes : (1) silylene extraction, (2) homolytic cleavage, and (3) alkyl side chain elimination followed by polymer skeleton scission. Their EPR spectra supported the reaction routes (1) and (3), but not route (2). Todesco et al. also reported UV light induced radical formation in the solution of poly[dimethylsilane-co-methyl(1-naphtylsilane] in methyltetrahydrofran.[2] However, their EPR spectrum is not consistent with that of the silyl radicals since the species they observed exhibited large hyperfine coupling. Thus, it appears that while silyl radical formation must be the ubiquitous results of homolytic cleavage of silicon skeleton on photolysis, it has not been directly observed so far.

Many investigations have been reported for small oligosilane molecules. Silyl radical formation for alkyl substituted, silicon-centered molecules was observed and confirmed by several research efforts in the 1970's. Benett et al.[3] and Krusic et al.[4] reported trimethylsilyl radical formation for UV light exposure to trimethylsilane in di-t-butyl peroxide solution at 153K. The observed EPR spectrum showed surprisingly small hyperfine splitting (0.634 mT for β-hydrogen) compared with t-butyl radical. Benett et al.[5] and Cooper et al.[6] also presented the EPR spectra of dimethyl-(trimetylsilyl)silyl radicals generated by UV light exposure for pentamethyldisilane solution in di-t-butyl peroxide. The coupling constant of β-hydrogen for this radical (0.821 mT) was somewhat larger in comparison with Me_3Si·, and It was ascribed to the conjugative interaction with the neighboring silicon atom. These small silane molecules serve as models for the repeat unit in longer polysilanes.

The present section describes the direct observation of silyl radicals in solid phase poly(dimethylsilane).

Table 4-1-1. Coupling constants of poly(dimethylsilane) radical

Radicals	Coupling Constants (mT)	
	β-H	γ-H
PDMS	0.813	0.046
Me_3SiMe_2Si·[a]	0.821	0.047

a Data quoted from Benett et al. (Ref. 3,5)

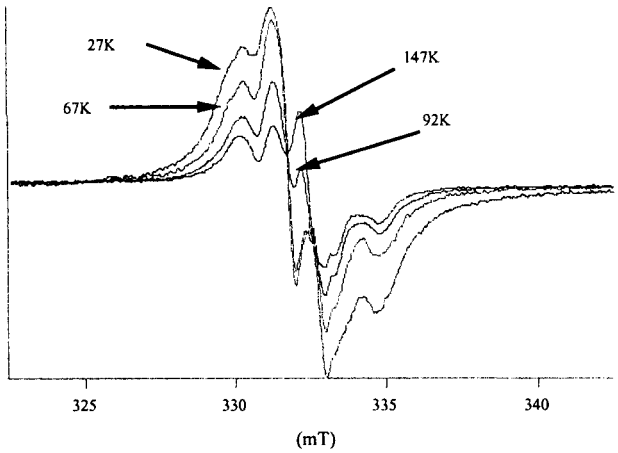

Figure 4-1-1. Temperature dependence of EPR signals of γ-ray irradiated poly(dimethylsilane) solid.

4-1-2 Experimental

Poly(dimethylsilane) was synthesized by the conventional sodium condensation (Wultz Coupling) method with a dichlorodimethylsilane monomer that was pre-

pared by Shinetsu Chemical Co. LTD. Polymerization was carried out in Ar atmosphere and in 100ml toluene as a reflux solvent. The monomer (5g) was added to the reaction vessel and mixed with melted sodium metal for 6-12 hours. The precipitated polymer was filtered and washed by 500ml of toluene, methanol and tetrahydrofran (THF), respectively.

Electron spin resonance measurements were carried out using a Varian X-band EPR spectrometer. The microwave power used as typically 0.2mW, and in the observation carried out above 250K, it was increased to 5mW.

Polymer samples were evacuated down to 10^{-4} Pa in suprasil quartz cells and irradiated by ^{60}Co γ-ray source in the Chemistry Division at Argonne National Laboratory with the dose of 1.9-5 kGy. Irradiation was carried out at 77K. After irradiation, samples were transferred to liquid helium cryostat in the EPR spectrometer, and EPR studies were carried out at temperatures 4K - 250K.

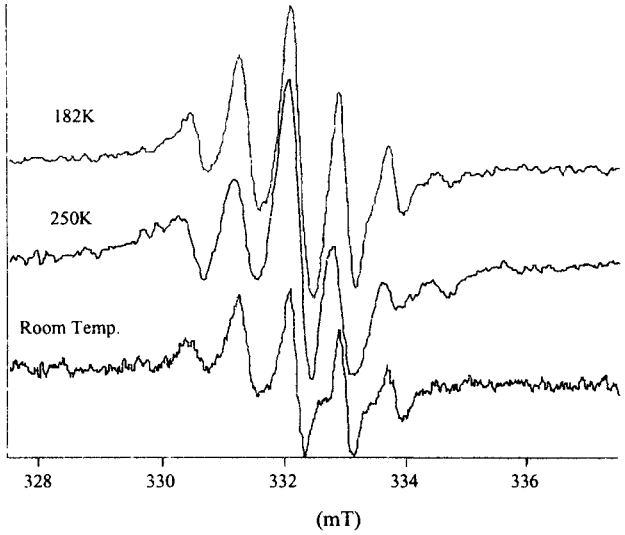

Figure 4-1-2. Temperature dependence of PDMS EPR signals between 182K and room temperature.

4-1-3 Results and Discussion

Figure 4-1-1 shows the temperature dependence of EPR spectra of poly(dimethylsilane) (PDMS) irradiated at 1.9kGy by the γ-ray source. The spectrum at extremely low temperature (20-40K) consisted of four lines with the coupling constant of ~1.5 mT. The shapes of the spectrum did not drastically change with increasing temperature up to 150K. However, the four lines split into more structures in the higher temperature region over 150K. This is illustrated in figure 4-1-2. The high temperature spectrum consists of seven lines split by ~0.8 mT. This value of coupling constant of silyl radicals shows good agreement with the data of previous work carried out for smaller silane molecules mentioned above.

The simulated spectrum of silyl radicals is presented in figure 4-1-3 together with the spectrum observed in PDMS at room temperature. The simulations were carried out using the coupling constants of β and γ hydrogens summarized in table 4-1-1. This simulation supports the view that the observed spectrum is due to silyl radicals that were formed by the main chain scission of the polymer induced by γ-ray irradiation. This silyl radical species is very stable in solid PDMS compared with other oligosilane materials, even at room temperature.

Figure 4-1-4 shows the difference in the spectra before and after annealing to room temperature. Both signal intensity and shape are markedly different in these two spectra.

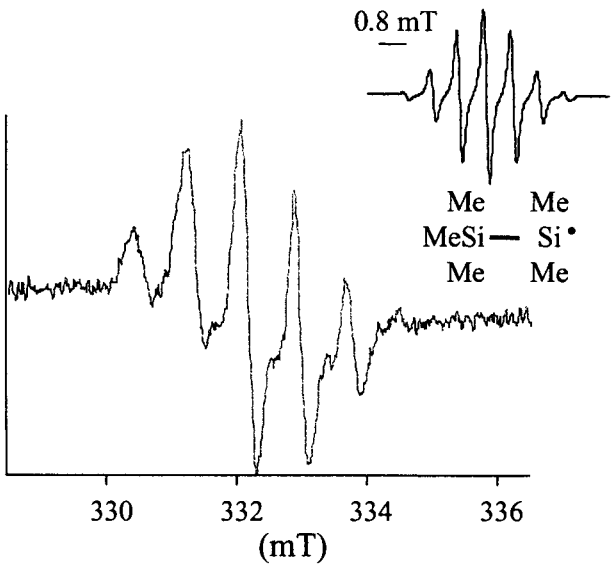

Figure 4-1-3. EPR Spectrum of γ-ray irradiated (3.9kGy) poly(dimethylsilane) solid at room temperature with a calculated EPR spectrum of a silyl radical, $(CH_3)_3Si$ $(CH_3)_2Si^{\cdot}$.

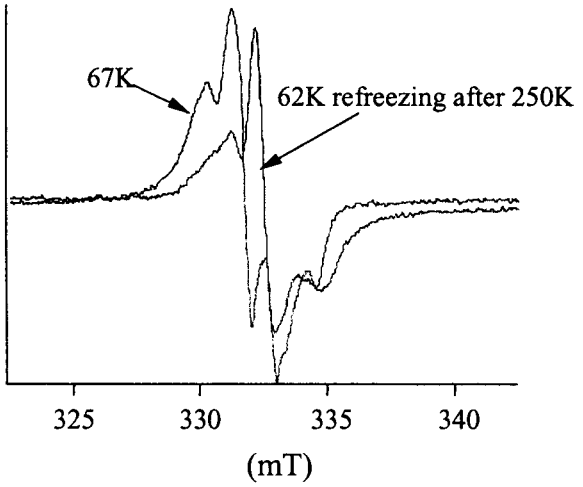

Figure 4-1-4. EPR spectra of poly(dimethylsilane) before and after heating.

Significantly, the initial four line feature disappeared after annealing, and only one broad line remained, except for a sharp background signal ascribed to color centers of quartz cell formed by γ-ray irradiation. This result implied the presence of reactive intermediate species other than the silyl radicals suggested earlier. While it seems likely that methyl radicals were produced as a result of radiolysis via the bond scission of methyl sub-

stituents on the polymer, the EPR spectra at low temperatures are not conclusive on this point. As McKinley et al. suggested,[1] the side chain elimination could occur in the photon-induced primary reactions of polysilanes. It may be that the elimination of methyl substituents from the polymer silicon skeleton competes with the homolytic cleavage of Si-Si bonds.

4-1-4 Summary

Radical species produced by the γ-ray irradiation of solid-state PDMS were investigated. High energy photons induce polymer main chain scission directly, and silicon-centered radicals were formed as a result of homolytic cleavage of silicon skeleton. The observed EPR coupling constants of the silyl radicals were essentially the same as the values observed in previous studies of small silane molecules. The spin density of the unpaired electron appeares to be localized on the silicon atoms.

In contrast, the EPR spectra in the low temperature region (<100K) suggest that other radical species may be present. This may indicate that competition between silyl radical formation and side chain eliminationis taking place at low temperatures. It can be concluded that in radiolysis of the polymer main chain scission predominates and represents the main degradation pathway of poly(dimethylsilane).

Section 4-1 Reference

[1] McKinly A. J.; Karatsu, T.; Wallraff, G. M.; Miller, R. D.; Sooriyakumaran, R.; Michl, *J. Organometalics* 1988, **7**, 2567.

[2] Todesco, R. V.; Kamat, P. V. *Macromolecules* 1986, **19**, 196.

[3] Benett, S. W.; Eaborn, C.; Hudson, A.; Hussain, H. A.; Jackson, R. A. *J. Organometallic Chem.* 1969, **16**, 36.

[4] Krusic, P. J.; Kochi, J. K. *J. Am. Chem. Soc.* 1969, 91, 3938.

[5] Benett, S. W.; Eaborn, C.; Hudson, A.; Jackson, R. A.; Root, K. D. J. *J. Chem. Soc,* A 1970, 348

[6] Cooper, J.; Hudson, A.; Jackson, R. A. *Mol. Phys.* 1972, **23**, 209.

4-2 Ion Beam Irradiation Effects on Polysilane

Radiation effects on poly(methylphenylsilane): PMPS, poly(di-n-hexylsilane): PDHS and poly(methylpropylsilane): PMPrS are described in the present chapter. PMPS solid films irradiated by a variety of high energy ion beams and electron beams show changes of solubility with a large LET (linear energy transfer; energy deposition rate of incident particles per 100Å) effects. Ion and electron (20 and 30 keV) beams induce mainly crosslinking of PMPS, while it was reported that UV light and γ-rays caused predominantly main chain scission on PMPS. The G-values of crosslinking increases with the values of LET of incident beams. PDHS has a clear phase transition temperature at around 312K with change of the silicon skeleton structure. Radiation induced reactions differed greatly above and below this temperature, showing large emission spectral changes. High LET ion beams induced main chain crosslinking in the polymer. PDHS behaved as a negative-type resist material below 312K, although it had been previously confirmed that PDHS had shown positive-type resist properties for UV light, electron beams, X-rays, low LET proton beams at any temperature range and for higher LET He ion beams at a temperature above 312K. The beams caused heterogeneous reactions of crosslinking and main chain scission in the films. The relative efficiency of the crosslinking was drastically changed in comparison with that of main chain scission. The anomalous change in the molecular weight distribution was analyzed with increasing irradiation fluence, and the ion beam induced reaction radius ; track radius was determined for the radiation sources by the function of molecular weight dispersion.

4-2-1 Introduction

The transient species and the electronic properties of polysilanes have been already described in the previous sections. Silicon containing polymers and their reactions induced by electron beam irradiation play a significant role in two layer resist processes which is one of the most important future technologies of electron beam microlithography.[1] In addition, polysilanes may play an important role in ion beam lithography, a technology which is recieving renews interest as a candidate for the manufacture of semiconductors in the future.[2]

It was reported by Trefonas et al. that films of high molecular weight poly(n-hexylmethylsilane) showed a UV absorption spectral shift and molecular weight reduction upon exposure to UV light (the wavelength was 313 nm).[3] Zeigler et al.,[4] Hofer et al.[5] and Miller et al.[6] reported that photovolatilization was caused by excimer laser irradiation (248nm - 306nm) for alkyl substituted polysilanes. Based on their results, polysilanes have been investigated as potential positive photoresist materials because of these results of UV photolysis. In addition to the UV studies, the radiation effects of γ-rays on a variety of polysilanes, and the G-values for main chain scission and crosslinking (number of chain scissions or crosslinks/100eV of absorbed dose) were determined as well. According to the data, main chain scission is predominant and G(s)/G(x) ratios are more than 10 in each sample.[7]

Further, several groups have investigated the potential of polysilane derivatives for electron-beam lithography. Miller et. al. reported that poly(di-n-pentylsilane) could be imaged by electron-beam, and the sensitivity of the material was very high (the fluence of 10-20 $\mu C/cm^2$) as a positive resist material.[8] Taylor and co-workers studied different materials in similar experiment on the electron-beam imaging characteristics of three polysilane copolymers.[9] These materials showed low sensitivity as positive resists (the fluence of 50 $\mu C/cm^2$ or more) and low contrast for the electron-beam, leading the author to speculate that the high vacuum conditions made the efficiency of crosslinking increase, and as a result, the sensitivity and contrast got worse.

It has been suggested that spatial distribution of deposited energy by charged ions has played a significant role in the chemical reactions occurred in the target materials. Ion beam irradiation and its induced modification have been vigorously investigated for polymer materials because ion irradiation has been expected to cause heterogeneous and peculiar reaction based on the high dense excitation. It enables to develop novel reaction system leading to new materials which can not be obtained by bulk chemical reactions. The models of the energy distribution have been experimentally and theoretically suggested by many groups. The detailes will be discussed in the section 4-4 from the view point of micro dosimetry, revealing that the theoretically predicted energy distribution was not the universal function that was able to apply for the elucidation of ion beam induced reaction systems.

To date, the auhtor is unaware of LET effect on polysilane derivatives as ion beam resist materials, though ion beams have been applied to the modification of polysilanes.[10] In this section, the radiation sensitivity of polysilanes for several kinds of ion and electron beams, especially G-values of crosslinking, have been studied from the view point of ion and electron beam lithography and future modification. It is also discussed that molecular weight distribution of polysilanes was extraordinary changed with ion beams. Both main chain scission and crosslinking reactions of polysilanes are able to regard as reactions occurred in ion tracks: intratrack reactions.

4-2-2 Experimental

Poly(methylphenylsilane) ; PMPS, poly(di-n-hexylsilane): PDHS and poly(methylpropylsilane): PMPrS were prepared by the reaction of dichlorosilane with sodium in refluxing toluene. The reaction was carried out under an atmosphere of predried argon. The chlorosilane was purchased from Shinetsu Chemical Inc., and distilled prior to use. The molecular weight of PMPS sample was measured by gel permeation chromatography (GPC) with tetrahydrofuran (THF) as eluent. The PMPS

used in this experiment has bimodal molecular weight distribution, and the high molecular weight peak was cut off by filtration. The sample had a molecular weight of 1.1 x 10^4 determined by polystyrene calibration standards. The PMPS samples were dissolved in xylene and spin-coated on Si wafers. The thickness of the films was 0.5 mm. These films were irradiated by 20, 30 keV electron beams, 2 MeV H^+,He^+ and N^+ ion beams from a Van de Graaff accelerator[11] in a vacuum chamber ($<10^{-6}$ Torr) at room temperature. Ion beam irradiation was done at the Research Center for Nuclear Science and Technology, University of Tokyo. Electron beams irradiation was done at energy of 20, 30 keV by the LSI laboratory, NTT corporation. After irradiation, the solubility of irradiated polysilanes films was evaluated in iso-amylalcohol, a developer used to obtain positive patterns in the UV photolysis of polysilanes, and the irradiated polysilanes was confirmed not to dissolve in the solvent. All samples were developed in xylene for 2 minutes and rinsed in methyl alcohol. Irradiated part of film, where gel was generated, was insoluble in xylene. The thicknesses of the remaining films after development were measured. The normalized thickness was defined as the ratio of the thickness after irradiation to that before.

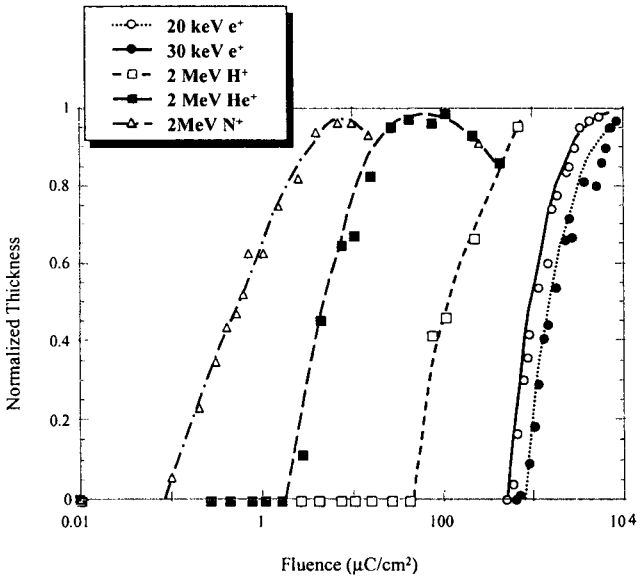

Figure 4-2-1. The relation between normalized thickness (gel fraction) and fluence.

The loss of kinetic energy of ions in traversing the polysilane thin films was estimated from the stopping powers of each constituent element of polysilane on the basis of Bragg's additivity rules.[12] Although the stopping powers of each element depend on the energy of incident ions, the films were so thin that the energy losses were very low compared with initial energy of the ions, and could be neglected except for N^+ ions. In the case of N^+ ion beam, the energy deposition in a film amounts to 30 percent of initial energy. Through this calculation process, the absorbed doses of each sample were obtained. The effects of backscattering were estimated only for electron beams, because they were negligible for ion beams.

IR spectra were measured for samples irradiated by ion beams with FT-IR spectrometer. Investigation of molecular weight change with irradiation was carried out by GPC for 2 MeV He^+ irradiated samples.

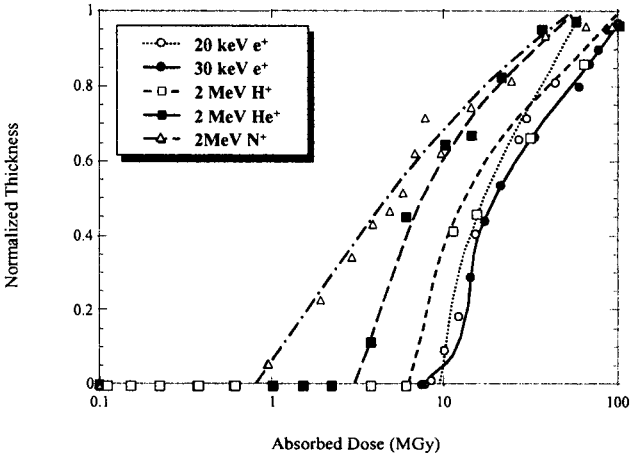

Figure 4-2-2. The relation between normalized thickness and absorbed dose.

Table 4-2-1. Difference in the behavior of gelation with substitution patterns of polysilanes[a]

Polymers	LET eV/nm	Df μC/cm²	Dg MGy	G(x)	G(s)
PMPS	21	2.8	3.3	0.17	0.069
PDHS	18	1.5	2.5	0.61	0.29
PMPrS	17	1.2	1.9	0.71	0.49

a Df and Dg gelation fluence and dose, respectidvely; G(x) and G(s), G-values of crosslinking and main chain scission, respectively.

4-2-3 Results and Discussion

Figure 4-2-1 shows sensitivity curves of PMPS films for irradiation of 20, 30 keV electron beams, 2 MeV H^+, He^+ and N^+ ion beams. Gel was generated for any kinds of beams, even in the case of electron beams, and the gel fraction corresponds to the normalized thickness. Figure 4-2-2 shows the sensitivity curves which was calibrated by the absorbed dose. All substituted polysilanes became insoluble against any kinds of solvents for 2 MeV He^+ irradiation. The gelation fluences and doses are summarized in table 4-2-1. Even in the values of gelation dose, the gelation dose becomes small with increasing values of LET, as shown in figure 4-2-3.

According to the statistical theory of crosslinking and scission of polymers induced by radiation, the behavior of gelation is expressed by the following equation (Charlesby-Pinner relationship),[13]

$$s + s^{1/2} = p_0/q_0 + m / q_0(M_n)_0 D \qquad (4\text{-}2\text{-}1)$$

$$s = 1 - g \qquad (4\text{-}2\text{-}2)$$

where p_0 is the probability of scission, q_0 the provability of crosslinking, s the sol fraction, g the gel fraction, m the molecular weight of a unit monomer, $(M_n)_0$ the number average molecular weight before irradiation, and D is absorbed dose. And then, each G-value is related to the values of p_0 and q_0 as follows,

$$G(x) = 4.8 \times 10^3 \times q_0 \qquad (4\text{-}2\text{-}3)$$

$$G(s) = 9.6 \times 10^3 \times p_0 \qquad (4\text{-}2\text{-}3)$$

where G(x) is the G-value of crosslinking and G(s) is the G-value of main chain scission. With these equations, crosslinking G-values are calculated and summarized in table 4-2-1 together with gelation fluences and doses. It is clear that the efficiency of crosslinking becomes larger with the increase of the LET of incident beams, and it is so-called LET effects. The following measurements can give some more information about the reactions caused by these irradiation.

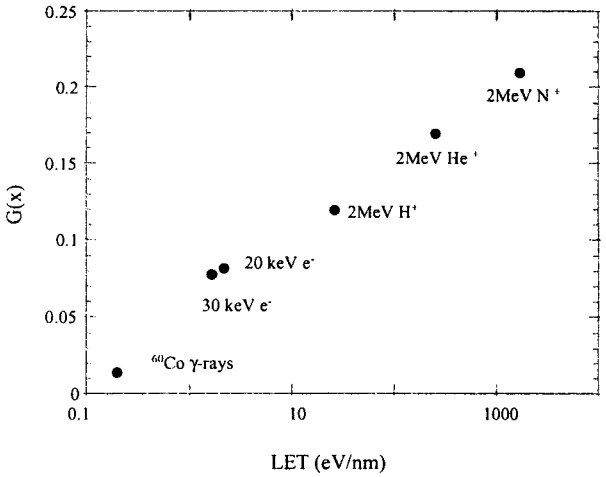

Figure 4-2-3. The relation between LET of radiations and crosslinking G-values.

(1) IR spectra of PMPS

IR-spectra of PMPS film were changed by the irradiation of 2 MeV He^+ ion beam as shown in figure 4-2-4. Peak assignment which is shown in the figure is based on several previous studies.[14] Sharp peaks become broader and larger with the irradiation. Broadening of peaks (4) in fig. 4-2-4 is maybe due to oxidation, and it is likely to produce siloxane structure. Peaks (5) become broader, too, and it shows the increase of Si-C bonds. According to the data of SiC IR-spectra,[10] solid SiC has a strong and broad absorption feature at 800 cm^{-1}. Comparing peaks (2) and (3) before irradiation with those after, the height of the peaks after irradiation becomes considerably low. This is ascribed to the loss of methyl and phenyl substituents from polymer backbone, and similarly the dissociation can be observed in the peaks of (1) which correspond to C-H strechings of methyl and phenyl substituents. Another change is observed around 2200 cm^{-1} with slightly increasing. It may be due to increase of Si-H bonds as a result of main chain scission and hydrogen terminated chain ends.

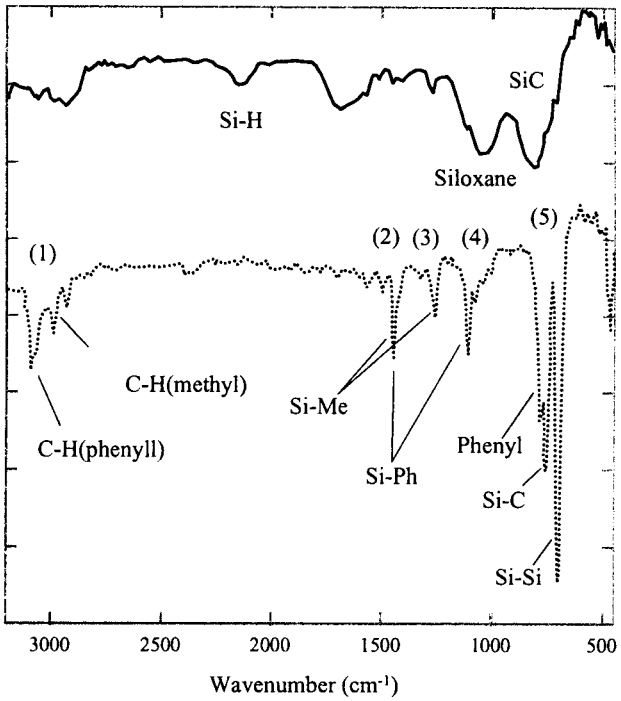

Figure 4-2-4. Changes in IR spectra as increasing dose of He^+ ion beam. (a): before irradiation, (b): after irradiation (572 MGy)

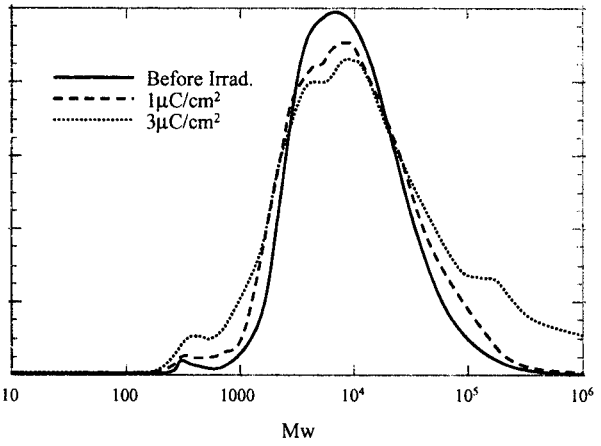

Figure 4-2-5. Changes of molecular weight induced by He^+ ion beam irradiation. (a): initial distribution, (b): 1 $\mu C/cm^2$, (c): 3 $\mu C/cm^2$

(2) Molecular weight changes around gelation dose

Film samples for molecular weight measurement were irradiated at the fluence of 1 and 3 $\mu C/cm^2$ by He^+ ion beam, and the data are shown in figure 4-2-5 with initial distribution. The shoulder in the high molecular weight region (10^5-10^6) raises with the irradiation, which is proof of the crosslinking described before. However, one peak appears in the low molecular weight side. It is also due to the dissociation of substituents from polymer backbone shown in IR-spectra.

The results of these measurements indicate considerable changes in molecular structure of solid state PMPS, especially breakdown of Si-Si bond structure in polymer backbone. In spite of this fact, the macroscopic behavior

of solid PMPS is a typical behavior of a crosslinking polymer. It is considered that the increasing Si-C bonds grow into silicon carbide network, therefore large molecules may be produced. On the other hand, the Si-C bonds cause rearrangement of polymer backbone, and as a result, the succession of σ-conjugation is broken down. It is supported by UV absorption band decrease with the ion beam irradiation.[15]

4-2-4 Summary

Ion (2 MeV) and electron (20 and 30 keV) beams induce mainly crosslinking in PMPS even though UV-light and γ-rays cause predominantly main chain scission. The G-values of crosslinking become larger as the values of LET of radiation increase. These phenomena are due to so-called LET effects. That is, the polysilane resist behave as a negative resist for *high* LET radiation, and also behave as a positive resist for *low* LET radiation. Further, in the case of low energy electron beam (20-30 keV), which is one of the *middle* LET range beams, the predominant reaction can be changed by polymer molecular structure. Therefore, it is quite important to elucidate the difference in the electron beam induced reactions of polysilanes.

Ion beam irradiation induces molecular structure changes of PMPS, such as dissociation of substituents, or generation of siloxane structure and Si-C bonds. Especially generation of Si-C bonds is important because increasing Si-C bonds maybe grow into silicon carbide network, and they also mean the rearrangement of polymer backbone. It is very interesting characteristics of PMPS that the main chain scission and rearrangement are simultaneously induced by the ion beam irradiation.

Section 4-2 Reference

[1] Bowden, M. J. ACS Symposium Series 266; American Chemical Society; Washington DC; 1984; p.39.

[2] Taylor, G.N.; Wolf, W.W.; Moran, J.M. J. Vac. Sci. Technol. 1981, 19, 872.

[3] Trefonas, P.; West, R.; Miller, R.D.; Hofer, D. J. Polym. Sci., Polym. Lett. Ed. 1983, 21, 823.

[4] Zeigler, J.M.; Harrah, L.A.; Johnson, A.W. Proc. SPIE 1985, 539, 166.

[5] Hofer, D. C.; Miller, R. D.; Willson, C. G. Proc. SPIE 1984, 469, 16.

[6] for a review, Miller, R. D.; Michl, J. Chem. Rev. 1989, 89, 1359

[7] Miller, R.D. Advanced in Chemistry Series 224; American Chemical Society; Washington DC; 1990; p.413.

[8] Miller, R.D.; Rabolt, J.F.; Sooriyakumaren, R.; Fickes, G.N.; Fleming, W.; Farmer, B.L.; Kuzmany, H. ACS Symposium Series 360; American Chemical Society; Washington DC; 1988; p.43.

[9] Taylor, G.N.; Hellman, M.Y.; Wolf, T.; Zeigler, J.M. Proc. SPIE 1988, 920, 274.

[10] Venkatesan, T.; Wolf, T.; Allara, D.; Wilkens, B.J.; Taylor, G.N. Appl. Phys. Lett. 1983, 43, 934.

[11] Kouchi, N.; Tagawa, S.; Kobayashi, H.; Tabata, Y. Radiat. Phys. Chem. 1989, 34, 453.

[12] Northcliffe, L.C.; Schilling, R.F. Nucl. Data. Tables A7, 1970, 233.

[13] Charlesby, A. Proc. R. Soc. London Ser. A, 1954, 222, 60; Charlesby, A. Proc. R. Soc. London Ser. A,1954, 222, 542; Charlesby, A. Proc. R. Soc. London Ser. A, 1954, 224, 120.; Charlesby, A.; Pinner, S. H. Proc. R. Soc. London Ser. A, 1959, 249, 367.

[14] Ban, H.; Sukegawa, K. J. Appl. Polym. Sci. 1987, 33, 2787.; Zhang, X.H.; West, R. J. Polym. Sci. 1984, 22, 159. ; Zhang, X.H.; West, R. J. Polym. Sci. 1984, 22, 225.; Wesson, J.P.; Williams, T.C. J. Polym. Sci. 1980, 18, 959.; Holler, I. J. Electrochem. Soc. 1982, 129, 180.; Scilling, F.C.; Bavoy, F.A.; Lovinger, A.J.; Zeigler, J.M. Advanced in Chemistry Series 224; American Chemical Society; Washington, DC; 1990; p.341.

[15] Unpunlished results.

4-3 Temperature Dependence of Radiation Induced Reactions

The present section describes radiation induced solubility changes and emission spectra of poly(di-n-hexylsilane) and their temperature dependence on. Poly(di-n-hexylsilane) has a clear phase transition temperature at around 312K with change of the silicon skeleton structure. Radiation induced reactions differed greatly above and below this temperature, showing large emission spectral changes. High LET (linear energy transfer; energy deposition rate of incident particles per 100Å) ion beams induced main chain crosslinking in the polymer. PDHS behaved as a negative-type resist material below 312K, although it had been previously confirmed that PDHS had shown positive-type resist properties for UV light, electron beams, X-rays, low LET proton beams at any temperature range and for higher LET He ion beams at a temperature above 312K.

4-3-1 Introduction

Polysilane derivatives and their reactions induced by electron beam (EB) irradiation are also of great interest due to the significant role they play in the two-layer resist process, which is one of the most important developing technologies of electron beam microlithography. Miller et al. reported that alkyl substituted polysilanes could be made patterns using EB with high sensitivity as a positive resist.[1] Taylor et al. studied polysilane copolymers as EB resist materials.[2] However, the polymers showed low sensitivity as positive resist materials and low contrast for EB. They concluded that the high vacuum conditions increased the efficiency of crosslinking, leading to low sensitivity and contrast. On the contrary, it is possible that the increasing temperature made the skeleton structure change leading to different reaction routes and the low efficiency of chain scission.

The ion beam lithography technique is receiving renewed interest as a candidate for the manufacture of semiconductors, because it realizes more detailed patterns than conventional UV lithography techniques. Ion beam induced reactions of polysilanes were investigated by the authors and Venkatesan et al.[3] Alkyl and aryl substituted polysilanes were crosslinked by irradiation and behaved as negative resists. Electron paramagnetic resonance (EPR) spectroscopy was carried out by the authors and identified the predominant reactive intermediates of the silicon based polymer materials.[4] It reported the detection of side chain neutral radicals and silicon centered radicals showing high stability. Incident ions caused high dense excitation in limited volume of the solid polymer. The radical, especially the silyl radical, was concentrated along the ion projectile and reacted to produce polymer gel. However, it was also anticipated for ion beam irradiation that phase transition of the polymer affected the concentration of radicals resulting drastic change of reaction pattern. In the present section, ion beam induced reactions were studied in poly(di-n-hexylsilane) (PDHS) which showed clear phase transition from the well-ordered liquid crystalline phase to the disordered random amorphous phase at around room temperature. Thus, PDHS is appropriate to investigate the relationship between temperature and beam-induced reactions because both the ordered and disordered phases have been well studied and eluci-

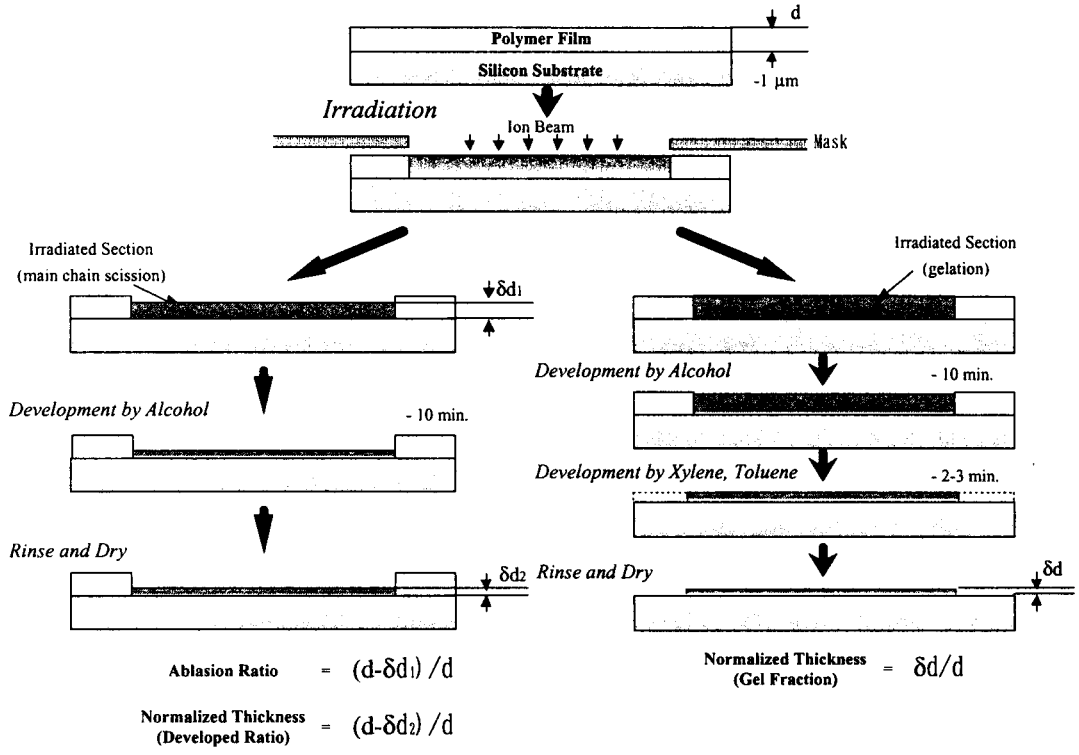

Figure 4-3-1 Schematic experimental procedure.

dated.[5] The obtained results will be discussed in relation to the temperature dependence on photo-induced reactions.

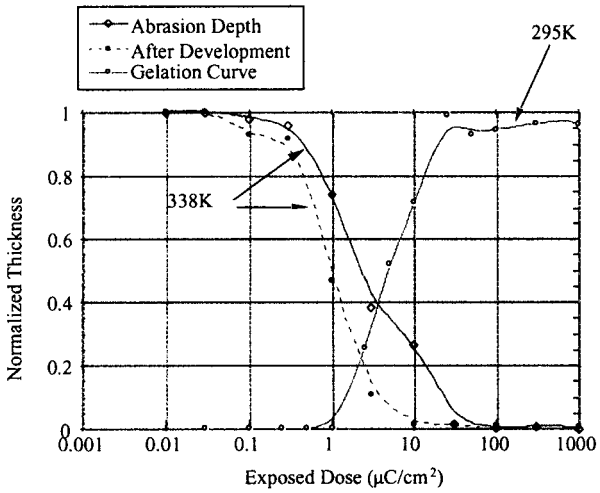

Figure 4-3-2. Sensitivity curves of PDHS irradiated by 2 MeV He+ ion beam at 295 K and 338 K.

4-3-2 Experimental

PDHS was prepared by the reaction of di-n-hexyl-dichlorosilane with sodium in refluxing toluene. The reaction was carried out under an atmosphere of predried argon.[6] Chlorosilane was purchased from Shinetsu Chemical Inc., and doubly distilled prior to use. The molecular weight of the PDHS sample was measured by gel permeation chromatography (GPC System, Shimadzu LC 6A) with tetrahydrofuran (THF) as the eluent. The chromatograph was equipped with two columns of TSK Gel from Toyo Soda Co. The PDHS bimodal molecular weight distribution peaked at 1.2×10^4 and 8.9×10^5, and the molecular weight distribution was controlled by reaction time and additives (12-crown-4 and 15-crown-5 ethers). Two molecular weight components were separated by fractional precipitation. PDHS had the molecular weight of Mn = 3.9×10^4 and Mw = 8.8×10^4, determined by polystyrene calibration standards. PDHS was dissolved in toluene and spin-coated on Si wafers at 1 μm thick. These films were irradiated in a vacuum chamber (< 5×10^{-6} Torr) by 2 MeV He^+ ion beams from a Van de Graaff accelerator which was previously described in the section 4-2. Temperature was controlled in the range of 200 K to 354 K by a cryostat in the vacuum chamber. Film thickness was measured by a surface profiler, Kosaka Laboratory SE-2300. Irradiation and the following procedures are summarized in figure 4-3-1. The solubility of all irradiated PDHS films was evaluated in iso-amylalcohol, a developer used to obtain positive patterns in the UV photolysis of polysilanes. Development by xylene or toluene was conducted for 2 min for all the polymer films confirmed to be insoluble in alcohol. The thickness of the remaining films after development was also measured. The normalized thickness was defined as the ratio of the thickness after irradiation to that before irradiation.

Other PDHS films were prepared for each of the following measurements by solvent casting at 3 μm thick, then irradiated under the same conditions and fluence. Irradiated PDHS was dissolved into THF followed by the measurement of molecular weight distribution using the GPC system. Fluorescence spectra were also measured by a Perkin Elmer LS-50B spectrometer for the irradiated PDHS films. The loss of kinetic energy of ions in traversing polymer films was estimated by Braggs additivity rules and the Monte-Carlo simulation using TRIM 91 code.[7]

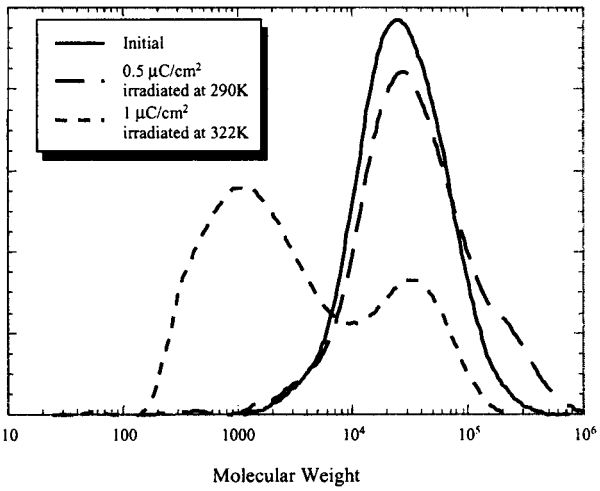

Figure 4-3-3. Molecular weight distribution of PDHS, initial distribution and after irradiation of 2 MeV He^+ ion beam at 290 K and 322 K.

4-3-3 Results and Discussion

Figure 4-3-2 shows the sensitivity curves of PDHS films for 2 MeV He^+ ion beam irradiations at 338 K and 295 K. The behavior of PDHS completely changed with the phase transition phenomenon. The fraction of removed film by ablasion or development was estimated based on the equations in fig. 4-3-1. Ablasion of polymer molecules was observed when the films were irradiated at 338 K. The depth of ablasion reached the entire thickness of the films, therefore wet development to remove the polymer film by ion beam irradiation is not necessary. Wet development by alcohol dissolved the remaining films and improved the sensitivity for ion beam irradiation. This feature indicated that main chain scission was predominantly induced by the ion beam irradiation at high temperature. PDHS apparently behaved like positive resist materials in this case. In spite of using the same ion beams, PDHS molecules were crosslinked by ion beam irradiation at 295 K. Crosslinked molecules grew into polymer gel and became insoluble in not only alcohol but also xylene and toluene. Thus, negative resist characteristics were obtained by irradiation below phase transition temperature.

Figure 4-3-3 shows the molecular weight distribution of PDHS. The shoulder in the high molecular weight region increases with irradiation at 290 K, indicating the crosslinking reaction. In contrast, molecular weight reduction was apparently observed in the PDHS irradiated at 322 K. It was unlikely that the distribution of irradi-

ated PDHS peaked independently at a considerably low molecular weight region. This feature was analyzed in The authors' previous works.[8] Ion beams caused heterogeneous reactions called inside track reactions in the solid polymer media.

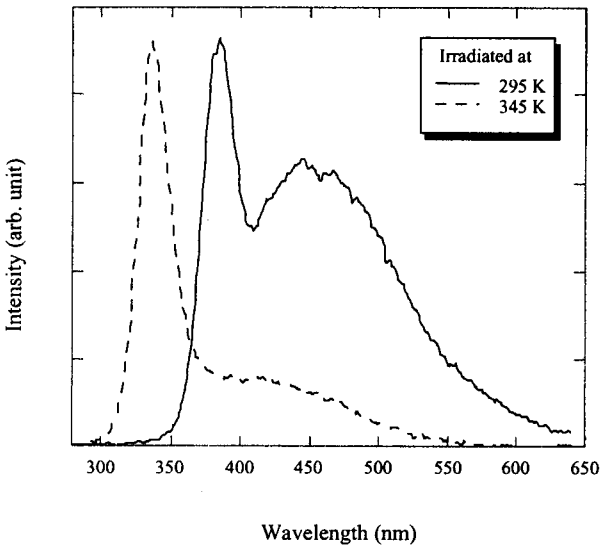

Figure 4-3-4. Fluorescence spectra of PDHS films after irradiation of 2 MeV He^+ ion beam at 295 K and 345 K.

The phase transition was studied for symmetrically and asymmetrically alkyl substituted polysilane derivatives.[9] PDHS exhibited transplaner conformations of the silicon skeleton and high crystallinity below phase transition temperature. However, overcoming an order-disorder transition at around 312 K, the solid state structure of PDHS turned into a hexagonal liquid crystalline phase upon heating.[5] The liquid crystalline phase was considered to allow for high mobility in the side chains.

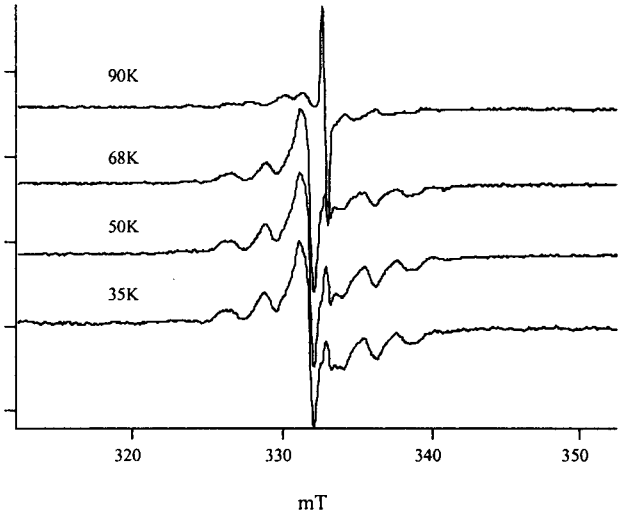

Figure 4-3-5. Temperature dependence of EPR signals on PDHS irradiated by ^{60}Co γ-rays at 3.9 kGy

Fluorescence spectra of irradiated PDHS films are illustrated in figure 4-3-4. The spectra was normalized by the intensity. Quantum efficiency became considerably low for the main emission band of PDHS irradiated at 345 K. Studies of photo-excited fluorescence spectra of solid state PDHS have resulted in the band peaked at 378 nm assigned to band exciton state. Irradiation at 345 K caused a large blue shift of the band in spite of the unchanged location of the band during irradiation at 295 K. The blue shift was due to the transition and quenching to hexagonal liquid crystalline phase by the irradiation. A new emission band was observed at 430-500 nm upon irradiation at 345 K. The long wavelength emission had typically been observed for structural defects induced (branched) polysilanes,[10] thus the emission was due to the self trapped exiton states of the crosslinked structure in silicon skeleton.

Reactive intermediates have been also investigated by the authors for solid state polysilane derivatives upon irradiation of a variety of radiation sources.[4] Irradiation primarily caused side chain dissociation and produced alkyl primary radicals at low temperature below 77K. Figure 4-3-5 illustrates the EPR spectra of PDHS irradiated by γ-rays at 77 K, and their changes with increasing temperature after refreezing at 4 K. The spectra suggested the presence of alkyl primary radicals and rapid extinction of the species with increased temperatures. The neutral radicals disappeared with increasing temperature up to 150 K because of recombination reactions. The authors reported that silicon-centered neutral radicals were also produced as a result of side chain dissociation and homolytic cleavage of the silicon skeleton. The silyl radicals had shown high stability and been identifiable even at room temperature.

Thus the silyl radicals were believed to play the role of the predominant reactive intermediates of crosslinking reactions induced by ion beam irradiation at low temperature. With high energy deposition rates, an incident ion particle produced high dense radicals in a limited spatial distribution called an ion track. Silyl radicals were closely packed in the track. Recombination reaction was promoted among the silyl radicals at 295 K, leading to crosslinking because of the low mobility of silyl radicals in the crystalline phase and the immediate extinction of alkyl radicals. At 338 K, silyl radicals spread and disappeared rapidly on account of the high mobility of the silicon chains and radical transfer reactions followed mainly by hydrogen extraction, leading to an increasing yield of main chain scission.

4-3-4 Summary

It had been reported that PDHS is applicable as a positive-type resist material for UV light, electron beams (10-100 keV), X-rays, γ-rays and MeV order proton beams in any temperature range. However, ion beam induced reactions were affected by the phase transition of PDHS. The predominant reaction changed from crosslinking into main chain scission with increasing temperatures. The transition was ascribed to ion beam induced *intratrack* reactions and neutral radical density which was influenced by the molecular motion. Thus, PDHS behaved as a negative-type resist material below 312 K, despite behaving as a positive-type resist material

above 312 K. It was important to maintain irradiation temperatures when the polymer was used as a resist material.

Section 4-3 Refernce

[1] R. D. Miller, J. F. Rabolt, R. Sooriyakumaren, G. N. Fickes, W. Fleming, B. L. Farmer and H. Kuzmany: ACS Symposium Series (American Chemical Society, Washington DC, 1988) Vol. 360, p.43.

[2] G. N. Taylor, M. Y. Hellman, T. Wolf and J. M. Zeigler: Proc. SPIE **920**(1988)274.

[3] S. Seki, H. Shibata, H. Ban, K. Ishigure and S. Tagawa: Radiat. Phys. Chem. **48**(1996)539.; S. Seki, H. Shibata, Y. Yoshida, K. Ishigure and S. Tagawa: Radiat. Phys. Chem. **49**(1997)389.; T. Venkatesan, T. Wolf, D. Allara, B. J. Wilkens and G. N. Taylor: Appl. Phys. Lett. **43**(1983)934.

[4] S. Seki, S. Tagawa, K. Ishigure, K. R. Cromack and A. D. Trifunac: Radiat. Phys. Chem. **47**(1996)217.

[5] H. Kuzumany, J. F. Rabolt, B. L. Farmer, R. D. Miller: J. Chem. Phys. **85**(1986)7413.; B. M. Klemann, R. West and J. A. Koutsky: Macromolecules **29**(1996)198.

[6] R. West: J. Organomet. Chem. **300**(1986)327.

[7] N. Kouchi, S. Tagawa, H. Kobayashi and Y. Tabata: Radiat. Phys. Chem. **34**(1989)453.; L. C. Northcliffe and R. F. Schilling: Nucl. Data Tables **A7**(1970)233.

[8] S. Seki, K. Kanzaki, S. Tagawa, Y. Yoshida, H. Kudoh, M. Sugimoto, T. Sasuga and T. Seguchi: to be published in Radiat. Phys. Chem., 50(1997)423.

[9] E. K. KariKari, B. L. Farmer, R. D. Miller and J. F. Rabolt: Macromolecules **26**(1993)3937.; B. M. Klemann, R. West and J. A. Koutsky: Macromolecules **29**(1996)198.

[10] K. Furukawa, M. Fujino and N. Matsumoto: Macromolecules **23**(1990)3423.

4-4 Microstructure of Ion Tracks in Polysilane

The solid films of poly(di-n-hexylsilane) were irradiated with a variety of high energy ion beams, electron beams, and ^{60}Co γ-rays of which LET ranges from 0.2 to 1620 eV/nm. The beams caused heterogeneous reactions of crosslinking and main chain scission in the films. The molecular weight of the polymer was traced to give the efficiency of crosslinking reactions: G(x) based on Charlesby-Pinner relationship. The value of G(x) increases from 0.042 to 0.91 with increasing values of LET. The author adopts a reaction model in a single ion track to the crosslinking reactions, and the expanding chemical track along an ion trajectory is responsible for the increasing crosslinking G-values. The theoretical aspects of the energy distribution in penumbra area give a good interpretation to the chemical track radii obtained in this study.

4-4-1 Introduction

The UV light induced scission reactions become a problem to use the polysilanes as electro-optical materials making the best use of the electronic properties of the polymers. The crosslinking reactions should play a significant role in the practical use of the polymer materials. The author's previous studies reported on reactive intermediates of polysilane derivatives irradiated by ion, electron and γ-rays.[1] Predominant reactive intermediates in polysilanes were assigned to silyl radicals showing great stability in comparison with carbon centered alkyl radicals.[1] The ion beam irradiation effects on polysilanes were also investigated, and the reactions in the polymers changed with the energy deposition rate of incident particle: linear energy transfer (LET) of radiation sources.[1] Polymers were crosslinked for high LET ion beam irradiation in spite of predominant main chain scission reaction for low LET radiation. The difference in radiation induced reactions was ascribed to a variation of density of stable reaction intermediates: silyl radicals generated by radiation. It has been suggested that spatial distribution of deposited energy by charged ions has played a significant role in the chemical reactions occurred in the target materials.[2] Models of the energy distribution was proposed experimentally and theoretically as "Track Core" and "Penumbra" models by Magee et al.,[3] Varma et al.,[4] Wingate et al.,[5] Katz et al.,[6] and Wilson.[7] In spite of the theoretical modeling effort, there are still unknown factors in the relationship between the ion track structure and the values of track radii that was experimentally obtained by the analysis of irradiation products.[8] Puglisi et al., Licciardello et al., and Calcagno et al. also reported the effects of ion beam bombardment to polystyrene leading to the aggregation of molecules and crosslinking reactions.[9] The anormal change in molecular weight distribution was ascribed to the intratrack reaction, however the estimated size of ion tracks was also larger than that of the track core. LaVerne et al. reported the considerable decrease in the radiation chemical yield for ferric production in the Fricke dosimeter. They suggested a model of a deposited energy density in an ion track, that depends on the LET and the atomic number of an irradiation particle.[10]

The author discuss the efficiency of crosslinking and main chain scission reactions induced by ion beams, EB, and γ-rays with a variety of LET ranging from 0.2 to 1620 eV/nm in the present section. The molecular weight of the polymer is traced as a function of absorbed dose giving G-values (number of reactions per absorbed 100 eV) of the reactions. Both reactions in polysilanes are able to regard as reactions occurred in an individual ion track: intratrack reactions. The simulation model of intratrack reactions reveals the chemical core to have different sizes with changing LET.

Table 4-4-1. The entry of radiation sources and PDHSa

Radiations	Entry	*Mn*	*Mw*
175MeV Ar^{8+}	PDHS-L	9.8×10^3	4.2×10^4
2MeV N^+	PDHS-L	1.1×10^4	5.6×10^4
160MeV O^{6+}	PDHS-L	1.3×10^4	3.9×10^4
225MeV O^{7+}	PDHS-L	1.3×10^4	3.9×10^4
2MeV He^+	PDHS-H	5.6×10^5	1.4×10^6
2MeV He^+	PDHS-L	1.1×10^4	5.6×10^4
220MeV C^{5+}	PDHS-L	1.3×10^4	3.9×10^4
20MeV He^{2+}	PDHS-L	9.8×10^3	4.2×10^4
2MeV H^+	PDHS-H	5.6×10^5	1.4×10^6
2MeV H^+	PDHS-L	1.1×10^4	5.6×10^4
20MeV H^+	PDHS-H	5.6×10^5	1.4×10^6
45MeV H^+	PDHS-H	5.6×10^5	1.4×10^6
20keV e^-	PDHS-H	5.6×10^5	1.4×10^6
30keV e^-	PDHS-H	5.6×10^5	1.4×10^6
^{60}Co γ-rays	PDHS-H	5.6×10^5	1.4×10^6

a *Mw* and *Mn*, weight and number average molecular weights, respectively.

4-4-2 Experimental

Poly(di-n-hexylsilane) (PDHS) was prepared by the reaction of di-n-hexyldichlorosilane with sodium in refluxing toluene. The reaction was carried out under an atmosphere of predried argon. The chlorosilane was purchased from Shinetsu Chemical Inc., and doubly distilled prior to use. The molecular weight of PDHS was measured by gel permeation chromatography (GPC System, Shimadzu Class VP-10) with tetrahydrofuran (THF) as an eluent. The chromatograph equipped with four columns : Shodex KF-805L from Showa Denko Co. LTD. PDHS has initially bimodal molecular weight distribution, and the molecular weight was controlled by reaction condition, reaction time and additives (12-crown-4 and diethylenegrycol-dimethylether as sodium activators). The high or low molecular weight peak was cut off by separatory precipitation leading to the low

molecular weight PDHS (PDHS-L) and high molecular weight PDHS (PDHS-H) with monomodal distribution. The molecular weights of the polymers were Mn = 0.98 ~ 1.3 x 10^4 and Mw = 3.9 ~ 5.6 x 10^4 for PDHS-L, and Mn = 5.6 x 10^5 and Mw = 1.4 x 10^6 for PDHS-H, respectively determined by polystyrene calibration standards. The PDHS samples were dissolved in toluene and spin-coated on Si wafers (0.5 μm thick), Kapton films (0.03 mm thick) and PEEK films (12 μm thick). The polysilane films were 1-3 μm thick for all ion beam irradiation. These films were irradiated in a vacuum chamber (< 5 x 10^{-6} hPa) with 2 MeV $^1H^+$, $^4He^+$, and $^{14}N^+$ ion beams from a Van de Graaff which was the same one used in the section 4-2. The ion beams from a cyclotron accelerator was also of use at Japan Atomic Energy Research Institute, Takasaki Radiation Chemistry Laboratory. The irradiation was performed under vacuum (< 5 x 10^{-6} hPa) at room temperature using 20 ~45 MeV $^1H^+$, 20 MeV $^4He^{2+}$, 220 MeV $^{12}C^{5+}$, 225 MeV $^{16}O^{7+}$, 160 MeV $^{16}O^{7+}$, and 175 MeV $^{40}Ar^{8+}$ ion beams. Table 4-4-1 summarizes the polymer entries and irradiation conditions. After irradiation, molecular weight distribution of irradiated PDHS films was measured by the GPC system. The loss of kinetic energy of ions in traversing polymer films was estimated by the TRIM 92 code.

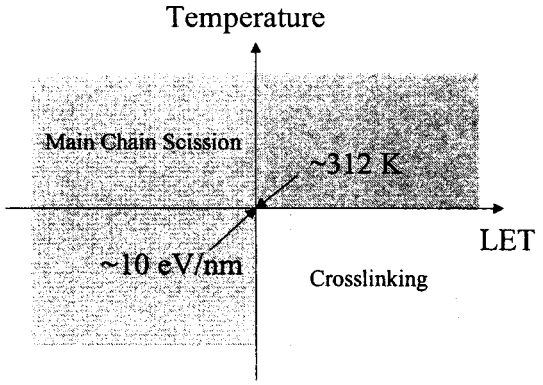

Figure 4-4-1. Schematic diagram of predominant reactions in PDHS.

4-4-3 Results and discussion

The MeV order ion beam irradiation already revealed to cause crosslinking reactions in polysilane derivatives making negative tone in the thin solid films. The behavior of PDHS drastically changed with the irradiation temperature and the value of LET of incident ions, i.e., the predominant reaction changed from crosslinking into main chain scission with increasing temperatures upon irradiation to high LET ion beams.[2] The main chain scission reactions also became predominant in PDHS irradiated with the low LET ion beams even below phase transition temperature, ca. 312 K. Figure 4-4-1 displays the diagram of ion beam induced reactions in PDHS. The efficiency of crosslinking reactions is expected to depend on the values of LET, thus the change in the molecular weight is traced as a function of absorbed dose.

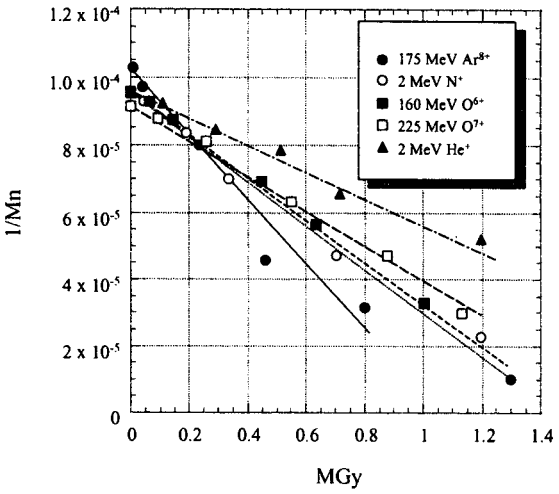

Figure 4-4-2. Charlesby-Pinner plotting of Mn to absorbed dose for 2MeV $^4He^+$, 225 MeV $^{16}O^{7+}$, 160 MeV $^{16}O^{7+}$, 2MeV $^{14}N^+$, and 175 MeV $^{40}Ar^{8+}$.

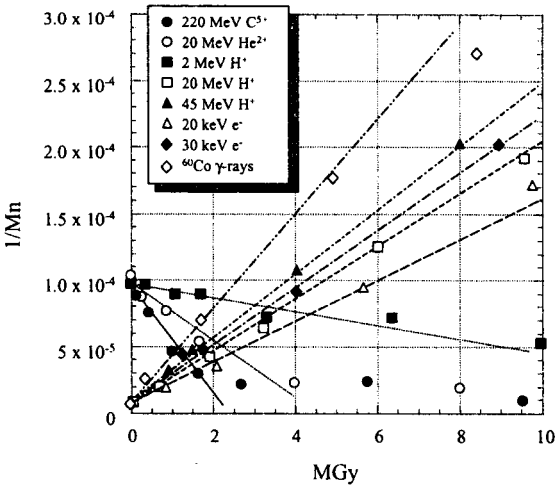

Figure 4-4-3. Charlesby-Pinner plotting of Mn to absorbed dose for ^{60}Co γ-rays, 20~30 keV e^-, 2 ~45 MeV $^1H^+$, 20 MeV $^4He^{2+}$, 220 MeV $^{12}C^{5+}$.

According to the statistical theory of crosslinking and scission of polymers induced by radiation, the number and weight average molecular weights is expressed by the following equation (Charlesby-Pinner relationship),[11]

$$1/M_n = 1/(M_n)_0 + (p_0 - 0.5q_0)\, D/m \qquad (4\text{-}4\text{-}1)$$

$$1/M_W = 1/(M_W)_0 + (0.5p_0 - q_0)\, D/m \qquad (4\text{-}4\text{-}2)$$

where p_0 is the probability of scission, q_0 the provability of crosslinking. Mn and Mw denote the number and weight average molecular weight with their initial values of $(M_n)_0$ and $(M_W)_0$, respectively. m is the molecular weight of a unit monomer, and D (MGy) is absorbed dose.

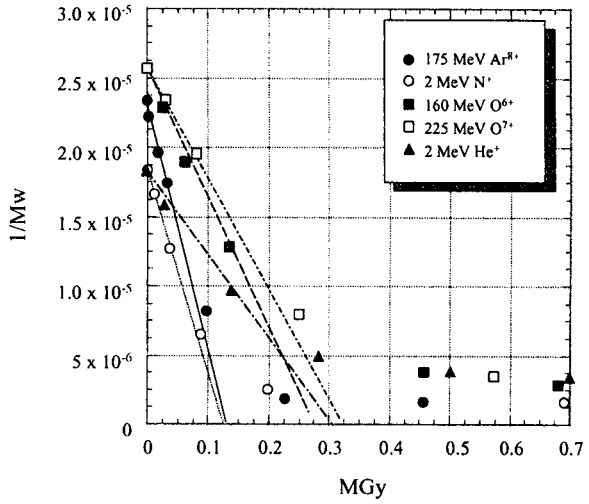

Figure 4-4-4. Charlesby-Pinner plotting of Mw to absorbed dose for 2MeV $^{4}He^{+}$, 225 MeV $^{16}O^{7+}$, 160 MeV $^{16}O^{7+}$, 2MeV $^{14}N^{+}$, and 175 MeV $^{40}Ar^{8+}$.

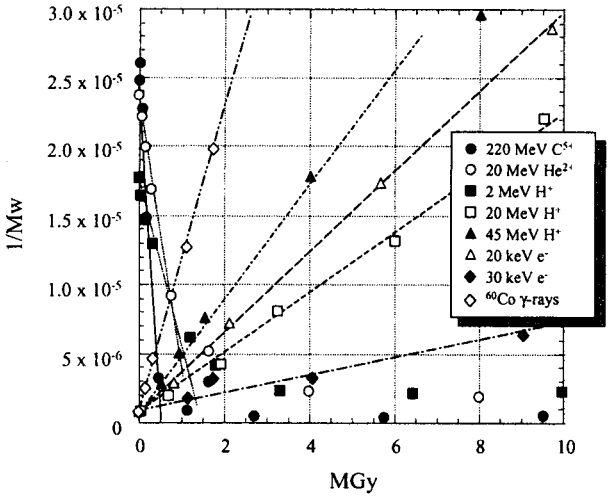

Figure 4-4-5. Charlesby-Pinner plotting of Mw to absorbed dose for ^{60}Co γ-rays, 20~30 keV e^{-}, 2 ~45 MeV $^{1}H^{+}$, 20 MeV $^{4}He^{2+}$, 220 MeV $^{12}C^{5+}$.

G-values of main chain scission and crosslinking are estimated by the equations (4-2-3) and (4-2-4) in the section 4-2 using the values of p_0 and q_0, giving the values of G(x) and G(s). The calculated values of G(x) and G(s) are summarized in table 4-4-2. PDHS molecules grow into a polymer gel upon irradiation to the high LET ion beams, and the geletion dose: Dg is also shown in table 4-4-2. The molecular weights of PDHS are measured by GPC at the range of absorbed dose below Dg. Figures 4-4-2 and 4-4-3 plot 1/Mn vs. D, which present a relationship in equation 1. The Charlesby-Pinner relationship apparently gives good interpretation to the change in 1/Mn for low LET radiation such as γ-rays, EB, and high energy proton beams. However, the linear relationship is no longer effective to fit 1/Mn vs. D of high LET ion beams at high dose (> 1 MGy) as displayed in fig. 4-4-2. The solid PDHS films become partially insoluble against THF in the range of D, which is responsible to the non-linearity at high dose region. The slope of the plotting mainly reflects the probability of chain scission, and it suddenly drops down at the LET increased from 2.7 to 17 eV/nm. The irradiated part of PDHS films actually turns from positive to negative tone, thus the threshold of LET seems to locate around 10 eV/nm. Mw of PDHS is also plotted to D in the figures 4-4-4 and 4-4-5. The linear relationship in equation (4-4-2) also gives better fitting in fig. 4-4-5. Generally, Mw is more sensitive than Mn to the change in the molecular weight distribution, and it reflects the rapid decrease in 1/Mw which is shown in fig. 4-4-5.

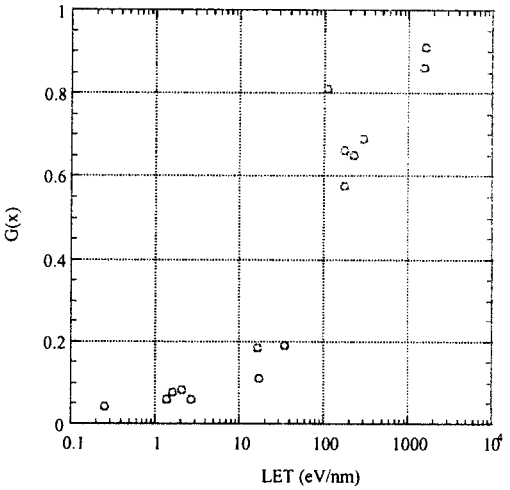

Figure 4-4-6. Semi-logarithmic plotting of the calculated G(x) vs. LET.

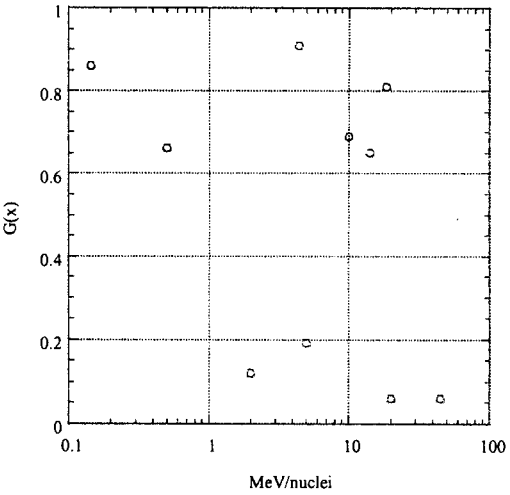

Figure 4-4-7. Semi-logarithmic plotting of the calculated G(x) vs. particle velocity : MeV/nuclei.

The negative slope of the fitting indicates that the crosslinking reactions become predominant for the irradiation, and the slope turns from positive into negative at the same threshold of ca. 10 eV/nm.

Figure 4-4-6 shows semi-logarithmic plotting of the calculated G(x) against LET. G(x) increases with the increasing LET. G(x) is also plotted as a function of particle velocity in figure 4-4-7. Apparently, fig. 4-4-6 gives a better fitting than that in fig. 4-4-7.

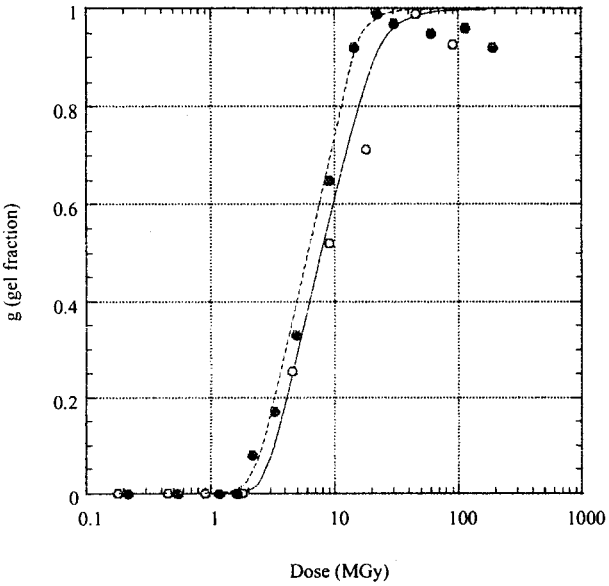

Figure 4-4-8. Sensitivity curves of PDHS-L (solid) and PDHS-H (dashed) for 2 MeV $^4He^+$ ion beam irradiation.

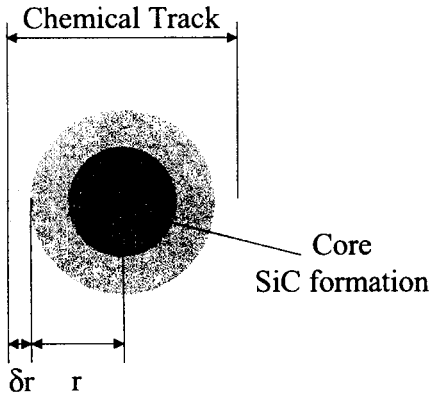

Figure 4-4-9. Schematic representation of cross section of a ion track: the chemical track and core.

The G(x) is estimated in both PDHS-L and PDHS-H for 2MeV $^1H^+$ and $^4He^+$ ion beams. Both polymers show little difference in the G(x) determined by the trace of the molecular weight change as shown in fig. 4-4-6, indicating the G(x) not to depend on the initial molecular weight of PDHS. However, a small fraction of the insoluble gel was also formed by the irradiation at the dose lower than Dg. The gel fractions of both PDHS-L and PDHS-H are plotted vs dose of 2 MeV He^+ irradiation in figure 4-4-8.

There is little difference in the sensitivity curves of the polymers though PDHS-H has the 50 times higher values of Mn than that of PDHS-L. The values of Dg are almost same for PDHS-L and PDHS-H as summarized in table 4-4-3. The behavior of gelation is already discussed in the section 4-2 based on the statistical theory of crosslinking and scission of polymers induced by radiation (Charlesby-Pinner relationship).[11] The eqns. (4-2-1) and (4-2-3) were obtaind for the evaluation of p_0 and q_0: the provability of main chain scission and crosslinking, and the eqns. (4-2-3) and (4-2-4) give the values of G(x) and G(s) using p_0 and q_0. The G-values obtained by the gel fraction measurement: $G(x)_g$ and $G(s)_g$ are summarized in table 4-4-3. The apparent G-values depend on the initial molecular weight of polymers, and the extremely low values are observed for PDHS-H. This suggests that the large number of crosslinking points is formed in a polymer molecule for the high LET ion beam irradiation, and the G-values of crosslinking seemingly decreases because the statistical theory treats the model of micro gels which have a crosslinking points per a molecule. The authors previous study reported anomalous change in the molecular weight distribution of PDHS irradiated by high LET ion beams.[1] It was attributed to microscopically heterogeneous reactions caused along incident ion projectile, giving ion track

Table 4-4-2. G-values of crosslinking and main chain scission upon irradiation to a variety of radiation sources.

Radiations	LET (eV/nm)	Dg[a] (MGy)	G(x)[b]	G(s)[b]	Type[c]
175 MeV Ar^{8+}	1620	0.81	0.91	0.17	CL
2 MeV N^+	1580	0.89	0.86	0.17	CL
160 MeV O^{6+}	300	3.1	0.69	0.064	CL
225 MeV O^{7+}	230	3.4	0.65	0.10	CL
2 MeV He^+	180	3.3[d]	0.66	0.33	CL
220 MeV C^{5+}	110	2.9	0.81	0.35	CL
20 MeV He^{2+}	35	5.4	0.19	0.16	CL
2 MeV H^+	17	6.8[d]	0.12	0.11	CL
20 MeV H^+	2.7	-	0.059	0.27	CS
45 MeV H^+	1.4	-	0.061	0.32	CS
20 keV e^-	2.1	-	0.083	0.28	CS
30 keV e^-	1.6	-	0.078	0.32	CS
^{60}Co γ-rays	0.25	-	0.042	0.45	CS

[a] D_g, gelation dose; [b] G(x) and G(s), G-values of crosslinking and main chain scission, respectively; [c] CL and CS denote predominant reactions as crosslinking and chain scission, respectively. [d] The values were obtained for PDHS-L.

Table 4-4-3. Gelation dose and G-values of PDHS determined by gel fraction measurements[a].

Polymer	for 2 MeV He^+			for 2 MeV H^+		
	D_g	$G(x)_g$	$G(s)_g$	D_g	$G(x)_g$	$G(s)_g$
PDHS-L	3.3	0.61	0.29	6.8	0.10	0.09
PDHS-H	3.1	0.092	0.044	6.3	0.015	0.0095

[a] Dg, gelation dose; $G(x)_g$ and $G(s)_g$, G-values of crosslinking and main chain scission, respectively determined by the gel fraction measurement.

radii for a variety of ion beams. The LET dependence of ion track radii is similar to that of G(x) obtained in this study. The volume of a single ion track should be responsible to the increasing G(x). The schematic view of a single track is illustrated in figure 4-4-9. The author suggests the following empirical equation that gives the better interpretation to the gel formation in polysilanes,

$$s = \{1-(r+\delta r)\}^f$$
$$g = 1-\{1-(r+\delta r)\}^f \qquad (4\text{-}4\text{-}3)$$

where r is the radius of a chemical track, δr is the differential radius of a track, and f is the fluence of the incident ion beams. The fittings in figure determine the values of r + δr, giving r + δr = 6.0 nm for PDHS-L, and r + δr = 6.2 nm for PDHS-H at 2 MeV $^4He^+$ irradiation. The ion track radius of 2 MeV $^4He^+$ was already reported to be 5.9 ± 1.5 nm for PDHS, showing good agreement with the values obtained in this study. The track radii of the other ion beams are also determined by the same way as summarized in table 4-4-4. Several previous experimental studies have also been suggested a variety of radii for tracks induced by ion beams.[8-10] The values of radii were determined by Koizumi et al. in the same LET range of incident ions, which were varying from 2 nm to 5 nm.[8] The present values of radii indicate similar to the experimentally obtained values, and locate in the middle of "Core" and "Penumbra" sizes suggested by theoretical aspects.[3,12] According to the study, the following formula was suggested to give the values of the coaxial energy density deposited at penumbra by the incident ions,

$$\rho(r) = \frac{LET}{2}\left[2\pi r^2 \ln\left(\frac{e^{1/2}r_p}{r_c}\right)\right]^{-1} \qquad r_c < r \le r_p \qquad (4\text{-}4\text{-}4)$$

where ρ is the deposited energy density, r_c and r_p are the radii of core and penumbra area, and e is the charge of an electron. Table 4-4-4 also summarizes the calculated values of r_c and r_p.[12] The density of the reactive intermediates controls the crosslinking reaction in PDHS, which is supported by the presence of a LET threshold (ca. 10 eV/nm) to obtain a polymer gel. Thus ρ_c is adopted as the required energy density for the predominance of crosslinking in PDHS. The following expression of form gives the relation between the track radii and LET,

$$\pi r^2 = \frac{LET}{4\rho_c}\left[\ln\left(\frac{e^{1/2}r_p}{r_c}\right)\right]^{-1} \qquad (4\text{-}4\text{-}5)$$

Then we get,

$$r \propto \left(\frac{1}{4\pi\rho_c}\right)^{1/2}\sqrt{LET_{eff}} \qquad (4\text{-}4\text{-}6)$$

where

$$LET_{eff} = \frac{LET}{\ln(r_p/r_c)} \qquad (4\text{-}4\text{-}7)$$

Figure 4-4-10 plots the experimentally obtained radii: r + δr vs LET_{eff}. The value of the radii is proportional to LET_{eff}, indicating that the equation (4-4-3) provides a good interpretation to the chemical track radii obtained in this study. The slope of fig. 4-4-10 gives ρ_c at 0.13 eV/nm^3.

The eq. 4-4-4, however, gives the energy density at a particular radius: r in the penumbra area. The effects of migration or diffusion of reactive intermediates are not taken into accounts for the estimation of ρ_c. The distribution of crosslinking points in an ion track is expected not to exactly reflect the radial energy density but to be averaged over the radii. Thus the averaged energy density is estimated by the integration of eq. 8. The total deposited energy: E_t at r is give by the next expression of form,

$$E_t = \frac{LET}{2} + \frac{LET}{4}\left[\ln\left(\frac{e^{1/2}r_p}{r_c}\right)\right]^{-1} + \int_{r_c}\rho_p(r)\cdot 2\pi r dr \qquad (4\text{-}4\text{-}8)$$

Then we get the averaged energy density: ρ(r) at a particular radius,

$$\rho(r) = \frac{E_t}{\pi r^2} = \frac{LET}{\pi r^2}\left[1-\frac{1}{2}\left\{\ln\left(\frac{e^{1/2}r_p}{r_c}\right)\right\}^{-1}\ln\left(\frac{r_p}{r}\right)\right] \qquad (4\text{-}4\text{-}9)$$

Table 4-4-4. Track parameters and experimental radii of a track for a variety of ion beams.

Radiations	LET (eV/nm)	r_c[a] (nm)	r_p[a] (nm)	LET$\{\ln(r_p/r_c)\}^{-1}$ (eV/nm)	$r + \delta r$[b] (nm)
175 MeV Ar^{8+}	1620	1.03	6.0×10^2	254	7.0
2 MeV N^+	1580	0.180	9.0	404	6.8
160 MeV O^{6+}	300	1.50	2.1×10^3	41.4	6.1
225 MeV O^{7+}	230	1.80	3.4×10^3	30.5	5.9
2 MeV He^+	180	0.320	37	37.9	6.0
220 MeV C^{5+}	110	2.00	4.7×10^3	14.2	6.6
20 MeV He^{2+}	35	1.00	8.0×10^2	5.24	3.2
2 MeV H^+	17	0.673	2.4×10^2	2.89	2.5
20 MeV H^+	2.7	2.10	5.3×10^3	0.345	1.7[c]
45 MeV H^+	1.4	3.00	1.5×10^4	0.164	1.8[c]

[a] Calculated from Ref. 34 and 35 . [b] Estimated in this study by the fitting of gelation curves. [c] Estimated by the G-values of crosslinking.

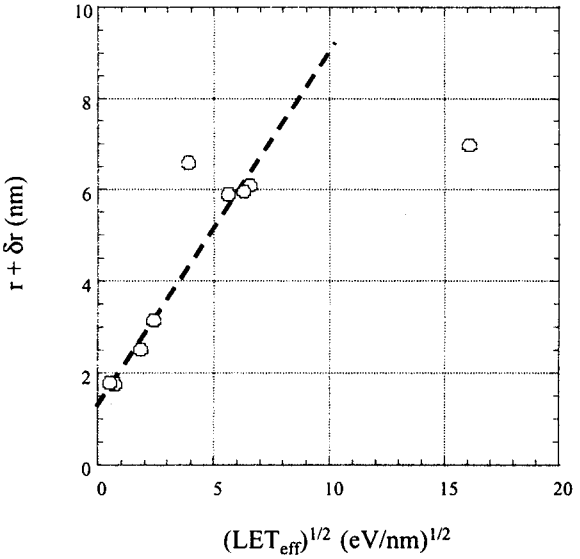

Figure 4-4-10. The relationship between the calculated LET_{eff} and the experimentally obtained radii of chemical track ($r + \delta r$)

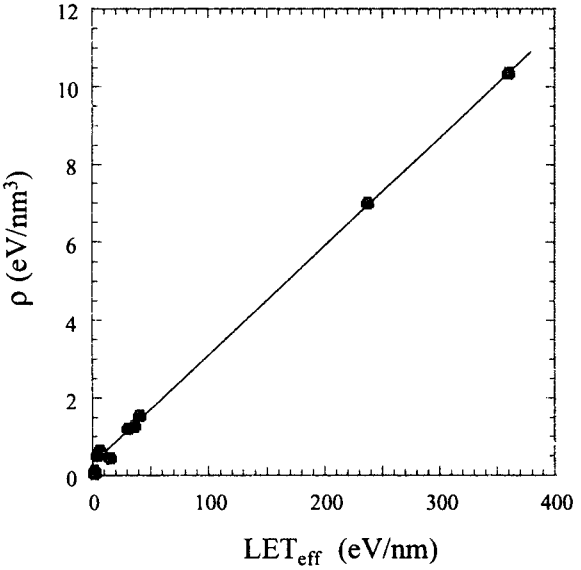

Figure 4-4-11. The relationship between the calculated LET_{eff} and the averaged energy density at the track radii obtained in the present study.

Fig. 4-4-11 plots the value of ρ at the experimentally obtained radius for each ion beam versus LET_{eff}. The values of ρ the averaged energy density rapidly increase with an increase in LET, leading to be 10 eV/nm^3 for 175MeV Ar^{8+} beams. The higher values of ρ are obtained than that estimated as ρ_{cr} at the track radii for high LET ion beams in spite of representing the similar values of ρ as ρ_{cr} for lower LET beams. This indicates that at the center part of ion tracks, the number of crosslinking points is predicted to be extremely larger than the number that is enough to make polymer gels (*Mn*/m per a molecule). Several groups reported that the IR spectra of polysilane indicated the Si-C ceramics formation upon irradiation to 2 MeV $^4He^+$ ion beam, however the conversion ratio was still ca. 25-30 % at 20 MGy despite of the gel fraction reaching at 100 %.[1,13] This may suggest that the Si-C ceramics structure is formed only in the core part of ion track as illustrated in fig. 4-4-9.

4-4-4 Summary

Crosslinking and main chain scission reactions were investigated for ion beam irradiation to PDHS films. The changes in Mn and Mw of PDHS showed good agreement with the Charlesby-Pinner relationship at the range of low absorbed dose. The G-value of crosslinking increased from 0.042 to 0.91 with increasing values of LET. The expanding chemical track along a ion trajectory may be responsible to the increasing G-values of crosslinking. The reaction model in a single track was applied to the gelation of PDHS, suggesting the chemical track radii of a variety of ion beams. The ion track model gives a good interpretation to the expanding track radii with an increase in LET of the ion beams.

Section 4-4 Reference

[1] Seki, S., Tagawa, S., Ishigure, K., Cromack, K. R., Trifunac. A. D. *Radiat. Phys. Chem.* 1996, **47**, 217.; Seki, S.; Cromack, K. R.; Trifunac, A. D.; Yoshida, Y.; Tagawa, S.; Asai, K.; Ishigure, K. *J. Phys. Chem.* 1998, **B102**, 8367.; Seki, S., Shibata, H., Yoshida, Y.,

Ishigure, K., Tagawa, S. *Radiat. Phys. Chem.* 1996, **48**, 539.; Seki, S., Kanzaki, K., Kunimi, Y., Tagawa, S., Yoshida, Y., Kodoh, H., Sugimoto, M., Sasuga, T., Seguchi, T., Shibata, H. *Radiat. Phys. Chem.* 1997, **50**, 423.

[2] Seki, S., Kanzaki, K., Yoshida, Y., Tagawa, S., Shibata, H., Asai, K., Ishigure, K. *Jpn. J. Appl. Phys.* 1997, **36**, 5361.

[3] Magee, J. L., Chattarjee, A. Kinetics of Nonhomogenious Processes; G. R. Freeman Ed.; Chapter 4; 1987; p.171

[4] Varma, M. N., Baum, J. W., Kuehner, A. J. *Radiat. Res.* 1975, **62**, 1.; Varma, M. N., Baum, J. W., Kuehner, A. J.. *Radiat. Res.* 1977, **70**, 511.

[5] Wingate, C. L., Baum, J. W. *Radiat. Res.* 1976, **65**, 1.

[6] Katz, R., Sinclair, G. L., Waligorski, M. P. R. *Nucl. Tracks Radiat. Meas.* 1986, **11**, 301.

[7] Wilson, W. E. *Radiat. Res.* 1994, **140**, 375.

[8] Kurshev, V. V., Koizumi, H., Ichikawa, T., Yoshida, H., Shibata, H., Yoshida, Y., Tagawa, S. *Radiat. Phys. Chem.* 1994, **44**, 521.; LaVerne, J. A., Schuler, R. H. *J. Phys. Chem.* 1987, **91**, 5770.; Koizumi, H., Ichikawa, T., Yoshida, H., Shibata, H., Tagawa, S., Yoshida, Y. *Nucl. Instr. Meth. Phys. Res.* 1996, **B117**, 269

[9] Puglisi, O., Licciardello, A. *Nucl. Instr. Meth. Phys. Res.* 1994, **B91**, 431.; Licciardello, A., Puglisi, O. *Nucl. Instr. Meth. Phys. Res.* 1994, **B91**, 436.; Calcagno, L., Percolla, R., Foti, G. *Nucl. Instr. Meth. Phys. Res.* 1994, **B91**, 426.

[10] LaVerne, J. A., Schuler, R. H. *J. Phys. Chem.* 1994, **98**, 4043.

[11] Charlesby, A. *Proc. R. Soc. London Ser.* 1954, **A222**, 60; Charlesby, A. *Proc. R. Soc. London Ser.* 1954, **A 224**, 120.; Charlesby, A., Pinner, S. H. *Proc. R. Soc. London Ser.* 1959, **A 249**, 367.

[12] Magee, J. L., Chattarjee, A. *J. Phys. Chem.* 1980, **84**, 3529.; Chattarjee, A., Magee, J. L. *J. Phys. Chem.* 1980, **84**, 3537.; Butts, J. J., Katz, R. *Radiat. Res.* 1967, **30**, 855.

[13] Venkatesan, T., Wolf, T., Allara, D., Wilkens, B. J., Taylor, G. N. *Appl. Phys. Lett.* 1983, **43**, 934.

4-5 Radiation Effects on Hole Drift Mobility

The radiation effects on hole drift mobility in polysilane derivatives were studied in the present section. The values of hole drift mobility (about 10^{-4} cm^2/V sec) obtained by the DC Time-of-Flight (TOF) measurement were improved by ion beam irradiation for in poly(methylphenylsilane) (PMPS) and poly(di-n-hexylsilane) (PDHS). The irradiated PMPS showed five times higher values of hole drift mobility than the non irradiated one. Their low photo-induced carrier yield, one of the highest barrier to use polysilanes as photoconductors, was also improved by the irradiation. The mechanism of the mobility improvement will be discussed in relation with the model of changes in the silicon skeleton structure induced by the irradiation.

4-5-1 Introduction

The hole transport is one of the most practical features of polysilane derivatives. Several studies have been intensively carried out on this feature of polysilanes as mentioned in the chapter 3,[1] and reported the highest values of hole drift mobility as the amorphous polymer materials without any dopants. However the value of hole drift mobility in polysilane (about 10^{-4} cm^2/V sec) is not the highest value in comparison with molecularly doped carbon backbone polymers with π-conjugated system such as polyacetylene.[2] Thus further improvement in the values is needed to use the polymers as real photoconducting materials.

Polysilanes have been regarded as 1 dimensional silicon materials: analogs of 3 dimensional amorphous and crystalline silicon. It is well known that those materials show higher values of electron and hole mobility (10^{-1} - 10^{1} cm^2/V sec) than the values of hole mobility in polysilanes. The carrier transport in 3-D amorphous and crystalline silicon is explained by the band conduction model in spite of the Poole-Frenkel hopping model applied to the explanation of the hole transport in 1-D polysilanes. The values of hole drift mobility in the amorphas polysilanes may be determined by next two processes : the presence of intermolecular and intersegment hopping barriers. It is common consensus that a polysilane molecule is divided into several σ-conjugated segments along the silicon skeleton. Therefore, hole transport is possibly determined by the hopping barrier between σ–conjugated segments as illustrated in figure 4-5-1. It is needed to elucidate which of intermolecular or intersegment hopping is the determinant process to the hole transport in polysilanes.

The improvement of low photo-induced carrier yield and high sensitivity for photodegradation is needed to use polysilanes as photoconductors. All kinds of linear polysilanes have no visible light absorption band but UV light absorption bands. Charge carriers are generated only for UV light (300 nm - 400 nm) exposure. The materials also show main chain scission for UV light exposure with high quantum efficiency. The experimental results suggested that UV light exposure causes not only charge carrier production but polymer main chain scission.

West et al. reported that crosslinked polysilanes showed increase of conductivity with the presence of electron acceptor.[3] The authors' previous studies also suggested that ion beam irradiation caused crosslinking of silicon skeletons leading to gelation of these materials.[4] The irradiated polysilanes grew into network silicon skeletons. The results suggested conversion from linear polysilane molecules to network polysilanes with higher dimensional silicon skeletons. Therefore the ion beam irradiation is expected to reduce the intermolecular hopping barrier, and also predicted to make holes highly mobile. It was also confirmed that ion beam irradiated polysilanes showed high resistivity to photodegradation with UV light because of their network silicon skeleton. Thus, ion beam irradiation can be an effective way to improve hole transport in polysilanes.

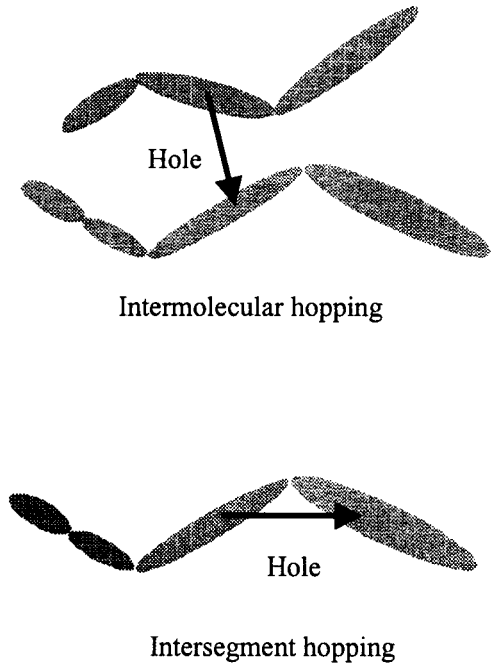

Figure 4-5-1. Schematic models of intermolecular and intersegment hopping in polysilanes

4-5-2 Experimental

Poly(methylphenylsilane) (PMPS) and poly(di-n-hexylsilane) (PDHS) were synthesized by the Wultz condensation with a methylphenyldichlorosilane for PMPS and a di-n-hexyl-dichlorosilane for PDHS as monomers respectively. All monomers were prepared by Shinetsu Chemical Co. LTD., and purified by distillation. Polymerization was carried out in Ar atmosphere and in 100 mL undecane as a reflux solvent. PDHS was synthesized in 100 mL toluene as a reflux solvent. The monomer was added to the reaction vessel and stirred with melted sodium metal for 4 hours. The reaction mixture containing PMPS and PDHS solution was poured into iso-propylalcohol after filtration to roughly eliminate

NaCl, and the precipitate was dried under vacuum. Toluene solutions of these polymers were transferred into separatory funnel with water, and poured into isopropylalcohol followed by reprecipitation using tetrahydrofran-methanol system. Molecular weight distributions of these polymers were measured by Toyosoda TSK-GEL gel permeation chromatography system. Obtained polymers have their weight average molecular weight : Mw = 7.1 x 10^4 for PMPS, and Mw = 8.5 x 10^5 for PDHS respectively.

Polymers were dissolved into toluene at 10-15 wt.% and casted on aluminum substrates at 10 μm thick. The remaining solvent was removed in vacuum oven during 5 hours at 120 °C, and the films were annealed. Nihon-Koshuha LGO-2N-200A nitrogen LASER (337 nm) was used as an excitation light source. The LASER pulses with 2 nsec width were strongly absorbed at the upper surface of polymer films through semitransparent Au top contacts, leading to plane-like charge packets. These carriers were forced to move by the applied electric fields, and the transient current was observed as voltage signals at terminate resistance. Predominately 1 kΩ - 10 kΩ terminate resistances were used to convert the transient current to voltage signals. Transient current was observed by the Sony/Tektoronics TDS350 and DSA601 digitizing oscilloscopes.

Ion beam irradiation was carried out by Van de Graaff accelerator at Research Center for Nuclear Science and Technology, The University of Tokyo. 2 MeV H^+ beam was irradiated to the film specimens of PMPS and PDHS at the fluence of 0.05-0.5 μC/cm^2. Energy deposition of 2 MeV H^+ beam in these media (10 μm depth) was estimated maximally 10 % of incident particle energy, then the irradiation was considered to be homogeneous.

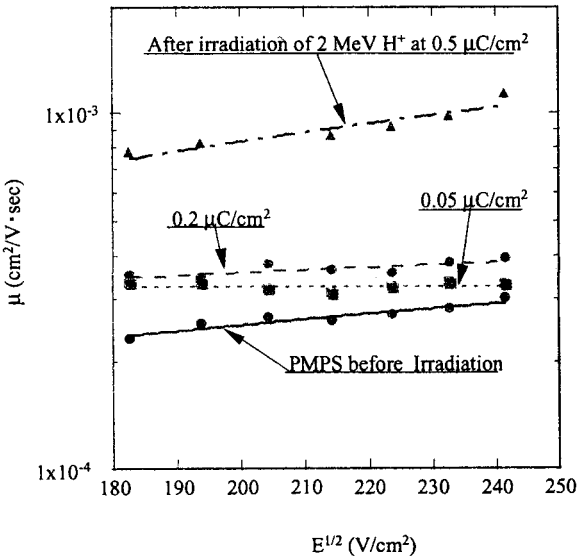

Figure 4-5-2 Arrhenius plot of hole drift mobility in poly(methylphenylsilane);PMPS films at electric field : E = 4.2x10^4 V/cm

4-5-3 Results and Discussion

Figure 4-5-2 shows temperature dependence of hole drift mobility in PMPS at the applied field of 4.0x10^4 V/cm. Next expression of form is introduced to deconvolute field and temperature dependence,

$$\mu = \mu_0 \exp\left[-\left(\varepsilon_0 - \beta E^{1/2}\right)/kT_{eff}\right] \quad (4\text{-}5\text{-}1)$$

where E denotes field, ε_0 denotes zero field limit activation energy, and $1/T_{eff} = 1/T - 1/T_0$, the same way as proposed by Grill, Pai and Chen et al. for hole transport in poly(vinylcarbazole).[5] Fig. 4-5-2 is represented by the extrapolation of the field dependence of hole drift mobility in PMPS. The obtained slope of the Arrhenius representation corresponds to activation energy of zero field limit ; ε_0 as shown in the equation (4-5-1). The result of ε_0 is estimated to be 0.39 eV in this PMPS media.

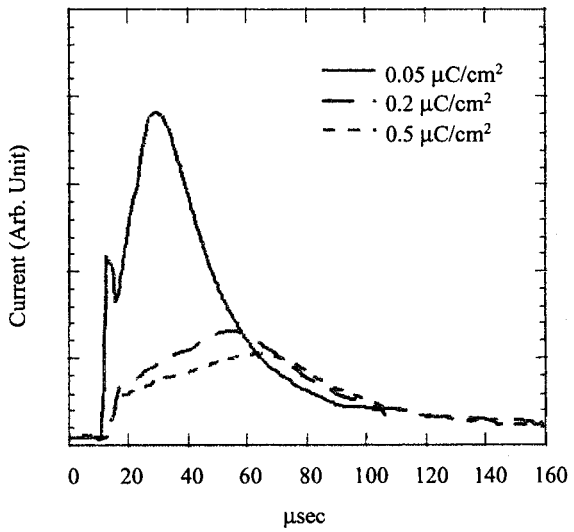

Figure 4-5-3. Changes in transient current pulse shapes of irradiated poly(methylphenylsilane)by 2 MeV H^+ ion beam at 298K, 4.2x10^4 V/cm

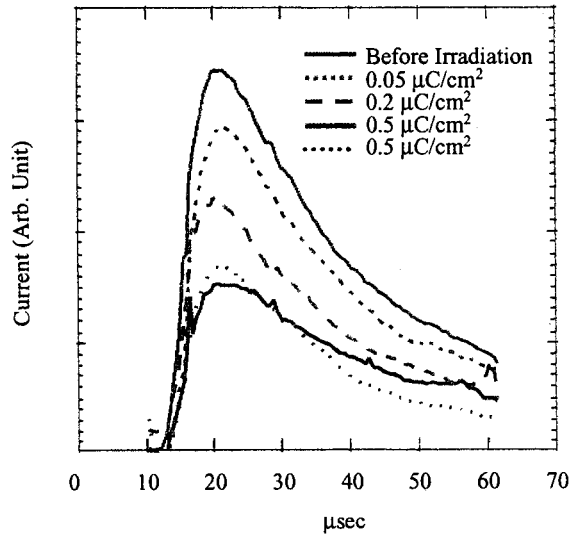

Figure 4-5-4. Changes in transient current pulse shapes of irradiated poly(di-n-hexylsilane)by 2 MeV H^+ ion beam at 298K, 4.2x10^4 V/cm

Figure 4-5-3 displays the ion beam induced changes in the TOF current-mode transit pulses collected on glassy PMPS media. These transit pulse shapes are obtained by the specimens irradiated by 2 MeV H^+ with the fluence of 0.05, 0.2 and 0.5 $\mu C/cm^2$, respectively. The lower current is obtained for the specimen before irradiation in comparison with these transit currents after irradiation. The values of transit time are estimated by the edges of transit pulse shapes. It is clear that the flight time is shortened by the ion beam irradiation. Another attractive change is the increase of carrier yield with the irradiation. The yield of holes is estimated by the integration of transient current. Especially for the specimen irradiated at 0.5 $\mu C/cm^2$, the yield is two times larger than that of before irradiation as summarized in table 4-5-1 (Normalized carrier yield means the ratio of carrier yield to the yield before irradiation.).

Figure 4-5-4 shows changes with the irradiation in the transit pulse shapes collected on the crystalline PDHS media. The ion beam irradiation was carried out at the same condition as PMPS, and the irradiation fluence was varied from 0.05 $\mu C/cm^2$ to 3 $\mu C/cm^2$. The transit pulses in fig. 4-5-4 is slightly distorted in comparison with the case of PMPS as shown in fig. 4-5-3, and it is impossible to distinguish a rectangular edges that presents the value of the transit time. The mobility seems to consist of multiple components for this polymer. However, it should be noted that pulse signals after irradiation showed faster decay than the pulse before irradiation, resulting in the generation of fast components of charge carrier mobility. The yield of charge carrier also increases with the irradiation similarly to the irradiation for PMPS. The yield of holes is once increased until the fluence reaching to 0.2 - 0.5 $\mu C/cm^2$, and decreases with further irradiation as summarized in table 4-5-1. In this case, the yield also becomes maximally two times larger than that of before irradiation.

Table 4-5-1. Changes in the carrier yield of PMPS and PDHS irradiated by ion beams

Fluence ($\mu C/cm^2$)	Normalized Carrier Yield	
	PMPS	PDHS
0	1	1
0.05	1.2	1.35
0.2	1.4	2.5
0.5	2.1	2.1
3	---	1.15

The values of hole drift mobility in polysilane derivatives have been reported to depend on the square root of electric field in Poole-Frenkel hopping model.[1,2] The electric field dependence in the PMPS also appears to obey the equation (4-5-1) even after the irradiation as summarized in figure 4-5-5. The values of zero field limit mobility are almost same for all irradiated samples in spite of the lower value observed for the specimen before irradiation. In this electric field range, the carriers are accelerated with the irradiation. The specimen irradiated at 0.5 $\mu C/cm^2$ shows five times larger value of mobility than that of before irradiation. The acceleration phenomenon of holes is fundamentally explained by a simple model of network structure generation as suggested in the authors' previous work.[6] Contrarily, lower values of hole drift mobility has been observed for structural defects induced polysilanes (chemically branched polysilanes).[7] Those structural defects induced polysilanes have also been investigated by means of the electron beam pulse radiolysis.[8] The experimental results showed hole localization around the sites of branched structures leading to decline of the hole drift mobility. Comparing the effects of ion beam irradiation to that of the chemically induced branched structure, the difference is in the dimensional change of silicon skeletons. Ion beam irradiation changes molecular structure of polysilanes into the 3-D Si network along incident ion tracks in spite of chemically induced branched structures meaning 2-D Si network structures.[9]

4-5-4 Summary

The values of hole drift mobility obtained in the present study corresponded to several previous data. The field dependence of hole drift mobility in PMPS was well explained by Poole-Frenkel type hopping model. The model was also effective to account for the field dependence even in the ion beam irradiated PMPS. The temperature and field dependence was deconvoluted for PMPS before irradiation, and the activation energy was estimated to be 0.39 eV.

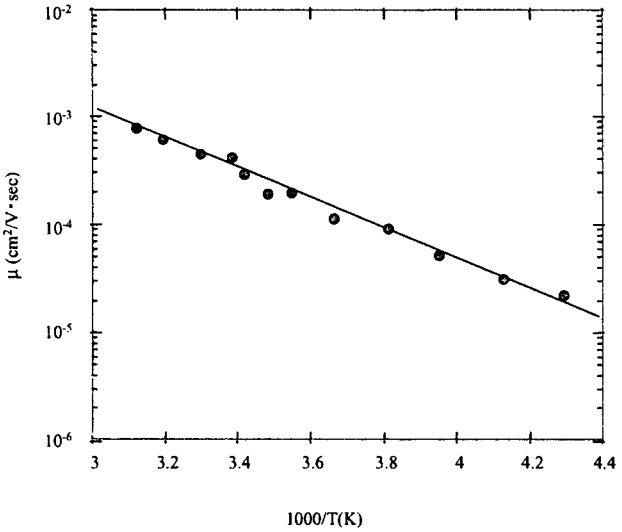

Figure 4-5-5. Semi-logarithmic plot of hole drift mobility μ vs $E^{1/2}$ $(V/cm)^{1/2}$ in ion beam irradiated polysilane films at 298K

Ion beam irradiation increased the values of hole drift mobility in glassy PMPS and crystalline PDHS, and the yield of charge carriers increased with the irradiation to the specimens of the PMPS and the PDHS. The yield of charge carrier was once increased until the fluence reaching to 0.2 - 0.5 $\mu C/cm^2$ followed by the decrease

with further irradiation. The yield became two times larger than that of before irradiation for both the PMPS and the PDHS. The acceleration was basically explained by a simple model of Si network structure generation induced by ion beam irradiation. Intermolecular hopping barrier was reduced by extended σ-conjugated system. The model of ion beam induced Si network structures is concluded to be 3-D cylindrical Si network structures generated by ion beam irradiation along incident ion tracks. The model is quite different from that of chemically induced 2-D network structures with Si branching.

Section 4-5 Reference

[1] for a review, Abkowitz M. A., Stolka M., Weagley R. J., McGrane K. M., Knier F. E. (1990) In Silicon Based Polymer Science, Advances in Chemistry Series 224 (Edited by Zeigler, J. M., Fearon, F. W. American Chemical Society: Washington DC.; Kepler R. G., Zeigler J. M., Harrah L. A., Kurtz S. R. (1987) Phys. Rev. B **35**, 2818.; Fujino M. (1987) Chem. Phys. Lett. **136**, 451.; Stolka M., Yuh H. J., McGrane K., Pai D. M. (1987) J. Polym. Sci., Polym. Chem. Ed. **25**, 823.; Abkowitz M. A., Knier F. E., Yuh H. J., Weagley R. J., Stolka M. (1987) Solid State Commun. **62**, 547.; Kepler R. G., Zeigler J. M., Harrah L. A., Kurtz S. R. (1984) Bull. Am. Phys. Soc. **29**, 509.; Kepler R. G., Zeigler J. M., Harrah L. A., Kurtz S. R. (1984) Bull. Am. Phys. Soc. **28**, 362.; Samuel L. M., Sanda P. N., Miller R. D. (1989) Chem. Phys. Lett. **159**, 227.; Phillpot S. R. (1987) Phys. Lett. **31**, 43.; Abkowitz M. A., Rice M. J., Stolka M. (1990) Phil. Mag. B **61**, 25.

[2] Rice M. J. (1979) Phys. Lett. A **71**, 152.; Su W. P., Schrieffer J. R., Heeger A. J. (1979) Phys. Rev. Lett. **58**, 937.

[3] West R. D., Djurovic L. D., Stearley P. I., Srinvasan K. S., Yu H. (1981) J. Am. Chem. Soc. **103**, 7352.

[4] Seki, S.; Shibata, H.; Ban, H.; Ishigure, K.; Tagawa, S. Radiat. Phys. Chem. 1996, **48**, 539.

[5] Pai D. M. (1970) J. Chem. Phys. **52**, 2285.; Gill W. D. (1972) J. Appl. Phys. **43**, 5033.; Chen I., Slowick J. H. (1975) Solid State Commun. **17**, 783.

[6] Seki, S., Shibata, H., Yoshida, Y., Ishigure, K., Tagawa, S. *Radiat. Phys. Chem.* 1996, **48**, 539.

[7] Seki, S.; Cromack, K. R.; Trifunac, A. D.; Yoshida, Y.; Tagawa, S.; Asai, K.; Ishigure, K. *J. Phys. Chem.* 1998, **B102**, 8367.

[8] Seki, S., Tagawa, S., Ishigure, K., Cromack, K. R., Trifunac. A. D. *Radiat. Phys. Chem.* 1996, **47**, 217.

[9] Furukawa K., Fujino M., Matsumoto N. (1990) Macromolecules **23**, 3423.; Bianconi P. A., Weidman T. W. (1988) J. Am. Chem. Soc. **110**, 2342.; Bianconi P. A., Schilling F. C., Weidman T. W. (1989) Macromolecules **22**, 1697.

Chapter 5 Conclusion

Neutral silyl radicals in solid aryl substituted polysilanes were less stable than radicals derived from dimethyl substituted polysilanes. The defect (branch) structure in the silicon skeleton appears to be able to stabilize silyl radicals, and highly branched silyl radicals exhibited remarkable stability, even close to room temperature.

The electronic states of excess electrons or holes were investigated by nano-second pulse radiolysis technique. The radical cations and anions of polysilanes displayed near UV and IR absorption maximums at ca. 3.2~3.4 eV and 0.5~1 eV, respectively. It can be concluded that excess electrons and holes are localized at the defect structures in specimens with more defects, while the charge was relatively delocalized in a conjugated segment in the polysilanes with fewer defects.

The author studied the hole transport properties in PMPS with controlled defect densities by the DC TOF technique. The observed TOF signals and hole drift mobilities in the polymers were analyzed on the basis of Bässler's disorder formalism. Hole transport in polymers with a lower defect density was dominated by the degree of fluctuation in the density of states, though the mobility was controlled by the intersite hopping distance in specimens with higher defect densities.

Radical species produced by the γ-ray irradiation of solid-state PDMS were investigated. High energy photons induce polymer main chain scission directly, and silicon-centered radicals were formed as a result of homolytic cleavage of silicon skeleton. The observed EPR coupling constants of the silyl radicals were essentially the same as the values observed in previous studies of small silane molecules. The spin density of the unpaired electron appeares to be localized on the silicon atoms.

Ion beam irradiation induces molecular structure changes of PMPS, such as dissociation of substituents, or generation of siloxane structure and Si-C bonds. Especially generation of Si-C bonds is important because increasing Si-C bonds maybe grow into silicon carbide network, and they also mean the rearrangement of polymer backbone. It is very interesting characteristics of PMPS that the main chain scission and rearrangement are simultaneously induced by the ion beam irradiation. However, ion beam induced reactions were affected by the phase transition of PDHS. The predominant reaction changed from crosslinking into main chain scission with increasing temperatures. The expanding chemical track along a ion trajectory may be responsible to the increasing G-values of crosslinking. The reaction model in a single track was applied to the gelation of PDHS, suggesting the chemical track radii of a variety of ion beams. The ion track model gives a good interpretation to the expanding track radii with an increase in LET of the ion beams.

Ion beam irradiation increased the values of hole drift mobility in glassy PMPS and crystalline PDHS, and the yield of charge carriers increased with the irradiation to the specimens of the PMPS and the PDHS. The yield of charge carrier was once increased until the fluence reaching to 0.2 - 0.5 $\mu C/cm^2$ followed by the decrease with further irradiation. The yield became two times larger than that of before irradiation for both the PMPS and the PDHS.

Finally, the author describes his impressions on the present materials: polysilanes as a general conclusion. Since 1992, the author have been studied the materials named polysilanes having silicon catenation as their main chains. In the early stage of this work, the author was fascinated by the polymeric materials because of their own and unique physical properties originated to the delocalized σ-electrons in the main chain. In spite of having a inorganic main chain, the polymer can be synthesized by procedures of organic chemistry in a glass flask. The nature of σ-conjugated system, which is the author's major objectives in these days, struck me at the moment when the author encountered to the materials.

However, to date, the author's thoughts on the materials have been gradually changed. The author might make some mistakes of the "unique" and something "special" feelings on polysilanes. Of course, the peculiar and interesting feature of polysilanes has not been faded a little now, but the nature of the other organic systems has revealed to be "unique", indicating that the author's sense on the organic chemistry has been very full of misunderstandings. The concepts of the chemical education might be wrong in the high school or the earlier education. The delocalization of σ-electrons certainly occurs even in the carbon based organic systems, and it received the general consensus in the nowadays physical chemistry. Moreover, almost all researchers are daily talking about the electron transfer through σ-bondings. Thus, the "unique" electronic structure of polysilanes should be ascribed to the degree of the electron migration over a σ-orbital. The polysilanes taught the author that the electrons could potentially be mobile even in the almost all σ-bonded organic materials, which are the essentials of Heisenberg's principle of uncertainty.

Although a huge amount of research has been carried out on the chemistry of carbon based materials since the last century, the studies on orgaopolysilanes have just started in the last decade in spite of silicon being one of the richest element on our planet. Thus, the possibility of the materials may be infinite, and scientifically the materials are still mysterious, now. It might be 20, 30, or more years later, the author believes that the organopolysilanes must get into limelight of the scientific and industrial world.

List of Publication

1. Publications

1) S. Seki, Y. Yoshida, S. Tagawa, K. Asai, Electronic Structure of Radical Anions and Cations of Polysilanes with Structural Defects, *Macromolecules* **32**, 1999, 1080-1086.

2) S. Seki, Y. Yoshida, S. Tagawa, K. Asai, K. Ishigure, K. Furukawa, M. Fujiki, N. Matsumoto, Effects of Structural Defects on Hole Drift Mobility in Aryl-substituted Polysilanes, *Phil. Mag.* **B79**, 1999, 1631-1646.

3) S. Seki, S. Tagawa, K. Ishigure, K. R. Cromack, A. D. Trifunac, Radical Stability of Aryl Substituted Polysilanes with Linear and Planar Silicon Skeleton Structures, *J. Phys. Chem.* **B102**, 1998, 8367-8371.

4) S. Seki, K. Kanzaki, Y. Kunimi, S. Tagawa, Y. Yoshida, H. Kudoh, M. Sugimoto, T. Sasuga, T. Seguchi, H. Shibata, LET Effects of Ion Beam Irradiation on Poly(di-n-hexylsilane), *Radiat. Phys. Chem.* **50**, 1997, 128-133.

5) S. Seki, K. Kanzaki, Y. Yoshida, S. Tagawa, H. Shibata, K. Asai, K. Ishigure, Positive-Neagative Inversion of Silicon Based Resist materials: Poly(di-n-hexylsilane) for Ion Beam Irradiation, *Jpn. J. Appl. Phys.* **36**, 1997, 5361-5364.

6) S. Seki, H. Shibata, Y. Yoshida, K. Ishigure, S. Tagawa, Radiation Effects on Hole Drift Mobility in Polysilanes, *Radiat. Phys. Chem*, **49**, 1997, 389-392.

7) S. Seki, H. Ban, H. Shibata, K. Ishigure, S. Tagawa, Radiation Effects of Ion Beams on Poly(methylphenylsilane), *Radiat. Phys. Chem.* **48**, 1996, 539-544.

8) S. Seki, S. Tagawa, K. Ishigure, K. R. Cromack, A. D. Trifunac, Observation of Silyl Radical in g-Radiolysis of Solid Poly(dimethylsilane), *Radiat. Phys. Chem.* **47**, 1996, 217-219.

9) S. Seki, M. Ando, T. Yamaki, Y. Nakashiba, K. Asai, K. Ishigure and S. Tagawa, Molecular interaction in langmuir-blodgett films of amphiphilic polysilanes, *J. Photopolym. Sci. Tech.*, **8**, 1995, 89-108.

2. Supplementary Publications

1) S. Seki, Y. Kunimi, K. Nishida, Y. Yoshida, and S. Tagawa, Electronic State of Radical Anions on Poly(methyl-*n*-propylsilane) Studied by Low Temperature Pulse Radiolysis, *J. Phys. Chem. B* in press.

2) S. Seki, Y. Yoshida, and S. Tagawa, Charged Radicals of Polysilane Derivatives Studied by Pulse Radiolysis, *Radiat. Phys. Chem.* in press.

3) K. Maeda, S. Seki, S. Tagawa, and H. Shibata, Radiation Effects on Branching Polysilanes, *Radiat. Phys. Chem.* in press.

4) Y. Yoshida, Y. Mizutani, T. Kozawa, A. Saeki, S. Seki, S.Tagawa and K. Ushida, Development of Laser-Synchronized Picosecond Pulse Radiolysis System, *Radiat. Phys. Chem.*, in press.

5) S. Tsuji, S. Seki, T. Kozawa and S. Tawaga, Reaction Mechanisms of Excimer Resists Studied by Laser Flash Photolysis, *J. Photopolym. Sci. Technol.*, 13 (2000), in press.

6) Y. Kunimi, S. Seki, and S. Tagawa, Free Volume in Poly(alkylphenylsilane) Probed by Positron Anihilaiton, *J. Photopolym. Sci. Technol.*, 13 (2000), in press.

7) S. Seki, Y. Kunimi, K. Nishida, K. Aramaki, and S. Tagawa, Optical Properties of Pyrrolyl-substituted Polysilanes, *J. Organomet. Chem.* **611** (2000) 62-68.

8) S. Seki, Y. Sakurai, K. Maeda, Y. Kunimi, and S. Tagawa, Studies on the Negative Resist Material Based on Polysilanes for EB and X-ray Lithography, *Jpn. J. Appl. Phys.* **39** (2000) 4225-4230.

9) Y. Kunimi, S. Seki, and S. Tagawa, Investigation on Hole Drift Mobility in Poly(*n*-hexylphenylsilane), *Solid State Commun.* **114** (2000) 469-472.

10) S. Seki, Y. Kunimi, Y. Sakurai, S. Tagawa, High-sensitive Negative Resist Materials Based on Polysilane Derivatives, *J. Photopolym. Sci. Technol.* **13** (2000) 395-396.

11) M. Tashiro, P. K. Pujari, S. Seki, Y. Honda, S. Ni-

shijima, and S. Tagawa, Studies on Thermally Induced Structural Changes in Silicon Based Polymers by Positron Annihilation, *Radiat. Phys. Chem.* **58** (2000) 587-592.

12) K. Mochida, N. Kuwano, H. Nagao, S. Seki, Y. Yoshida, and S. Tagawa, Radical Cation of Octaisopropylcyclotetragermane Generated by Pulse Radiolysis, *Inorg. Chem. Commun.* **2** (1999) 238.

13) S. Seki, K. Maeda, Y. Kunimi, Y. Yoshida, S. Tagawa, H. Kudoh, M. Sugimoto, T. Sasuga, T. Seguchi, T. Iwai, H. Shibata, K. Asai, and K. Ishigure, Ion Beam Induced Crosslinking Reactions in Poly(di-*n*-hexylsilane), *J. Phys. Chem. B* **103** (1999) 3043.

14) K. Mochida, N. Kuwano, H. Nagao, S. Seki, Y. Yoshida, and S. Tagawa, Radical Cation of Dodecamethylcyclohexagermane Generated by Pulse Radiolysis, *Chem. Lett.* (1999) 3.

15) S. Seki, Radiation Induced Reactions and Physical Properties of σ-conjugated Polymers, *Radioisotopes* **47** (1998) 382.

16) T. Yamaki, Y. Nakashiba, K. Asai, K. Ishigure, S. Seki, S. Tagawa, and H. Shibata, Intramolecular Exciplex Formation in Ammonium-type Amphiphilic Polysilanes, *Polymer* **39** (1998) 767.

17) S. Seki, S. Tsuji, K. Nishida, Y. Matsui, Y. Yoshida, and S. Tagawa, Photo-Induced Reaction Dynamics in Poly(di-*n*-hexylsilylene) by Excimer Laser Flash Photolysis, *Chem. Lett.* (1998) 1158.

18) Y. Matsui, S. Seki, T. Iwamoto, and S. Tagawa, Electronic Structure of Polysilanes Studied by Femtosecond Laser Flash Photolysis, *Chem. Lett.* (1998) 861.

19) K. Mochida, R. Hata, H. Chiba, S. Seki, Y. Yoshida, and S. Tagawa, Radical Anions of Oligogermanes, $Me(Me_2Ge)_nMe$ (n=2,3,5, and 10) Generated by Pulse Radiolysis, *Chem. Lett.* (1998) 263.

20) W. Zhao, S. Seki, Y. Yamamoto and S. Tagawa, Formation of Conjugated Double Bonds in Poly(vinylalcohol) Film under Irradiation with γ-rays at Elevated Temperatures, *Chem. Lett.* (1997) 183-184.

21) S. Seki, H. Shibata, Y. Yoshida, K. Ishigure, and S. Tagawa, Ion Beam Irradiation Effects on Polysilanes, *Radiat. Phys. Chem.* **49** (1997) 410-413.

22) T. Yamaki, Y. Nakashiba, K. Asai, K. Ishigure, S. Seki, S. Tagawa, and H. Shibata, Exciplex Emission from Amphiphilic Polysilanes Bearing Ammonium Moieties, *J. Nucl. Matter.* **248** (1997) 369-374.

23) K. Asai, T. Yamaki, S. Seki, K. Ishigure, and H. Shibata, Ion Bombardment Effect on Electronic States in CdS Fine Particles, *Thin Solid Films* **277** (1996) 169-174.

24) K. Asai, T. Yamaki, S. Seki, K. Ishigure, and H. Shibata, Surface Treatment Effect of Ion-irradiation on Size-Quantized Semiconductor Particles Incorporated into L.B. Films, *Thin Solid Films* **284-285** (1996) 541-544.

25) S. Seki, H. Shibata, S. Tagawa, Y. Yoshida, and K. Ishigure, Time-dependent Emission Spectra from Polysilane Thin Films Irradiated by MeV Ion Beams, *Nucl. Instr. Meth. Phys. Res. B* **105** (1995) 43-45.

26) K. Asai, S. Seki, T. Sato, K. Ishigure, and H. Shibata, Fast-ion-induced Fluorescence from j Aggregate of Cyanine Dye in Langmuir-Blodgett Films, *Thin Solid Films* **258** (1995) 286-291.

3. Proceedings

1) A. Saeki, Y. Yoshida, T. Kozawa, K. Ushida, S. Seki, and S. Tagawa, Study of Geminate Ion Recombination Process by Means of Laser-synchronized Picosecond and Subpicosecond Pulse Radiolysis, *Proceedings of the 8th Japan-China bilateral symposium on radiation chemistry* (2000) 10.

2) H. Habara, A. Saeki, Y. Kunimi, S. Seki, T. Kozawa, Y. Yoshida, and S. Tagawa, Study of Polysilane Mainchain Electronic Structure by Picosecond Pulse Radiolysis, *Proceedings of the 8th Japan-China bilateral symposium on radiation chemistry* (2000) 112.

3) K. Maeda, S. Seki, S. Tagawa, H. Shibata, and T. Iwai, Radiation Effects on Branched Polysilanes, *Proceedings of the 8th Japan-China bilateral symposium on radiation chemistry* (2000) 115.

4) Y. Matsui, S. Seki, and S. Tagawa, Transient Spectroscopy of Polysilanes Studied by Ultrashort Laser Pulses, *Proceedings of the 8th Japan-China bilateral symposium on radiation chemistry* (2000) 130.

5) S. Seki, K. Maeda, Y. Kunimi, S. Tagawa, Y. Yoshida, H. Kudoh, M. Sugimoto, Y. Morita, T. Seguchi, T. Iwai, H. Shibata, K. Asai, and K. Ishigure, Ion Track

Structure in Poly(di-*n*-hexylsilane), *JAERI-Conf.* **2000-001** (2000) 287.

6) M. Tashiro, S. Seki, P. K. Pujari, Y. Honda, and S. Tagawa, Microscopic Structures of Polysilanes Studied by Positron Annihilation Techniques, *JAERI-Conf.* **2000-001** (2000) 295.

7) Y. Kunimi, S. Seki, and S. Tagawa, Hole Drift Mobility in Poly(hexylphenylsilane), *JAERI-Conf.* **2000-001** (2000) 299.

9) M. Tashiro, S. Seki, P. K. Pujari, Y. Honda and S. Tagawa, Free-Volume Characterization of Polysilanes Using Positron Annihilation Spectroscopy, *J. Photopolym. Sci. Technol.* **12** (1999), 739-742.

11) M. Tashiro, P. K. Pujari, S. Seki, Y. Honda, T. Yamaguchi, R. Suzuki and S. Tagawa, Studies on the Thin Films of Poly(di-*n*-hexylsilane) Using Slow Positron Beam Technique, *J. Photopolym. Sci. Technol.* **12** (1999), 743-746.

12) S. Seki, Y. Sakurai, K. Maeda, Y. Kunimi, S. Nagahara, and Seiichi Tagawa, Reaction Mechanisms in Silicon-based Resist Materials: Polysilanes for Deep-UV, EUV, and X-ray Lithography, *Proc. SPIE* **3999** (2000) 423-431.

13) Y. Yoshida, Y. Mizutani, T. Kozawa, M. Miki, S. Seki, T. Yamamoto, A. Saeki, Y. Izumi, K. Ushida, and S. Tagawa, Geminate Ion Recombination of Electron and Radical Cations in Non-polar Liquid Studied by Laser-synchronized Pico- and Subpicosecond Pulse Radiolysis, *Proc. IEEE 13th ICDL* (1999) 579-582.

14) S. Seki, K. Nishida, Y. Kunimi, Y. Yoshida, and S. Tagawa, Electronic Structure of σ-conjugated System of Polysilanes Studied by Electron Beam Pulse Radiolysis, *Proc. IEEE 13th ICDL* (1999) 646-649.

15) S. Seki, K. Kanzaki, Y. Kunimi, Y. Yoshida, S. Tagawa, H. Kudoh, M. Sugimoto, and T. Seguchi, LET Effects of Ion Beam Irradiation on Poly(di-*n*-hexylsilane), *JAERI-Rev.* **97** (1997) 62-64.

16) Y. Yoshida, T. Yamamoto, K. Ushida, M. Miki, S. Seki, S. Okuda, Y. Honda, N. Kimura, and S. Tagawa, Development of a New Picosecond Pulse Radiolysis System by Using a Femtosecond Laser Synchronized with a Picosecond Linac. A Step to Femtosecond Pulse Radiolysis, *JAERI-Conf.* **97** (1997) 381-383.

17) S. Seki, K. Kanzaki, S. Tagawa, Y. Yoshida, H. Kudoh, M. Sugimoto, T. Sasuga, T. Seguchi, and H. Shibata, LET Effects of High Energy Ion Beam Irradiation on Polysilanes, *JAERI-Conf.* **97** (1997) 281-285.

18) S. Seki and S. Tagawa, Radiation Induced Modification and Physical Property Changes in Polysilanes, *KURRI-TR* **411** (1995) 1-10.

Acknowledgements

I have often climbed mountains since 10 years ago, because I belonged to the mountain climbing club. There are many famous walls even in Japanese Mountains, such as "Byobu" at Hodaka range, "Tsuitate" at Tanigawa mountains. When I climbed the length of a range or climbed up a rock, I often looked up the very faced mountain or wall, but I had never seen the top of the mountain or wall on the way of climbing before reaching the summit. Thus I just climbed up there with a little disappointment at every moments. Sometimes I encounter the similar situation of my research work to that of the mountain climbing. We never see the whole picture of our research works when we are very studying on the subject. Maybe the author can only recognize the right trajectory by looking back our footprints. It is viewed in this light that no one might not be able to see through the intrinsic whole picture of the science. Thus, I may miss some persons to acknowledge here, anyway,

The author firstly acknowledges Prof. S. Tagawa for his guidance throuout this work, and Prof. Y. Shirota, and Prof. Y. Kai for their helpful comments. The author is also indebted to Prof. Y. Yoshida, and Prof. Y. Yamamoto at ISIR Osaka University, Prof. K. Ishigure and Dr. K. Asai at Faculty of Engineering, the University of Tokyo for their proper directions and meaningful suggestions in the present work. The author would like to express appreciation to Mr. T. Yamamoto and Mr. S. Suemine at RL, ISIR Osaka University. The author's honest thanks are given to the graduate students in the University of Tokyo and Osaka University, Mr. M. Ando, Mr. T. Yamaki, Mr. K. Yonemura, Ms. K. Aramaki, Mr. K. Kanzaki, Mr. K. Nishida, Mr. Y. Nakashiba, Mr. Y. Kunimi, Mr. Y. Matsui, Mr. Y. Mizutani, Mr. M. Tshiro, Mr. K. Maeda, Mr. S. Tsuji, Mr. Y. Sakurai, and Mr. H. Habara for their experimental efforts. The author also thanks to Dr. K. Kobayashi, Ms. M. Miki, Ms. J. Nishibayashi, Ms. M. Okada, Dr. W. Zhao, Mr. S. Nagahara, Mr. M. Naito, Mr. K. Okamoto, Mr. T. Tanaka, and Mr. K. Yokoyama.

The author often used the facilities at a variety of laboratories, thus The author acknowledges Prof. H. Shibata, Dr. T. Iwai, Mr. M. Narui, Mr. T. Omata, and Ms. M. Osono at RCNST, the University of Tokyo for their efforts on the accelerator facility, and to Prof. Y. Katsumura at the University of Tokyo for useful advises. The author also thanks to Dr. M. Sugimoto, Dr. H. Kudoh, Dr. T. Sasuga, Dr. T. Seguchi, and Dr. Y. Morita at JAERI, Takasaki for their experimental supports on the cyclotron experiments, and to Dr. K. Furukawa, Dr. M. Fujiki, Dr. K. Takeda, and Dr. N. Matsumoto at NTT Basic Research Laboratories for their advises on the drift mobility measurements.

Other scientists experimentally assisted several parts of this work. The author appreciates to Dr. A.D. Trifunac, Dr. K.R. Cromack, Dr. D. Werst, and Dr. C.D. Jonah at Argonne National Laboratories for their collaborations on the EPR spectroscopy. Acknowledgements are also given to Prof. O. Itoh and Prof. A. Watanabe at ICRS, Tohoku University for their helps in the LASER experiments.